Supporting Information for

Regioselective –NO_2 Substitution Enables Tunable Photophysics and Molecular Packing in a Polycyclic 1,2-BN Heteroarene Framework

Carl Jacky Saint-Louis,[a]* Lingaraju Gorla,[a] Ophelia Adjei-sah,[a] Lilianna Kocai,[a] Miriam Raggs,[a] Zaynab Khan,[a] Misgana Idris,[a] Rajendra Prasad Nandi,[c] Blaise Williams,[a] Sanjay Dutta,[a] Petia Bobadova-Parvanova,[b] Frieder Jäkle,[c] Mohammad A. Halim,[a] and Masafumi Yoshinaga[a]

[a] Department of Chemistry and Biochemistry, Kennesaw State University, Kennesaw, GA, 30144, USA.; Tel: 1-470-578-6048
[b] Department of Chemistry and Fermentation Sciences, Appalachian State University, Boone, NC 28608, USA
[c] Department of Chemistry, Rutgers University-Newark, Newark, NJ, 07102, USA

*To whom correspondence should be addressed: csaintlo@kennesaw.edu

Table of Contents **Pages**

General Information

Starting materials were produced in the laboratory and solvents were purchased from commercial suppliers as reagent grade unless noted otherwise. *N*-bromosuccinimide (NBS) and 1,8-diazabicyclo[5.4.0]undec-7-ene (DBU) were purchased from TCI America, Inc. Solvents for workup and column chromatography, such as hexanes (Hex), ethyl acetate (EA), dichloromethane (DCM), and other chemicals such as benzene were obtained from commercial vendors and used without further purification. The NMR solvent $CDCl_3$ was purchased from Cambridge Isotope Laboratories; acetone-d_6 and DMSO-d_6 were purchased from Thermo Fisher Scientific.

Organic solutions were concentrated by rotary evaporation at ca. 12 Torr. All NMR spectra were recorded on a Bruker AM-400 spectrometer. ^{1}H NMR spectra were recorded at 400 MHz, $^{13}C\{^1H\}$ spectra at 100 MHz, and $^{11}B\{^1H\}$ spectra (sodium tetraphenylborate as standard) at 128 MHz; chemical shifts are expressed in parts per million (δ scale) downfield from TMS (δ = 0.00) and are referenced to residual protium in the NMR solvent (DMSO-d_6: δ = 2.50 and $CDCl_3$: δ = 7.26) for ^{1}H NMR, relative to the central $CDCl_3$ (δ = 77.16) and DMSO-d_6 (δ = 39.52) for $^{13}C\{^1H\}$ NMR and sodium tetraphenylborate as standard (δ = -6.61) for $^{11}B\{^1H\}$ NMR. Data are presented as follows: chemical shift, multiplicity (s = singlet, d = doublet, t = triplet, q = quartet, quint = quintet, m = multiplet and/or multiple resonances), coupling constant in Hertz (Hz), integration. FT-IR spectra were recorded on a PerkinElmer Spectrum 100 FT-IR spectrometer. All samples were placed over the detector and crushed using the anvil attached on the Perkin Elmer Spectrum 100 FTIR spectrometer featuring an attenuated total reflection (ATR) sampler equipped with a diamond crystal. Spectra were obtained in the range of 600-4000 cm^{-1}. Melting points were recorded using Mpa161 Digimelt Melting Point apparatus from Stanford Research Systems. Reactions were performed at room temperature (25 °C) or with heat using a silicone oil bath, and reaction condition temperatures were those of the oil bath unless noted otherwise. N_2 gas was purchased from Airgas. Thin-layer chromatography was performed using TLC silica gel 60 F_{254} aluminum sheets from Sorbtech. Flash column chromatography was performed using CombiFlash® R_f from Teledyne ISCO.

UV-vis data were collected on a Cary 60 UV-vis spectrometer (Agilent Technologies, Inc.), and fluorescence data were collected on a HORIBA Fluorolog QM-75-11-C Spectrofluorometer. Variable temperature fluorescence measurements were performed using a Horiba Fluorolog-3 spectrofluorometer equipped with an Oxford cryostat.

Mass Spectrometry

Mass spectrometry experiments were conducted with LTQ XL mass spectrometer (Thermo Fisher Scientific, Waltham, MA) equipped with DART source (IonSense, Saugus, MA). DART source was optimized by varying gas heater temperatures (200-400°C) and setting the helium gas flow rate at 2.0 mL/s. The DART mass spectra were acquired in the range of m/z 100–2000.

Computational Methods. All ground and excited states were studied at the M06-2X/6-311++G(d,p) level. Three different DFT functionals were tested: cam-B3LYP, M06-2X, and

ωB97X-D. The results showed that the M06-2X functional is in best agreement with the trends in experimentally observed maximum absorption wavelengths (Figure S64, Supporting Information). Therefore, M06-2X /6-311++G(d,p) calculations were used for all data reported in this manuscript. The solvent effects were taken into account using the Polarized Continuum Model (PCM). The first three singlet excitations were considered, and the lowest-energy excited singlet state was optimized to calculate the properties reported in this manuscript.
All calculations were performed using the Gaussian 16 program package. [Gaussian 16, Revision C.02, Frisch, M. J.; Trucks, G. W.; Schlegel, H. B.; Scuseria, G. E.; Robb, M. A.; Cheeseman, J. R.; Scalmani, G.; Barone, V.; Petersson, G. A.; Nakatsuji, H.; Li, X.; Caricato, M.; Marenich, A. V.; Bloino, J.; Janesko, B. G.; Gomperts, R.; Mennucci, B.; Hratchian, H. P.; Ortiz, J. V.; Izmaylov, A. F.; Sonnenberg, J. L.; Williams-Young, D.; Ding, F.; Lipparini, F.; Egidi, F.; Goings, J.; Peng, B.; Petrone, A.; Henderson, T.; Ranasinghe, D.; Zakrzewski, V. G.; Gao, J.; Rega, N.; Zheng, G.; Liang, W.; Hada, M.; Ehara, M.; Toyota, K.; Fukuda, R.; Hasegawa, J.; Ishida, M.; Nakajima, T.; Honda, Y.; Kitao, O.; Nakai, H.; Vreven, T.; Throssell, K.; Montgomery, J. A., Jr.; Peralta, J. E.; Ogliaro, F.; Bearpark, M. J.; Heyd, J. J.; Brothers, E. N.; Kudin, K. N.; Staroverov, V. N.; Keith, T. A.; Kobayashi, R.; Normand, J.; Raghavachari, K.; Rendell, A. P.; Burant, J. C.; Iyengar, S. S.; Tomasi, J.; Cossi, M.; Millam, J. M.; Klene, M.; Adamo, C.; Cammi, R.; Ochterski, J. W.; Martin, R. L.; Morokuma, K.; Farkas, O.; Foresman, J. B.; Fox, D. J. Gaussian, Inc., Wallingford CT, 2016.]]

Synthesis protocols

Preparation of methyl 2-(bromomethyl)-6-nitrobenzoate (**1a**)[1]

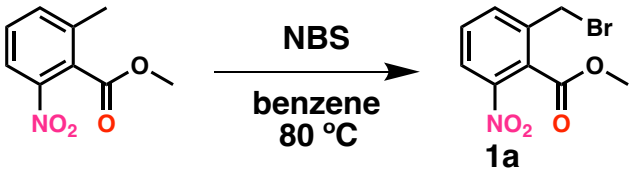

Methyl 2-methyl-6-nitrobenzoate (0.300 g, 1.56 mmol) was placed in a round bottom flask and dissolved in benzene (5.00 mL), followed by the addition of NBS (0.416 g, 2.34 mmol, 1.50 eq.) and benzoyl peroxide (0.006 g, 0.023 mmol, 0.010 eq.). The reaction mixture was allowed to stir at 80 °C under N_2 atmosphere for 24 h. The completion of the reaction was monitored via TLC (Hex: EA 5:1). Once the starting materials were completely consumed, the reaction mixture was allowed to cool to 22 °C then placed in an ice bath for 30 min. A colorless precipitate, succinimide, formed and was removed by gravity filtration. The excess benzene was removed under reduced pressure, and the orange residue was purified via flash column chromatography using (Hex: EA 5:1) to produce the product (**1a**), a white solid. (0.430 g, 1.57 mmol, 75.0 %). R_f: 0.45 (Hex:EA 5:1). M.p.: 81°C - 85°C. ^{1}H NMR (400 MHz, $CDCl_3$, 25 °C): δ (ppm) 8.07 (dd, *J* = 8.2, 1.1 Hz, 1H), 7.77 (dd, *J* = 7.8, 1.1 Hz, 1H), 7.59 (dd, *J* = 8.1 Hz, 7.9 Hz, 1H), 4.57 (s, 2H), 3.99 (s, 3H). ^{13}C {^{1}H} NMR (100 MHz, $CDCl_3$, 25 °C): δ (ppm) 165.60, 147.16, 137.63, 135.75, 130.71, 128.93, 124.24, 53.51, 27.89.

Preparation of methyl 2-(bromomethyl)-5-nitrobenzoate (**1b**)[2]

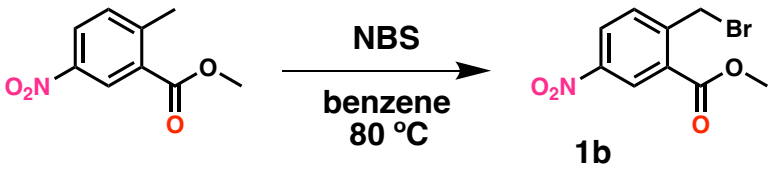

Following the experimental procedure of compounds **1a** presented above, methyl 2-methyl-5-nitrobenzoate (2.50 g, 12.8 mmol) was placed in a round bottom flask and dissolved in benzene (30.0 mL) followed by the addition of NBS (3.42 g, 19.2 mmol, 1.50 eq.) and benzoyl peroxide (0.031 g, 0.128 mmol, 0.010 eq.). The reaction mixture was allowed to stir at 80 °C under N_2 atmosphere for 24 h, and the completion of the reaction was monitored via TLC (Hex: EA 5:1). Once the starting materials were completely consumed, the reaction mixture was allowed to cool to 22 °C then placed in an ice bath for 10 min. Succinimide, a colorless precipitate formed, was removed by gravity filtration. The excess benzene was removed under reduced pressure, and the residue was purified via flash column chromatography using 5:1 Hex:EA to produce the product (**1b**), a white solid. (1.52 g, 5.55 mmol, 43.0 %). R_f: 0.45 (Hex:DCM 1:1). M.p.: 76°C -81°C. ^{1}H NMR (400 MHz, $CDCl_3$) δ 8.81 (d, *J* = 2.5 Hz, 1H), 8.33 (dd, *J* = 8.5, 2.5 Hz, 1H), 7.68 (d, *J* = 8.5 Hz, 1H), 5.00 (s, 2H), 4.01 (s, 3H). ^{13}C{^{1}H} NMR (101 MHz, $CDCl_3$, 25 °C) δ 165.11, 147.50, 146.17, 133.05, 130.35, 127.00, 126.51, 53.11, 29.32.

Preparation of methyl 2-(bromomethyl)-4-nitrobenzoate (**1c**)[3]

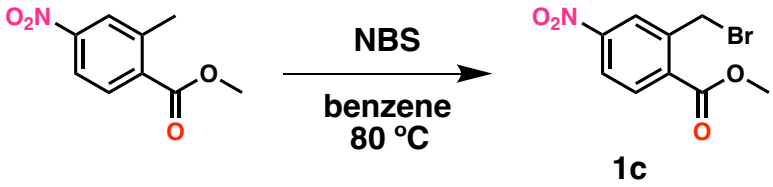

Following the experimental procedure of compounds **1a** presented above, methyl 2-methyl-4-nitrobenzoate (0.729 g, 3.74 mmol) was placed in a round bottom flask and dissolved in benzene (10.0 mL) followed by the addition of NBS (0.997 g, 5.60 mmol, 1.50 eq.) and benzoyl peroxide (0.009 g, 0.037 mmol, 0.010 eq.). The reaction mixture was allowed to stir at 80 °C under N_2 atmosphere for 24 h, and the completion of the reaction was monitored via TLC (Hex: DCM 1:1). Once the starting materials were completely consumed, the reaction mixture was allowed to cool to 22 °C then placed in an ice bath for 30 min. Succinimide, a colorless precipitate formed, was removed by gravity filtration. The excess benzene was removed under reduced pressure and the residue was purified via flash column chromatography using 1:1 Hex:DCM to produce the product (**1c**), a white solid. (0.555 g, 2.03 mmol, 54.0 %). R_f: 0.45 (Hex:DCM 1:1). M.p.: 65°C - 69°C. ^{1}H NMR (400 MHz, $CDCl_3$, 25 °C): δ 8.34 (d, *J* = 2.3 Hz, 1H), 8.21 (dd, *J* = 8.6, 2.3 Hz, 1H), 8.12 (d, *J* = 8.6 Hz, 1H), 4.97 (s, 2H), 4.01 (s, 3H). ^{13}C {^{1}H} NMR (100 MHz, $CDCl_3$, 25 °C): δ (ppm) 165.00, 150.41 145.18, 131.64, 129.84, 126.75, 123.76, 53.36, 35.58.

Preparation of methyl 2-(bromomethyl)-3-nitrobenzoate (**1d**)[4]

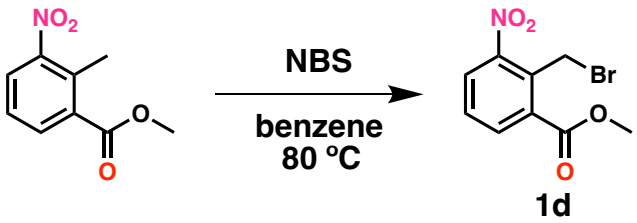

Following the experimental procedure of compounds **1a** presented above, methyl 2-methyl-3-nitrobenzoate (6.00 g, 30.7 mmol), benzene (62.0 mL), NBS (8.21 g, 46.1 mmol, 1.50 eq.) and benzoyl peroxide (0.112 g, 0.461 mmol, 0.010 eq.) were placed in a round bottom flask and reacted together for 48 h under N_2 atmosphere. Following, the completion of the reaction, the excess benzene was removed under reduced pressure. The organic layer extracted with EA (3x30.0 mL), washed with brine, dried over $MgSO_4$, and filtered. The product was concentrated in vacuo to yield the product (**1d**) as an orange solid without any further purification (7.53 g, 27.5 mmol, 89.0 %). R_f: 0.43 (Hex:EA 5:1). M.p.: 67 °C – 71 °C. ^{1}H NMR (400 MHz, $CDCl_3$, 25 °C): δ 8.10 (dd, *J* = 7.9, 1.4 Hz, 1H), 7.96 (dd, *J* = 8.1, 1.3 Hz, 1H), 7.54 (dd, *J* = 8.1 Hz, 7.9 Hz, 1H), 5.16 (s, 2H), 4.00 (s, 3H). ^{13}C {^{1}H} NMR (100 MHz, $CDCl_3$, 25 °C): δ (ppm) 166.03, 150.74, 134.86, 132.85, 132.54, 129.25, 127.98, 53.24, 22.86.

Preparation of 7-nitroisoindolin-1-one (**2a**)

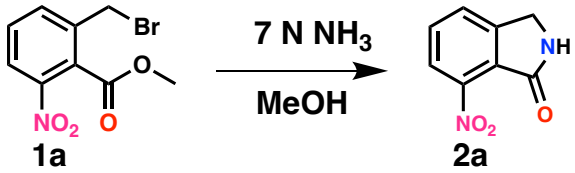

A round-bottom flask was charged with brominated product (**1a**) (2.00 g, 7.30 mmol), and 7 N NH_3 in MeOH (35.0 mL). The reaction mixture was placed in an ice bath and stirred overnight at 0 °C under N_2 atmosphere while slowly warming up to room temperature. The completion of the reaction was indicated via TLC (Hex:EA 5:1). The precipitate formed was filtered and washed with cold MeOH to yield product (**2a**) as a white powder without any further purification (0.856 g; 4.81 mmol, 66.0 %). M.p.: 223 °C - 227 °C. ^{1}H NMR (400 MHz, $CDCl_3$, 25 °C): δ (ppm) 7.80-7.70 (m, 3H), 6.93 (s, 1H, NH), 4.53 (s, 2H). ^{13}C {^{1}H} NMR (100 MHz, DMSO-d_6, 25 °C): δ (ppm) (101 MHz,) δ 165.42, 146.77, 145.99, 132.59, 127.64, 123.25, 121.56, 44.76. ATR-FTIR (cm^{-1}): 3173 (w), 3085 (w), 2876 (w), 1703 (s), 1619 (w), 1524 (s), 1468 (w), 1354 (s), 1280 (w), 1186 (w), 1155 (w), 1048 (w), 956 (w), 795 (w), 725 (s). HRMS (DART-MS) m/z: Calcd for $C_8H_7N_2O_3$, 179.0456 $(M + H)^+$; Found: 179.0833 $(M + H)^+$.

Preparation of 6-nitroisoindolin-1-one (**2b**)[2]

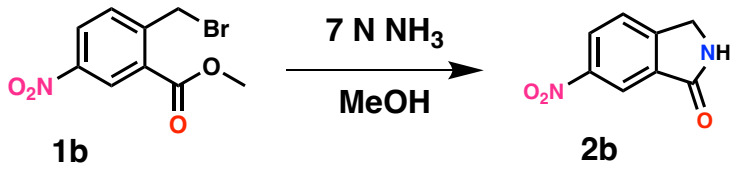

Following the experimental procedure of compounds **2a** presented above, a round-bottom flask was charged with the brominated product (**1b**) (1.50 g, 5.47 mmol), and 7 N NH_3 in MeOH (35.0 mL). The reaction mixture was placed in an ice bath and stirred overnight at 0 °C under N_2 atmosphere while slowly warming up to room temperature. The completion of the reaction was indicated by TLC (Hex:EA, 5:1). The precipitate formed was filtered and washed with cold MeOH to yield product (**2b**) as a white powder (0.430 g, 0.440 mmol, 44.0 %). mp 252–255 °C. ^{1}H NMR (400 MHz, $CDCl_3$) δ 8.73 (d, *J* = 1.6 Hz, 1H), 8.47 (dd, *J* = 8.2 Hz, 1.8 Hz, 1H), 7.67 (d, *J* = 8.2 Hz, 1H), 6.46 (s, 1H, NH), 4.59 (s, 2H). ^{13}C{^{1}H} NMR (101 MHz, DMSO-*d*$_6$, 25 °C) δ 167.94, 150.64, 147.80, 134.04, 126.25, 125.50, 117.73, 45.40

Preparation of 5-nitroisoindolin-1-one (**2c**)[5]

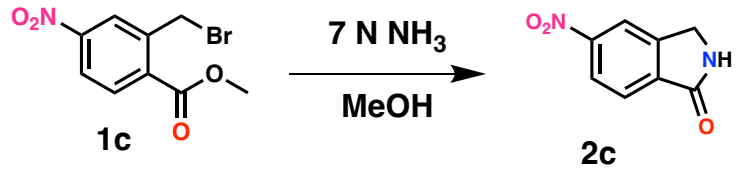

Following the experimental procedure of compounds **2a** presented above, a round-bottom flask was charged with the brominated product (**1c**) (2.00 g, 7.30 mmol), and 7 N NH_3 MeOH (35.0 mL). The reaction mixture was placed in an ice bath and stirred overnight at 0 °C under N_2 atmosphere while slowly warming up to room temperature. The completion of the reaction was confirmed via silica TLC in (Hex:EA 5:1). The precipitate formed was filtered and washed with MeOH to yield product (**2c**) as a white powder (0.950 g, 5.33 mmol, 73.0 %). M.p. 259 °C – 263 °C. ^{1}H NMR (400 MHz, $CDCl_3$, 25 °C): δ (ppm) 8.37 (m, 2H), 8.04 (d, J= 8.8 Hz, 1H), 6.67 (s, 1H, NH), 4.59 (s, 2H). ^{13}C {^{1}H} NMR (100 MHz, $CDCl_3$, 25 °C): δ (ppm) 168.79, 150.47, 144.19, 137.26, 125.07, 123.90, 118.96, 45.40.

Preparation of 4-nitroisoindolin-1-one (**2d**)[6]

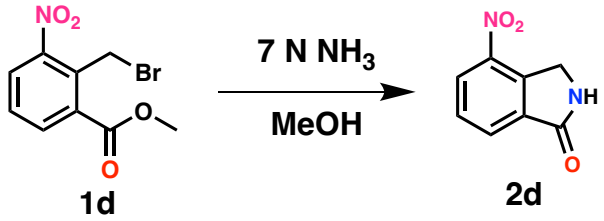

Following the experimental procedure of compound **2a** presented above, a round bottom flask was charged with brominated product (**1d**) (4.00 g, 14.6 mmol) and 7 N NH_3 MeOH (70.0 mL). The reaction mixture was placed in an ice bath and stirred overnight at 0 °C under N_2 atmosphere while slowly warming up to room temperature. The completion of the reaction was confirmed via TLC in (Hex:EA 5:1). The precipitate formed was filtered and washed with MeOH to yield a white powder as the crude product (**2d**). (1.86 g, 10.4 mmol, 72.0 %). M.p.: 245°C - 250°C. ^{1}H NMR (400 MHz, $CDCl_3$, 25 °C): δ 8.46 (dd, *J* = 8.2, 0.9 Hz, 1H), 8.23 (dd, *J* = 7.8, 0.9 Hz, 1H), 7.74 (t, *J* = 8.2 Hz, 8.1 Hz, 1H), 6.60 (s, 1H, NH), 4.95 (s, 2H). ^{13}C {^{1}H} NMR (100 MHz, DMSO-d_6, 25 °C): δ (ppm) 167.76, 143.46, 139.44, 135.84, 129.87, 129.54, 126.67, 46.07. ATR-FTIR (cm^{-1}): 3158 (w), 3084 (w), 2868 (w), 1700 (w), 1667 (m), 1631 (w), 1524 (m), 1443 (w), 1342 (s), 1275 (w), 1179 (w), 1052 (w), 915 (w), 824 (w), 768 (w), 728 (s). HRMS (DART-MS) m/z: Calcd for $C_8H_7N_2O_3$, 179.0456 $(M + H)^+$; Found: 179.1667 $(M + H)^+$.

5-hydroxy-8-nitrobenzo[3,4][1,2]azaborinino[6,1-a]isoindol-7(5H)-one (**8**)

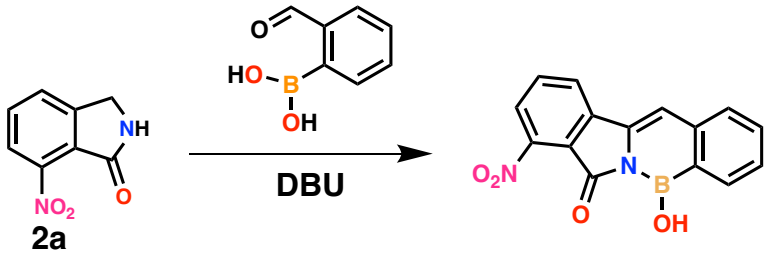

The isoindolinone ring closure product (**2a**) (0.300 g, 1.68 mmol, 1.25 eq.) and (2-formylphenyl) boronic acid (0.200 g, 1.34 mmol), were placed in a round bottom flask and dissolved in ethanol (6.72 mL, 200 proof). DBU (1.53 g, 10.1 mmol, 1.50 mL, 6.00 eq. of **2a**) was added to the mixture resulting in a white cloudy solution. The cloudy reaction mixture was allowed to stir at reflux under N_2 atmosphere for 48 h. After 48 h, the color of the solution changed from cloudy to homogeneous orange mixture. The reaction mixture was allowed to cool to room temperature and was placed in an ice-water bath at 0 °C for 15 min, followed by the addition of HCl (15.7 mL, 1 M) dropwise while the reaction mixture stirred vigorously resulting in an orange precipitate. The mixture was then cooled below 0 °C for 24 h in a freezer. After 24 h, the precipitate was vacuum-filtered and washed with cold HCl (1 M) and DI H_2O. Thereafter, allowed to dry overnight to produce (**8**) as an orange solid. (0.342 g; 1.17 mmol, 70.0 %). M.p.: Decomposes at 203.0 °C. ^{1}H NMR (400 MHz, $CDCl_3$, 25 °C): δ (ppm) 8.19 (d, J= 7.3 Hz, 1H), 8.05 (dd, J=7.6 Hz, 0.7 Hz, 1H), 7.97 (s, 1H, OH), 7.88 (dd, J= 7.9 Hz, 0.7 Hz, 1H), 7.84 (dd, J=7.8 Hz, 7.7 Hz, 1H), 7.62 (td, J= 7.5 Hz, 1.1 Hz, 1H), 7.55 (d, J= 7.7 Hz, 1H), 7.48 (td, J= 7.4 Hz, 1.1 Hz, 1H), 6.99 (s, 1H). ^{13}C {^{1}H} NMR (100 MHz, DMSO-d_6, 25 °C): δ (ppm) 167.52, 146.58, 140.92, 140.84, 135.78, 133.88, 133.67, 132.67, 128.82, 127.80, 125.53, 124.10, 119.90, 109.49. ^{11}B {^{1}H} NMR (sodium tetraphenyl borate as standard, 128 MHz, Acetone-d_6, 25 °C): δ (ppm) 30.7. ATR-FTIR (cm^{-1}): 3458 (w), 3057 (w), 1706 (s), 1621 (w), 1531 (s), 1478 (w), 1432 (w), 1351 (s), 1288 (s), 1173 (w), 1132 (w), 1095 (m), 1033 (w), 982

(w), 924 (m), 884 (m), 844 (w), 819 (m), 789 (w), 764 (w), 705 (s). HRMS (DART-MS) m/z: Calcd for $C_{15}H_{10}BNO_2$, 293.0733 $(M + H)^+$; Found: 293.1667 $(M + H)^+$.

Preparation of 5-hydroxy-9-nitrobenzo[3,4][1,2]azaborinino[6,1-*a*]isoindol-7(5*H*)-one (**9**)[2,7]

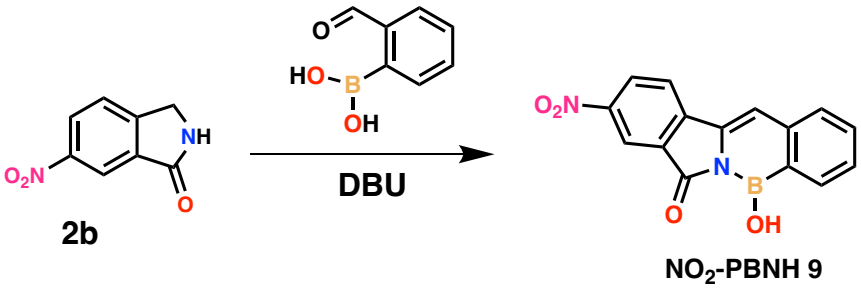

Following the experimental procedure of compound **8** presented above, the isoindolinone ring closure product (**2b**) (1.00 g, 5.61 mmol, 1.25 eq.) and (2-formylphenyl) boronic acid (0.670 g, 4.49 mmol), were placed in a round bottom flask and dissolved in ethanol (30.0 mL, 200 proof). DBU (4.10 g, 26.9 mmol, 4.00 mL, 6.00 eq. of **2b**) was added to the mixture, resulting in a dark red solution. The red reaction mixture was allowed to stir at reflux under N_2 atmosphere for 48 h. After 48 h, the color of the solution changed from red to homogenous orange reaction mixture. The reaction mixture was allowed to cool to room temperature and was placed in an ice-water bath for 15 min, followed by the addition of HCl (40.0 mL, 1 M) dropwise while the reaction mixture stirred vigorously, resulting in an orange reaction mixture. The mixture was then cooled below 0 °C for 24 h in a freezer. After 24 h, the precipitate was vacuum-filtered and washed with cold HCl (1 M) followed by DI H_2O. Following, trituration was performed in hot ethanol and vacuum-filtered to produce **9** as a dark red solid (0.650 g, 2.23 mmol, 50.0 %). mp 240–245 °C. ^{1}H NMR (400 MHz, $CDCl_3$, 25 °C) δ 8.77 (s, 1H), 8.55 (dd, *J* = 8.3 Hz, 1.3 Hz, 1H), 8.21 (d, *J* = 7.5 Hz, 1H), 7.95 (d, *J* = 8.3 Hz, 1H), 7.86 (s, 1H, OH), 7.64 (td, *J* = 7.5 Hz, 0.7 Hz, 1H), 7.58 (d, *J* = 7.8 Hz, 1H), 7.50 (td, 1H), 7.07 (s, 1H).^{13}C {^{1}H} NMR (100 MHz, DMSO-d_6, 25 °C): δ (ppm) 170.3, 148.6, 143.6, 140.9, 134.3, 133.8, 132.7, 130.2, 129.4, 129.1, 128.1, 122.9, 119.9, 111.1. ^{11}B {^{1}H} NMR (sodium tetraphenyl borate as standard, 128 MHz, acetone-d_6, 25 °C): δ (ppm) 30.2.

Preparation of 5-hydroxy-10-nitrobenzo[3,4][1,2]azaborinino[6,1-a]isoindol-7(5H)-one (**10**)

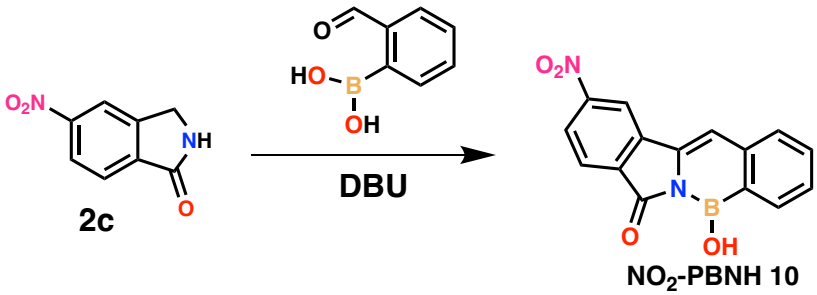

Following the experimental procedure of compound **8** presented above, the isoindolinone ring closure product (**2c**) (0.500 g, 2.81 mmol, 1.25 eq.) and (2-formylphenyl) boronic acid

(0.340 g, 2.25 mmol), were placed in a round bottom flask and dissolved in ethanol (15.0 mL, 200 proof). DBU (2.57 g, 16.86 mmol, 2.50 mL, 6.00 eq. of **2c**) was added to the mixture resulting in a dark red solution. The red reaction mixture was allowed to stir at reflux under N_2 atmosphere for 48 h. After 48 h, the color of the solution changed from red to orange. The reaction mixture was allowed to cool to room temperature and was placed in an ice-water bath for 15 min, followed by the addition of HCl (26.2 mL, 1 M) dropwise while the reaction mixture stirred vigorously, resulting in an orange reaction mixture. The mixture was then cooled below 0 °C for 24 h. After 24 h, the precipitate was vacuum-filtered and washed with cold DI H_2O. Following, trituration was performed in hot ethanol and vacuum-filtered to produce **10** as a dark red solid. (0.424 g, 1.45 mmol, 81.0 %). M.p.: Decomposes at 209°C. ^{1}H NMR (400 MHz, $CDCl_3$, 25 °C): δ (ppm) 8.64 (d, J= 1.7 Hz, 1H), 8.35 (dd, J= 8.4 Hz, 1.6 Hz, 1H), 8.20 (d, J= 7.3, 1H), 8.08 (d, J= 8.3 Hz, 1H), 7.87 (s, 1H, OH), 7.66 (td, J= 7.6 Hz, 1.0 Hz, 1H), 7.57 (d, J= 7.8 Hz, 1H), 7.47 (td, J= 7.2 Hz, 0.8 Hz, 1H), 7.03 (s, 1H). ^{13}C {^{1}H} NMR (100 MHz, $CDCl_3$, 25 °C): δ (ppm) 172.51, 151.87, 140.55, 139.73, 133.72, 133.44, 132.86, 132.75, 128.84, 128.08, 126.00, 124.18, 116.14, 109.99. ^{11}B {^{1}H} NMR (sodium tetraphenyl borate as standard, 128 MHz, acetone-d_6, 25 °C): δ (ppm) 30.6. ATR-FTIR (cm^{-1}): 3456 (w), 3105 (w), 1697 (s), 1644 (w), 1622 (w), 1603 (w), 1529 (s), 1456 (w), 1352 (s), 1289 (m), 1197 (w), 1162 (w), 1113 (w), 1030 (w), 971 (w), 859 (w), 793 (w), 760 (w), 710 (s), 683 (w). HRMS (DART-MS) m/z: Calcd for $C_{15}H_{10}BNO_2$, 293.0733 $(M + H)^+$; Found: 293.2500 $(M + H)^+$.

Preparation of 5-hydroxy-11-nitrobenzo[3,4][1,2]azaborinino[6,1-a]isoindol-7(5H)-one (**11**)

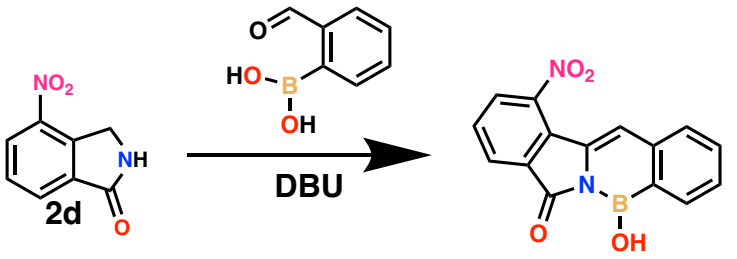

NO_2-PBNH 11

Following the experimental procedure of compound **8** presented above, the isoindolinone ring closure product (**2d**) (0.400 g, 2.25 mmol, 1.25 eq.) and (2-formylphenyl) boronic acid (0.270 g, 1.81 mmol), were placed in a round bottom flask and dissolved in ethanol (10.0 mL, 200 proof). DBU (2.06 g, 13.56 mmol, 2.0 mL, 6.00 eq. of **2d**) was added to the mixture resulting in a dark red solution. The red reaction mixture was allowed to stir at reflux under N_2 atmosphere for 48 h. After 48 h, the color of the solution changed from red to orange. The reaction mixture was allowed to cool to room temperature and was placed in an ice-water bath for 15 min, followed by the addition of HCl (21.1 mL, 1 M) dropwise while the reaction mixture stirred vigorously resulting in an orange reaction mixture. The mixture was then cooled below 0 °C for 24 h. After 24 h, the precipitate was filtered and washed with HCl (1 M) followed by cold DI H_2O. Following, the solid was allowed to dry overnight to produce **11** as a green solid (0.462 g; 1.58 mmol, 88.0 %). M.p: Decomposed at 206°C. ^{1}H NMR (400 MHz, $CDCl_3$, 25 °C): δ (ppm) 8.31 (dd, J= 8.0 Hz, 0.97 Hz, 1H), 8.25 – 8.15 (m, 3H), 7.68-7.60 (m, 4H),

7.49 (td, J= 7.3 Hz, 1.4 Hz, 1H). ^{13}C {^{1}H} NMR (100 MHz, $CDCl_3$, 25 °C): δ (ppm) 172.36, 144.45, 140.79, 133.33, 132.74, 132.39, 130.67, 130.36, 130.15, 130.01, 129.89, 129.53, 128.65, 117.28. ^{11}B {^{1}H} NMR (sodium tetraphenyl borate as standard, 128 MHz, acetone-d6, 25 °C): δ (ppm) 30.1. ATR-FTIR (cm^{-1}): 3455 (s), 3092 (w), 1704 (s), 1622 (m), 1528 (s), 1451 (w), 1396 (w), 1352 (m), 1328 (w), 1289 (m), 1175 (w), 1103 (w), 1080 (m), 1030 (w), 978 (m), 892 (w), 857 (w), 765 (s), 711 (s), 672 (w). HRMS (DART-MS) m/z: Calcd for $C_{15}H_{10}BNO_2$, 293.0733 $(M + H)^+$; Found: 293.1667 $(M + H)^+$.

NMR spectral characterization

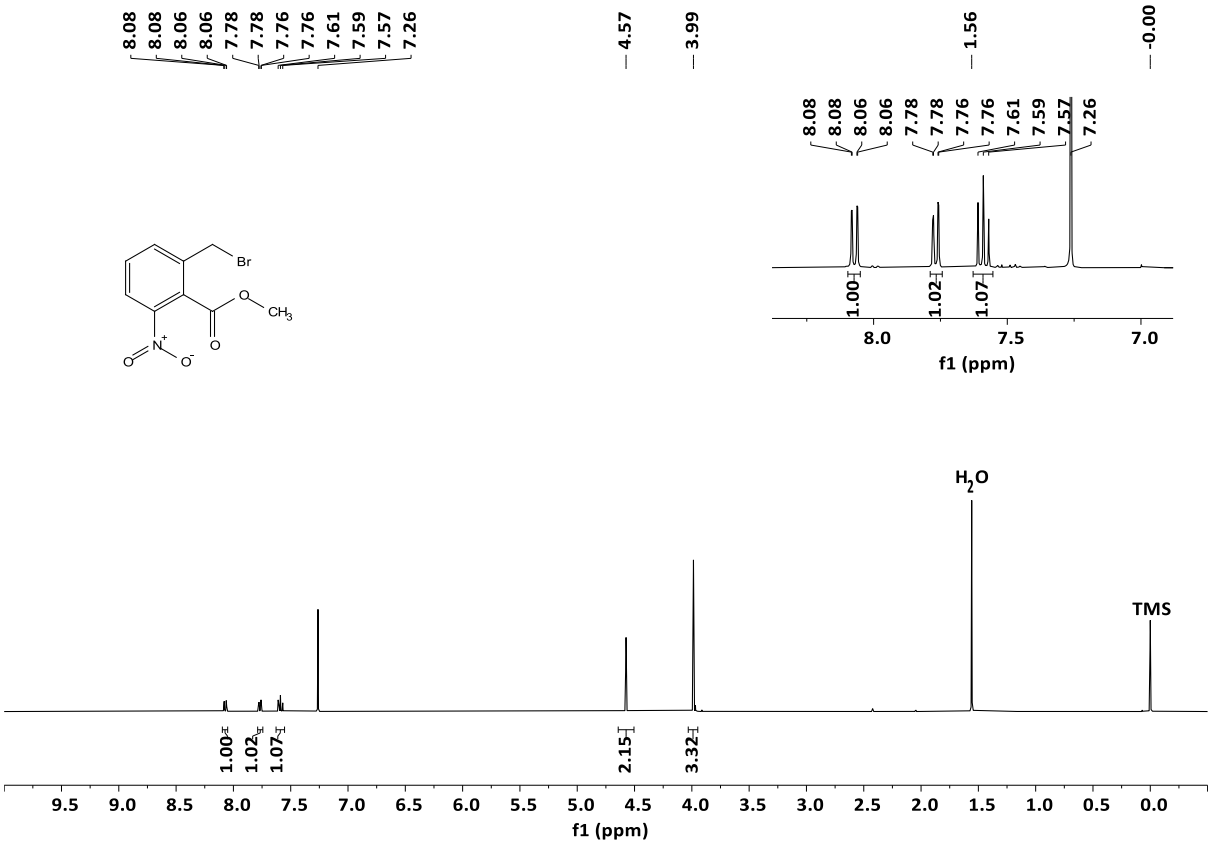

Figure S1.[1]H NMR spectrum (400 MHz) of **1a** in $CDCl_3$ at 25 °C

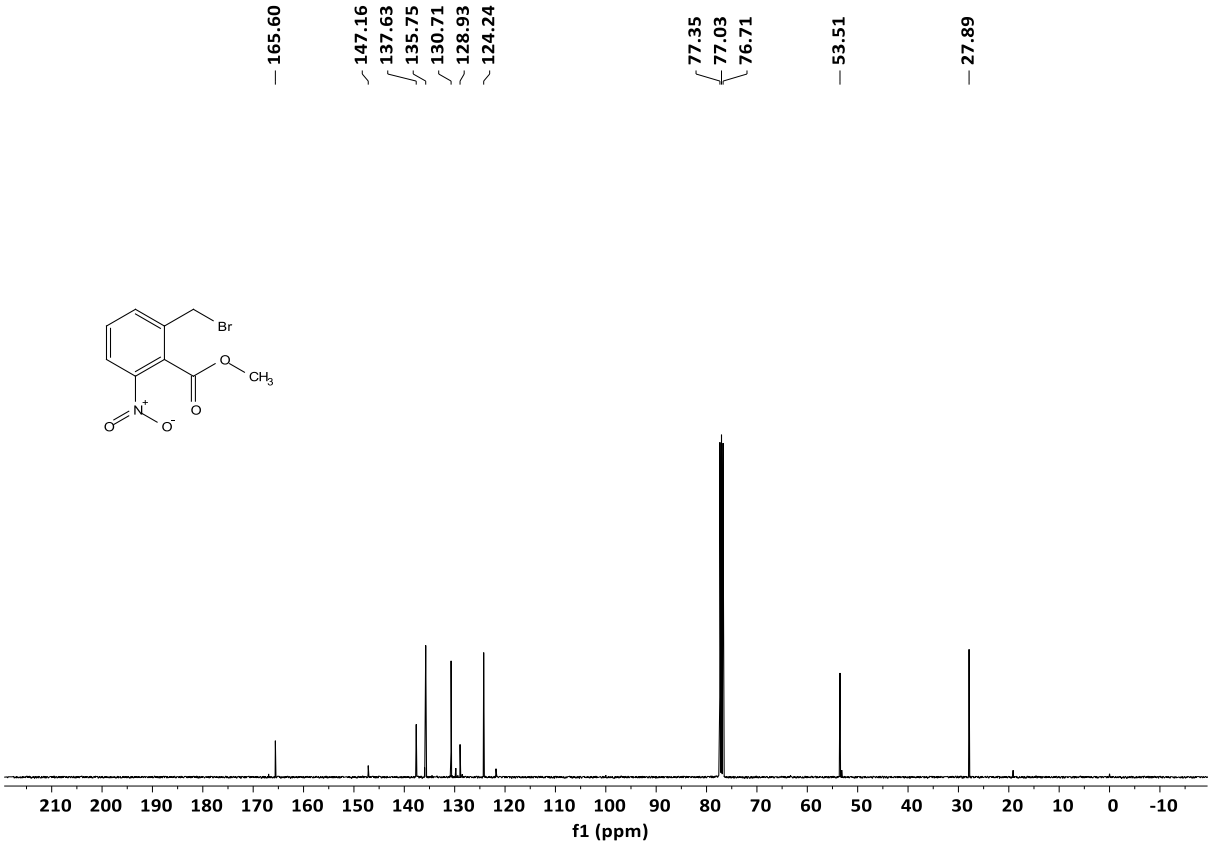

Figure S2.[13]C {[1]H} NMR spectrum (100 MHz) of **1a** in $CDCl_3$ at 25 °C

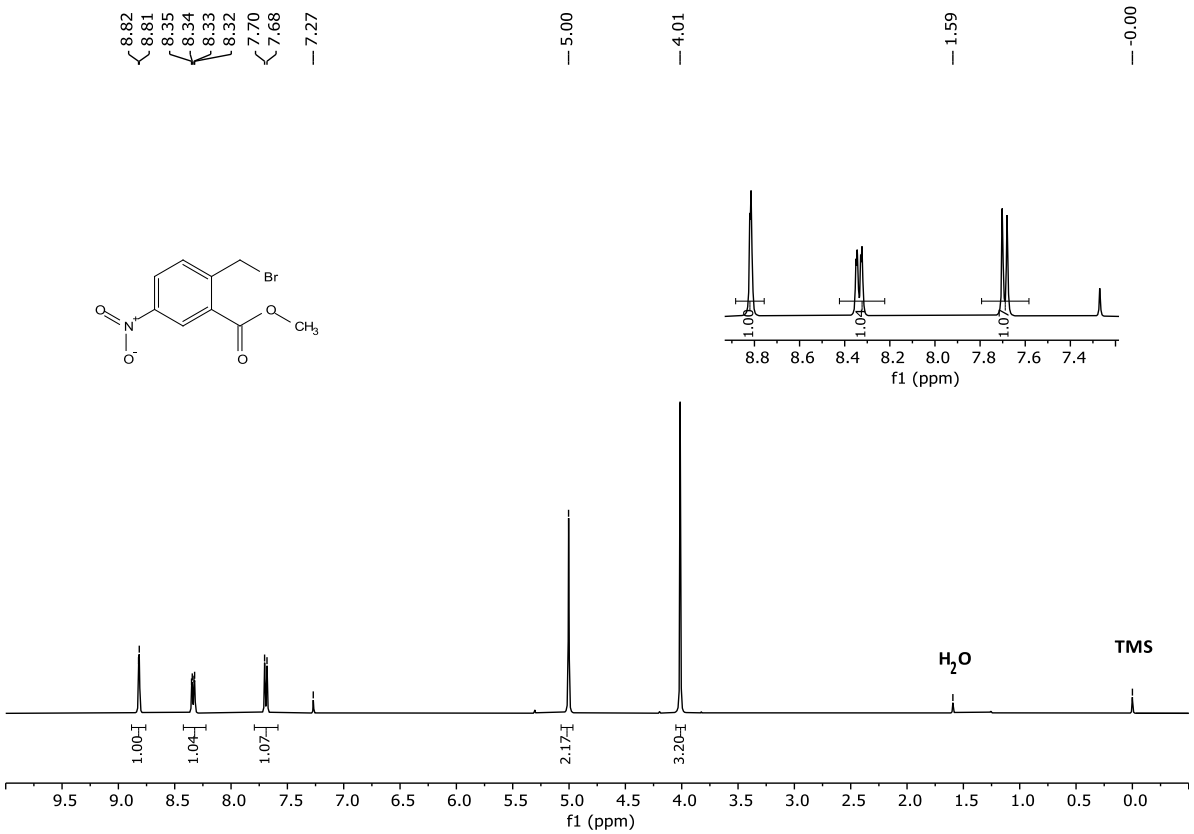

Figure S3. ^{1}H NMR spectrum (400 MHz) of **1b** in $CDCl_3$ at 25 °C

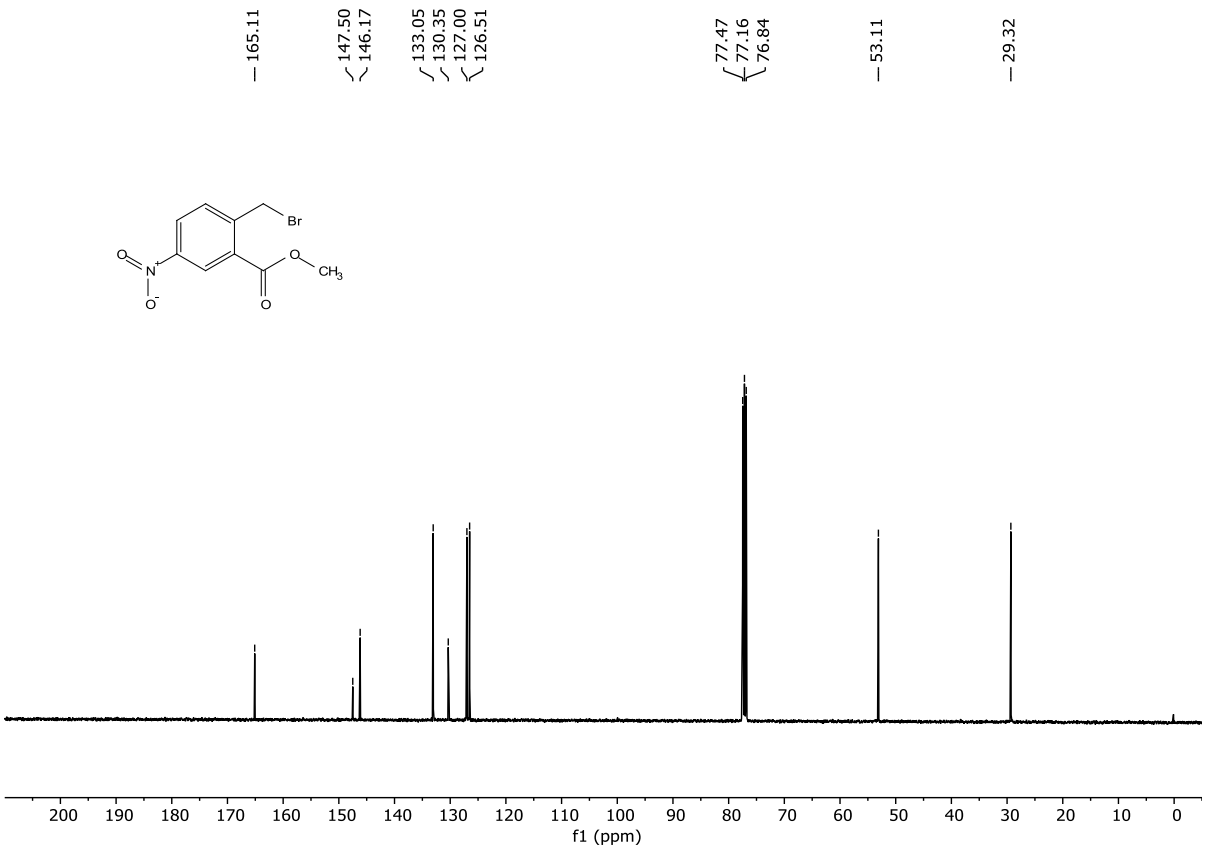

Figure S4. ^{13}C {^{1}H} NMR spectrum (100 MHz) of **1b** in $CDCl_3$ at 25 °C

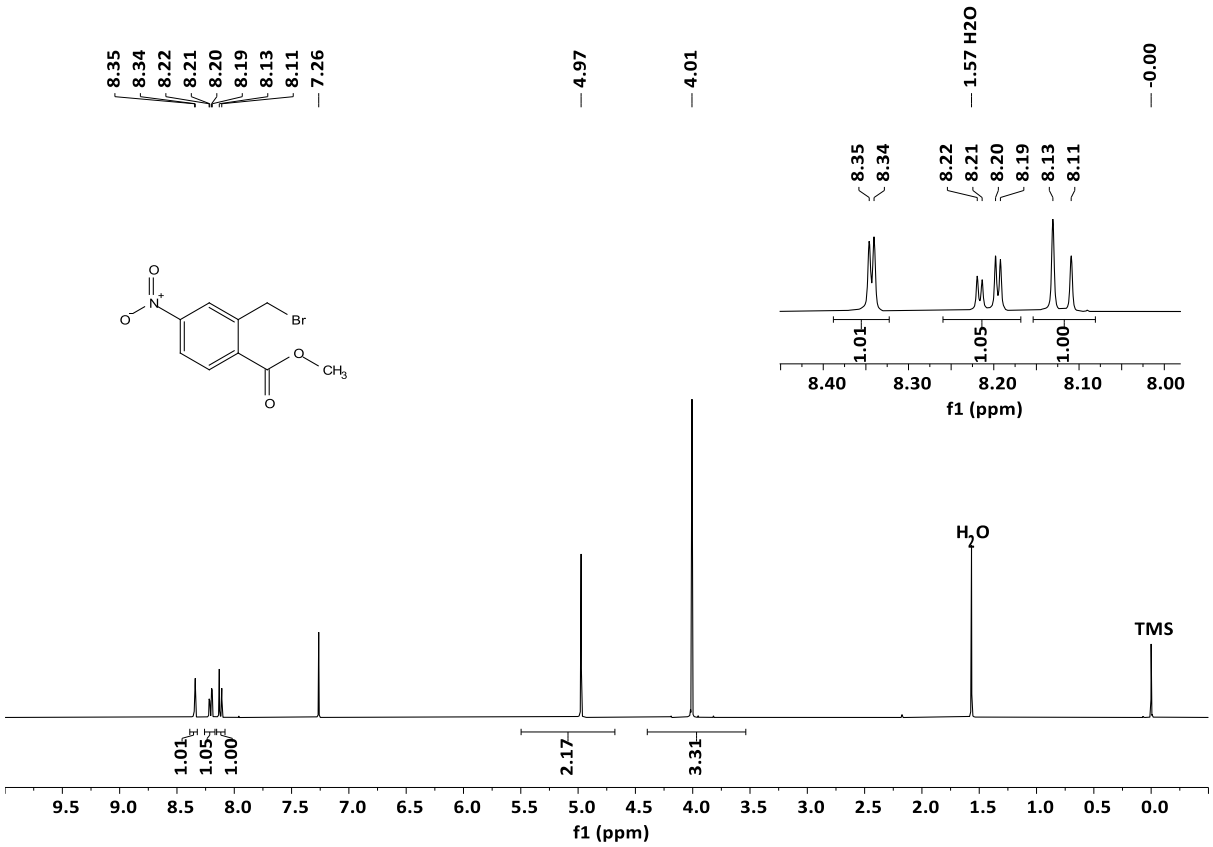

Figure S5. ^{1}H NMR spectrum (400 MHz) of **1c** in $CDCl_3$ at 25 °C

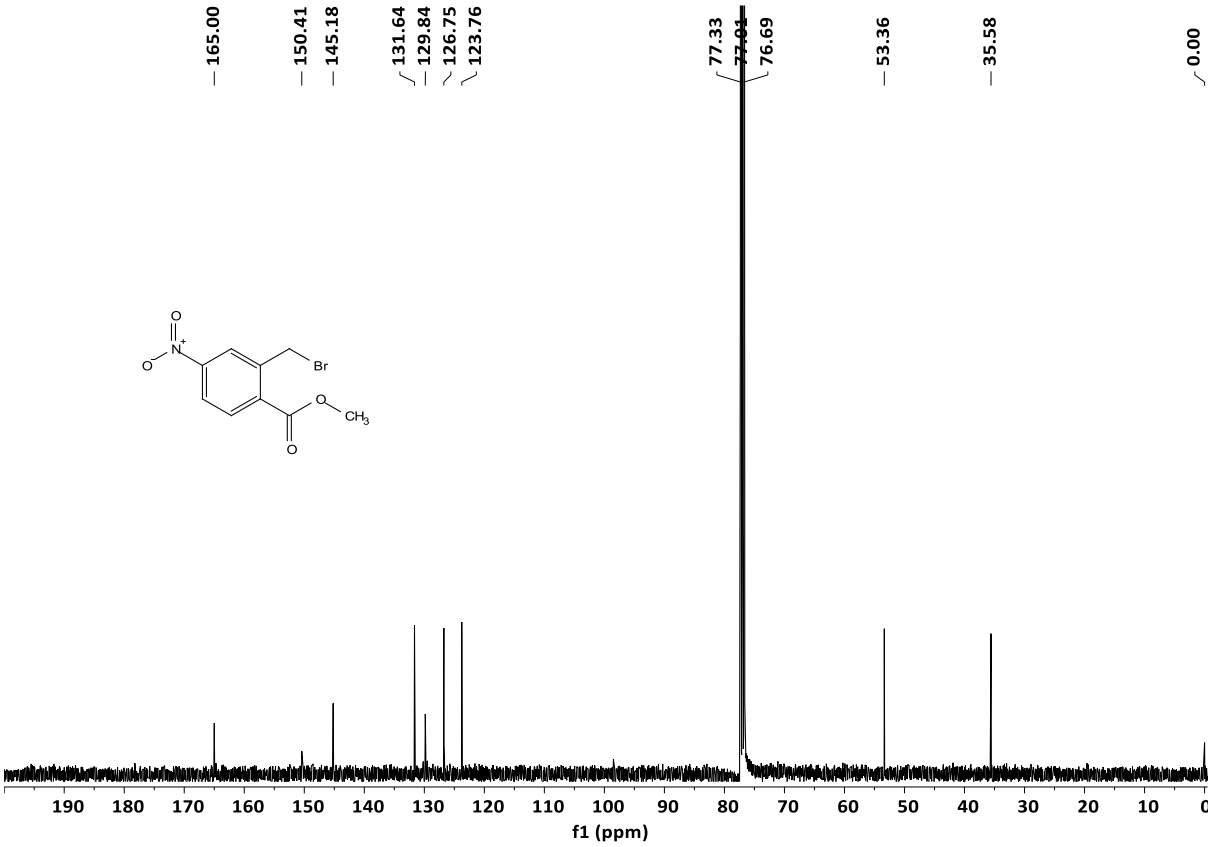

Figure S6. ^{13}C {^{1}H} NMR spectrum (100 MHz) of **1c** in $CDCl_3$ at 25 °C

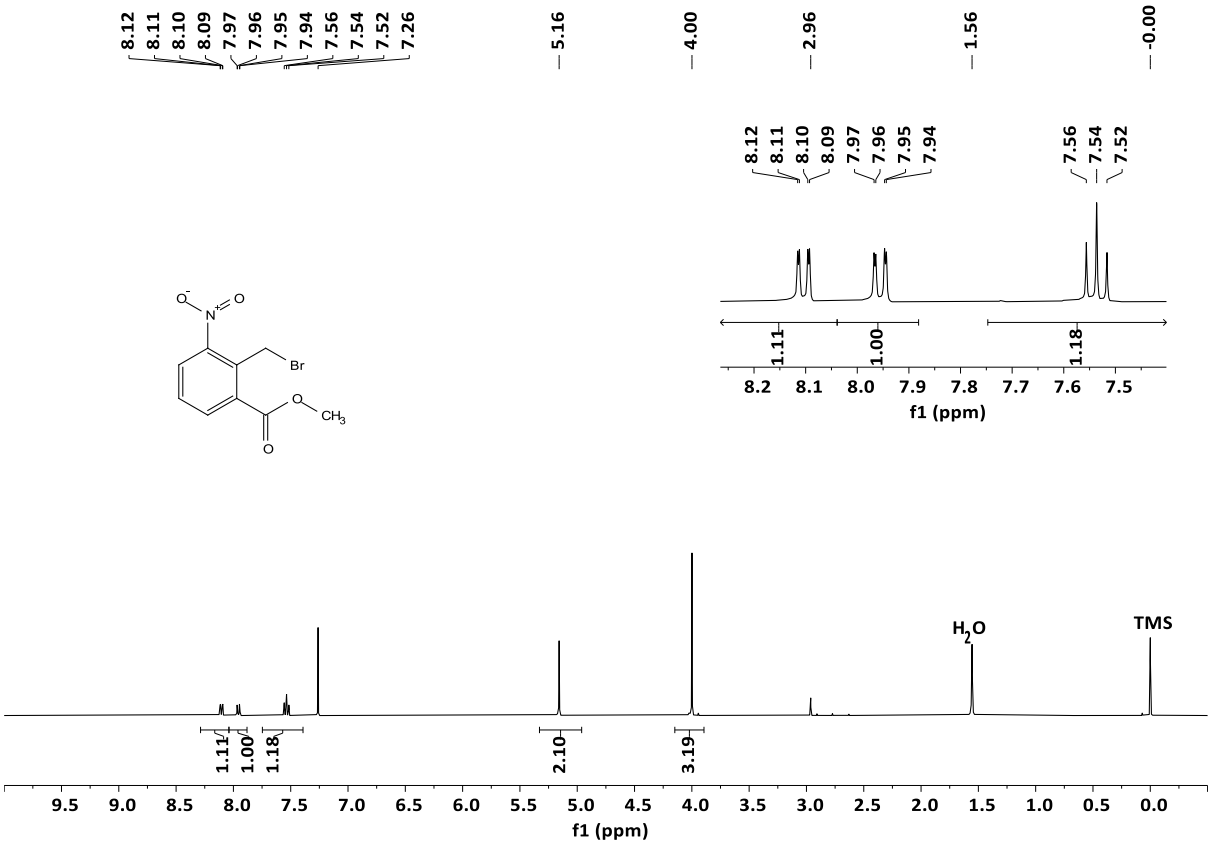

Figure S7.[1]H NMR spectrum (400 MHz) of **1d** in $CDCl_3$ at 25 °C

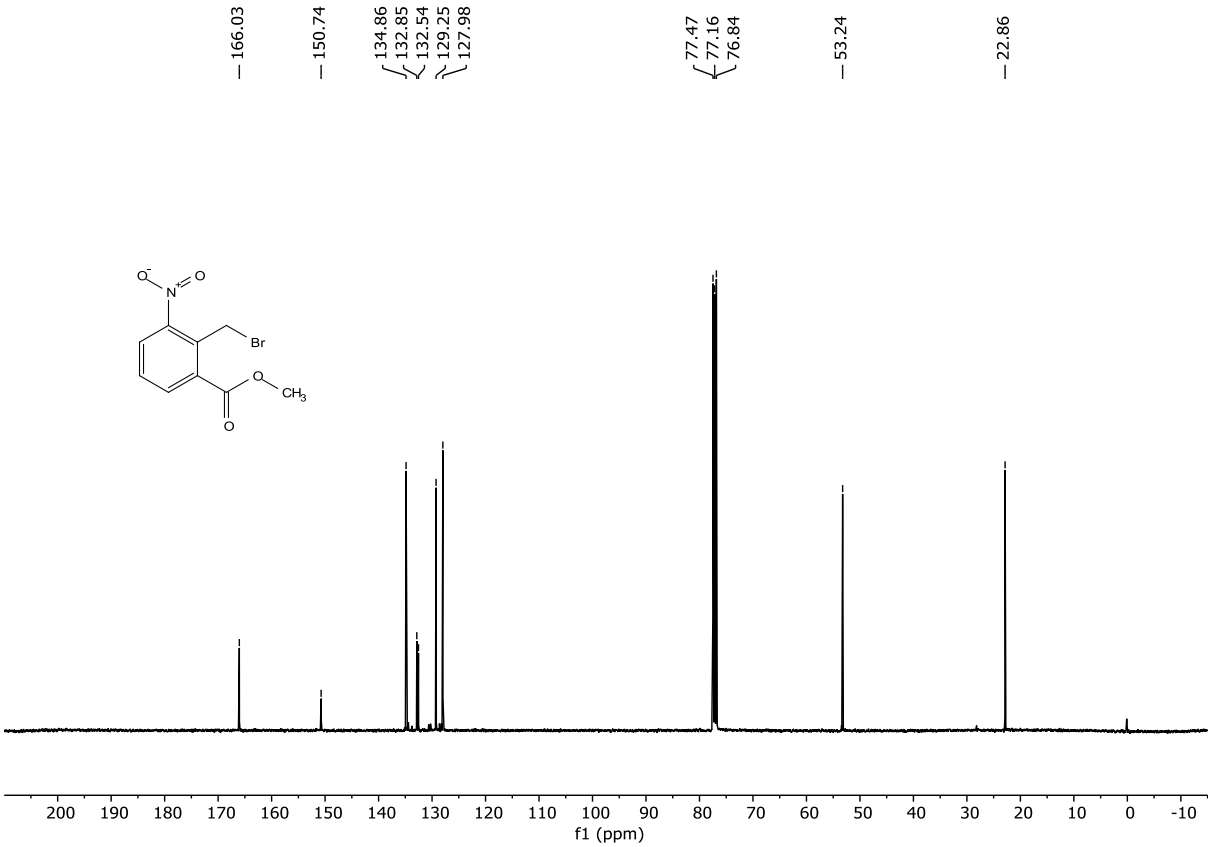

Figure S8.[13]C {[1]H} NMR spectrum (100 MHz) of **1d** in $CDCl_3$ at 25 °C

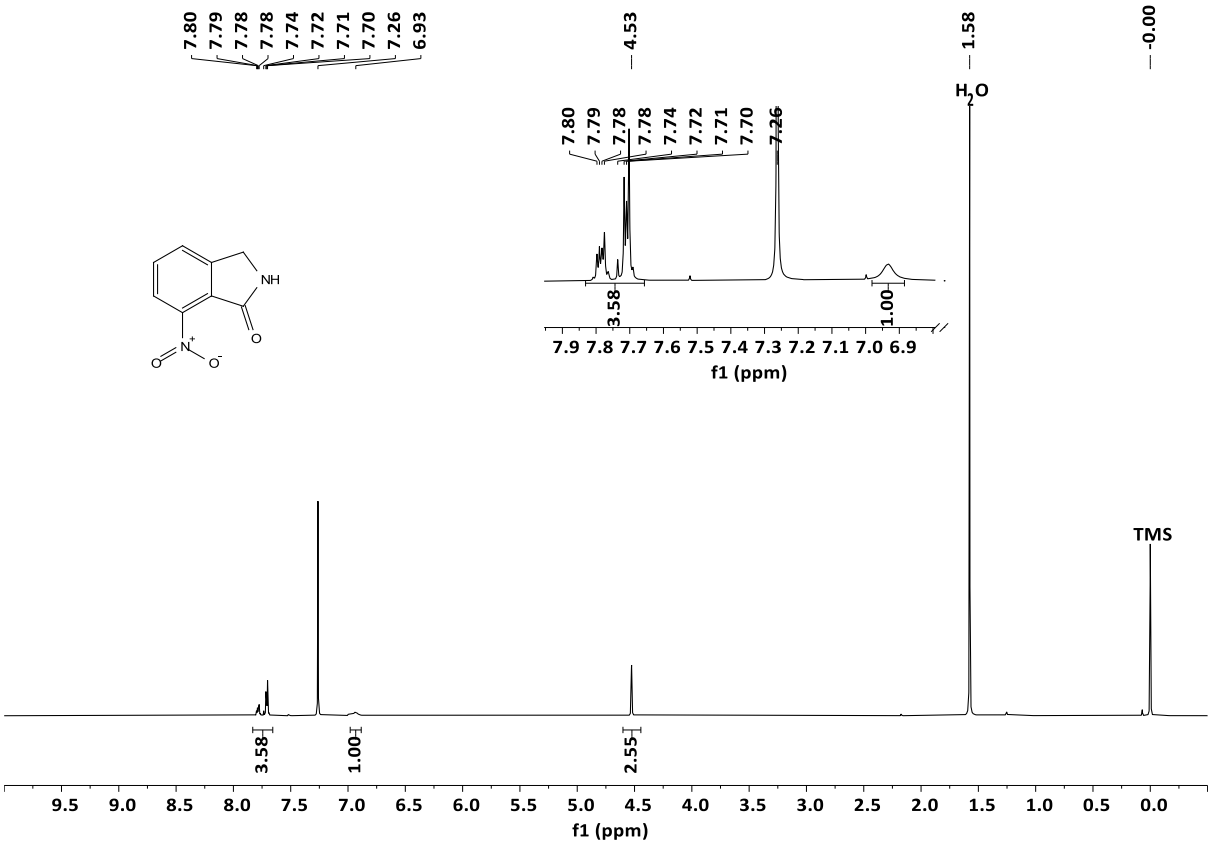

Figure S9.[1]H NMR spectrum (400 MHz) of **2a** in $CDCl_3$ at 25 °C

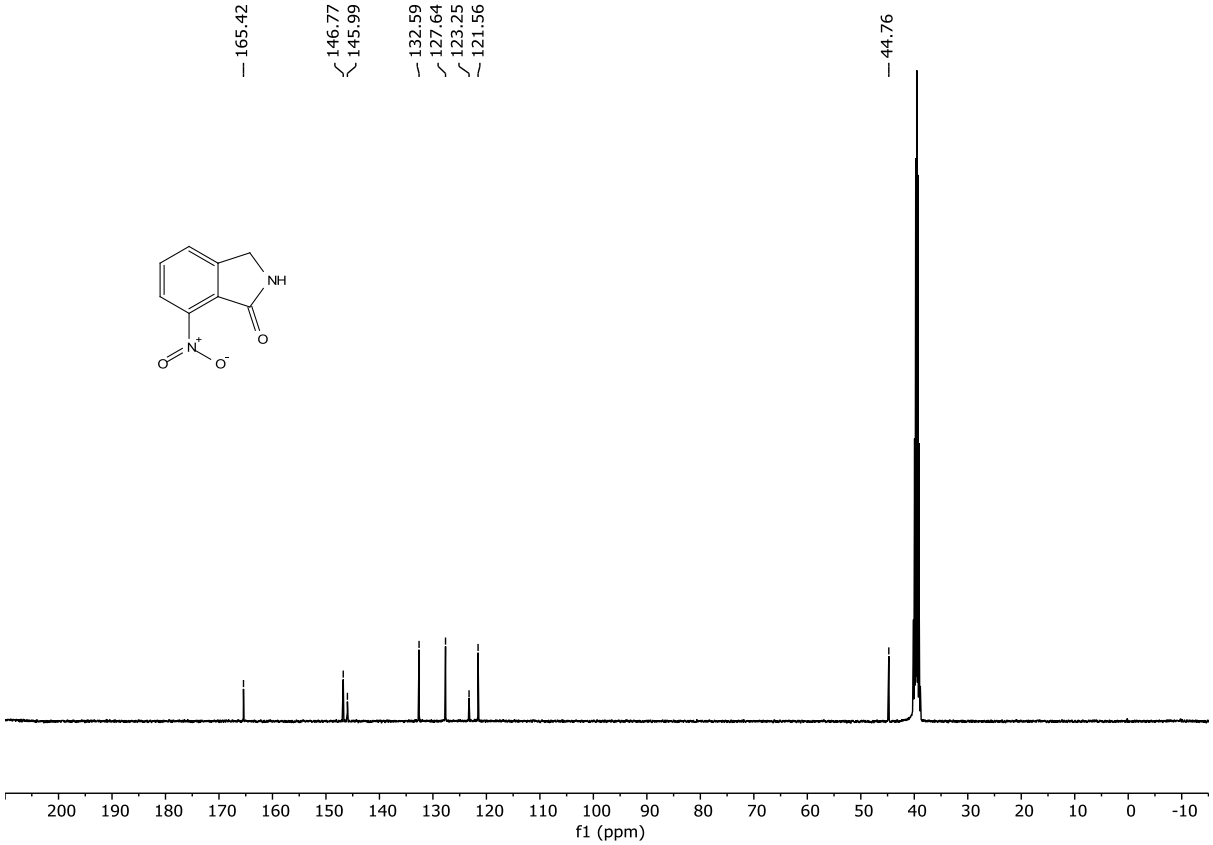

Figure S10.[13]C {[1]H} NMR spectrum (100 MHz) of **2a** in DMSO-d_6 at 25 °C

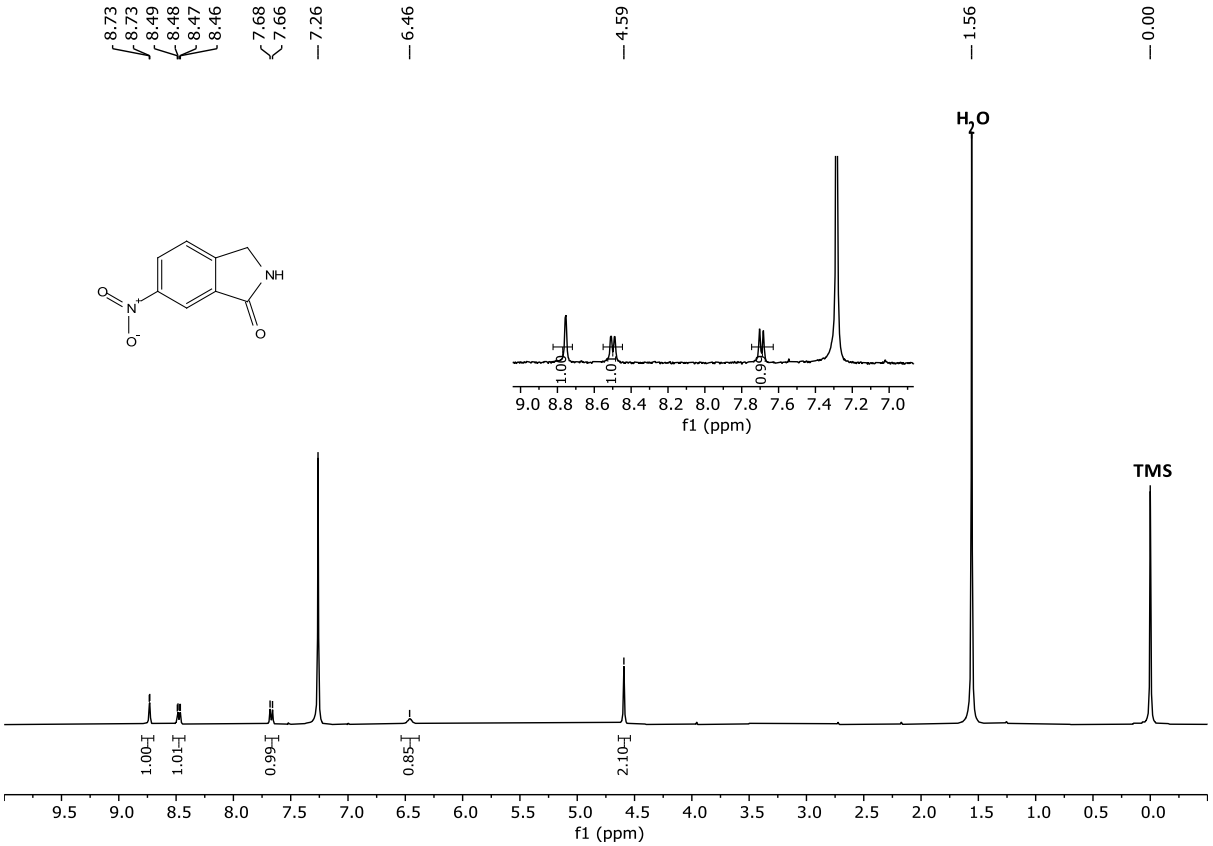

Figure S11. ^{1}H NMR spectrum (400 MHz) of **2b** in $CDCl_3$ at 25 °C

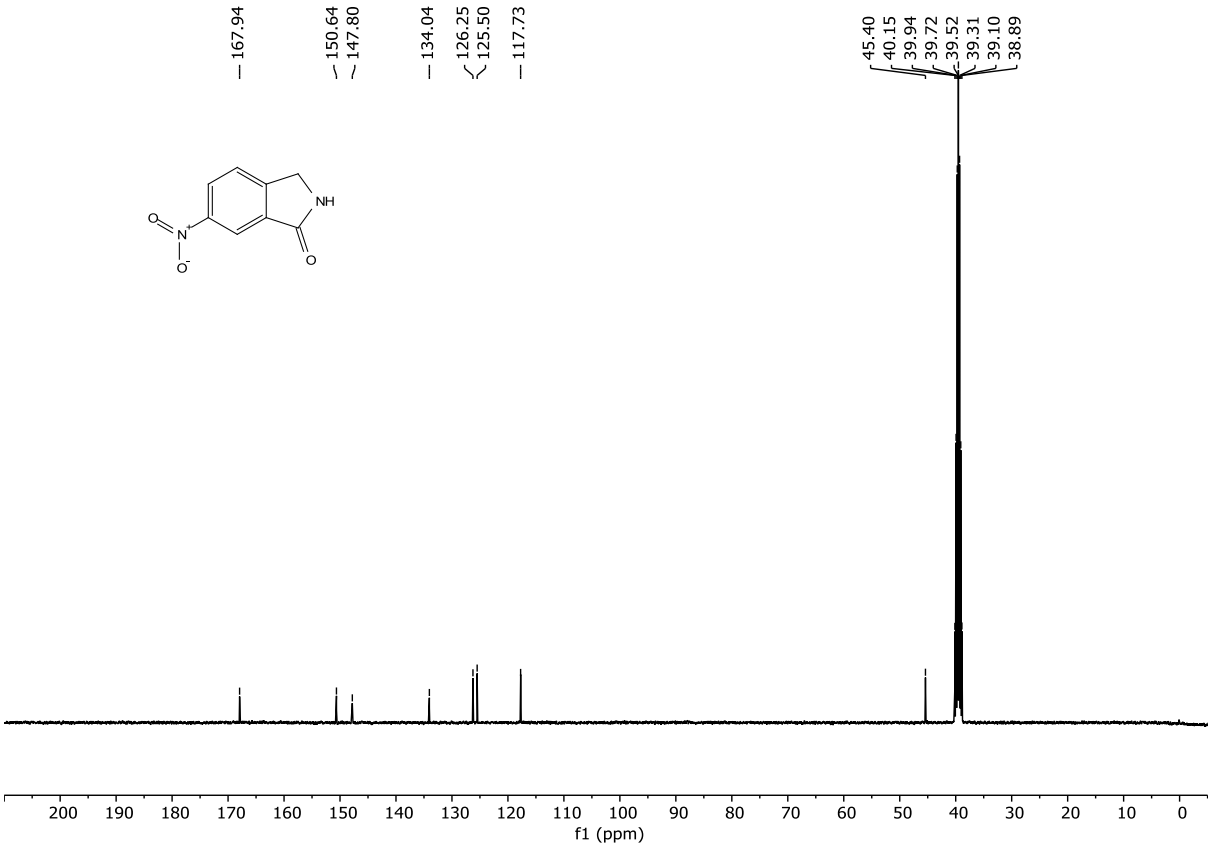

Figure S12. ^{13}C {^{1}H} NMR spectrum (100 MHz) of **2b** in DMSO-d_6 at 25 °C

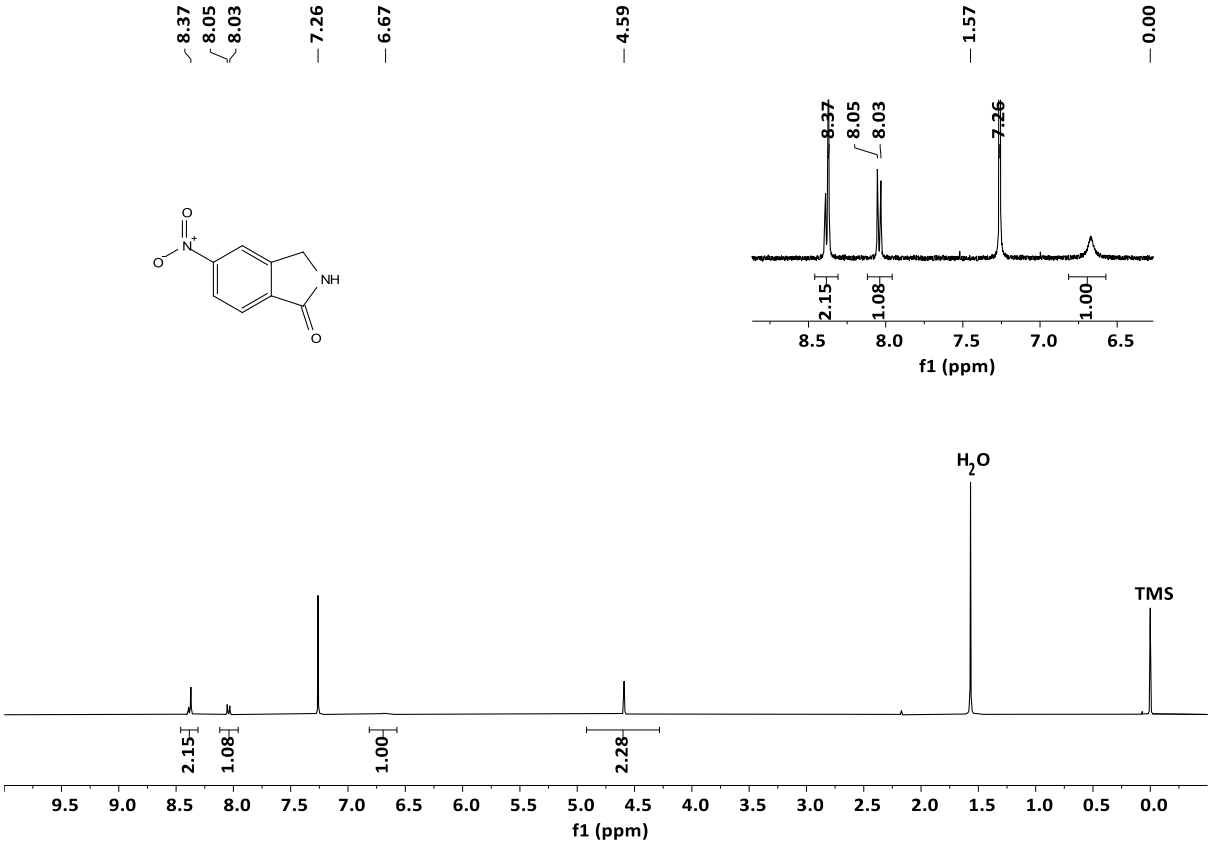

Figure S13. ^{1}H NMR spectrum (400 MHz) of **2c** in $CDCl_3$ at 25 °C

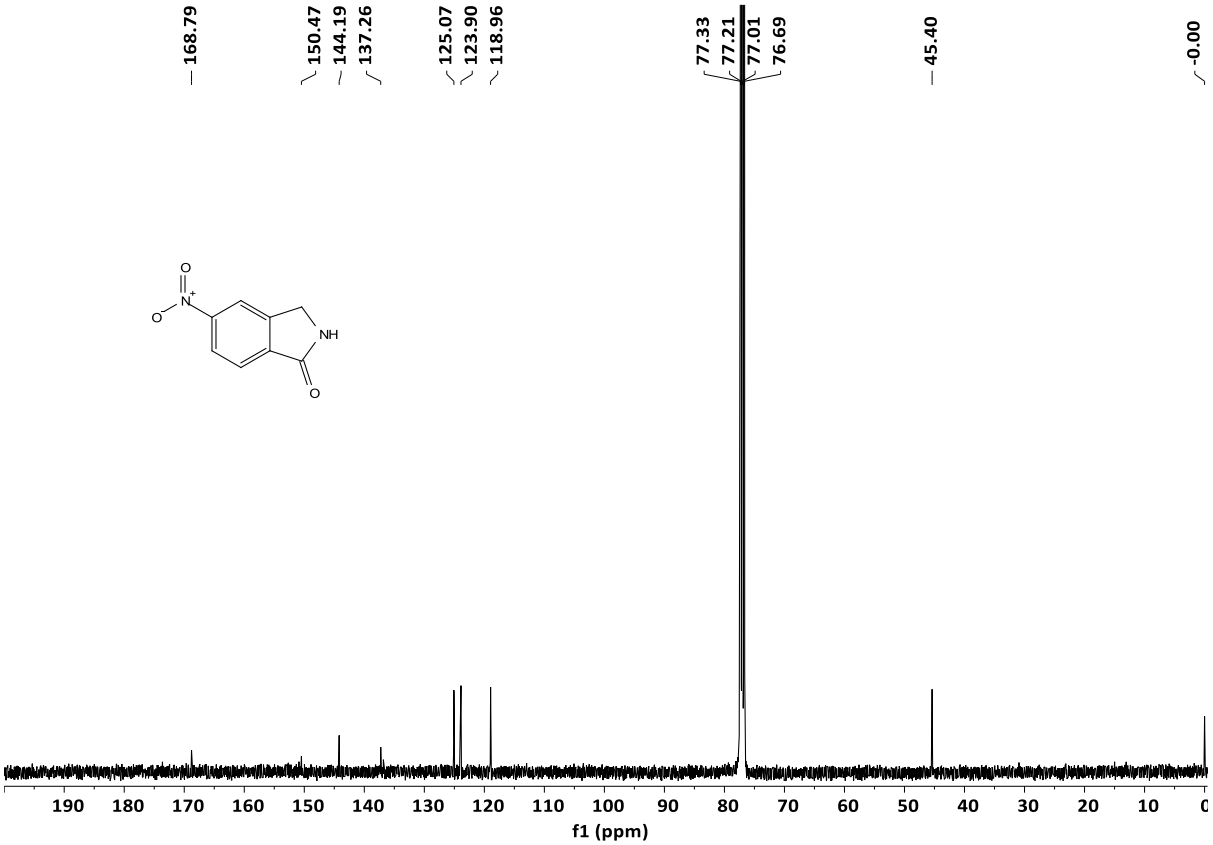

Figure S14. ^{13}C {^{1}H} NMR spectrum (100 MHz) of **2c** in $CDCl_3$ at 25 °C

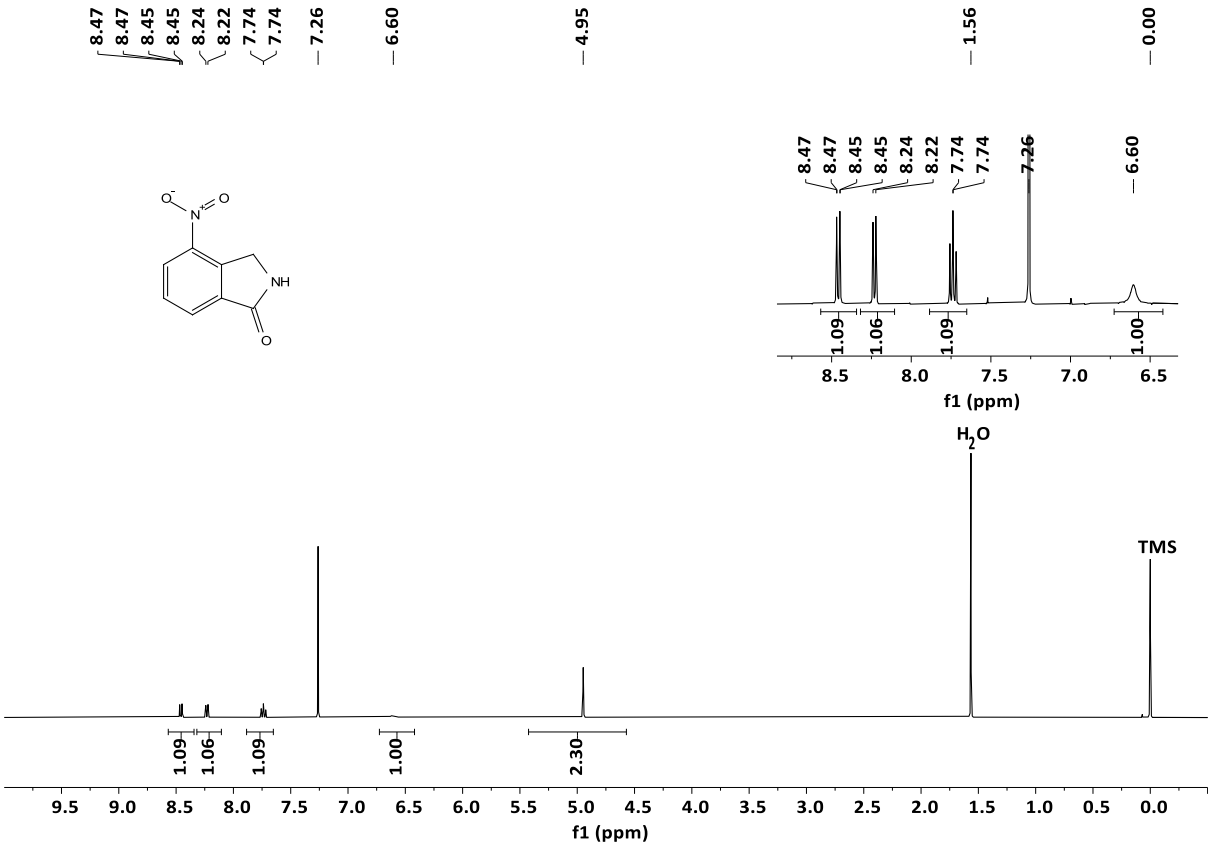

Figure S15. ^{1}H NMR spectrum (400 MHz) of **2d** in $CDCl_3$ at 25 °C

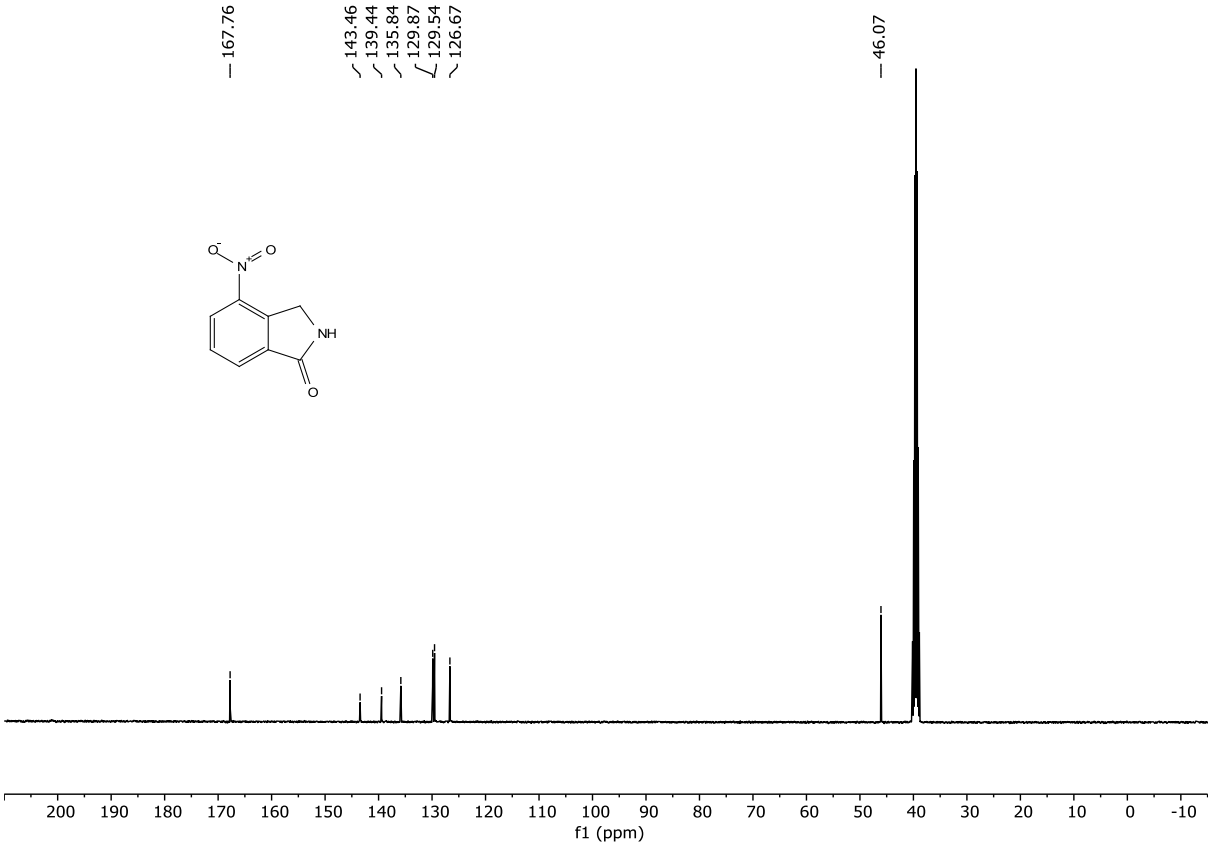

Figure S16. ^{13}C {^{1}H} NMR spectrum (100 MHz) of **2d** in DMSO-d_6 at 25 °C

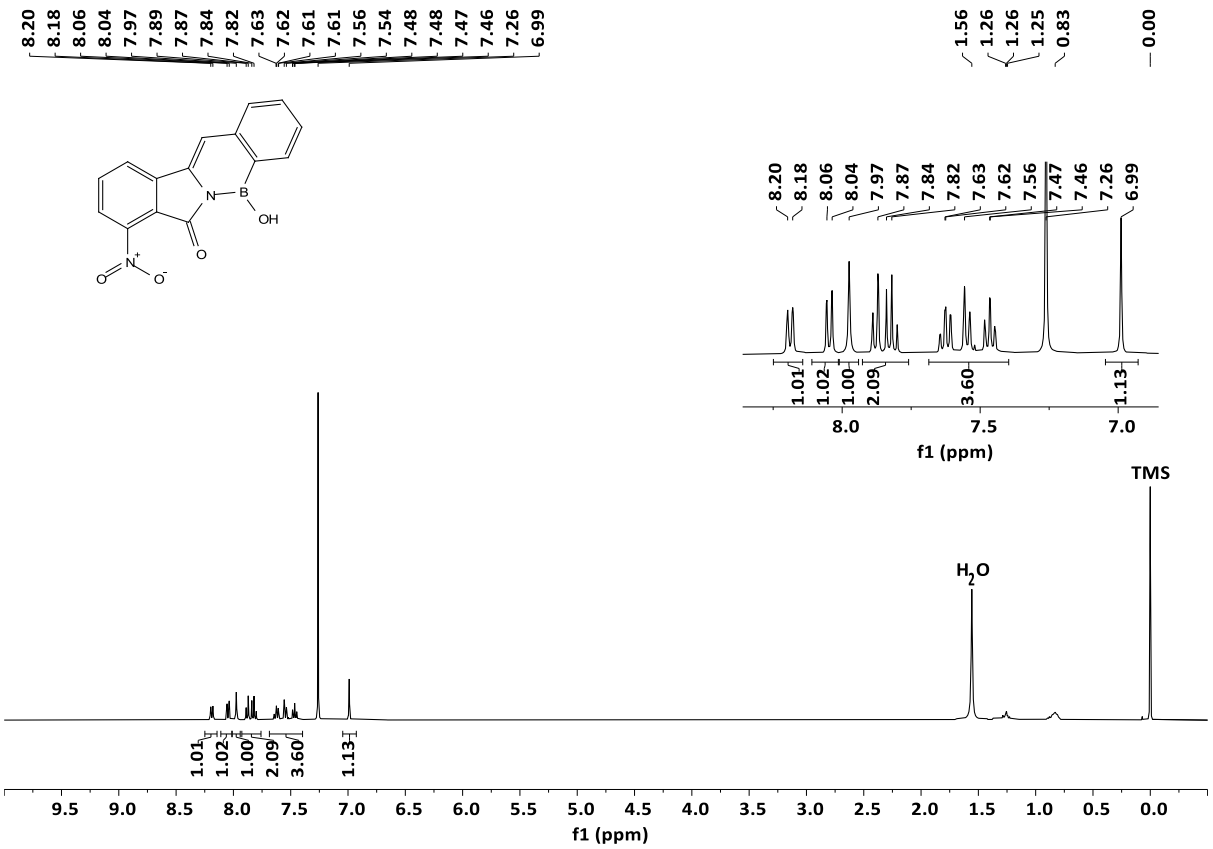

Figure S17. ^{1}H NMR spectrum (400 MHz) of **NO_2-PBNH 8** in $CDCl_3$ at 25 °C

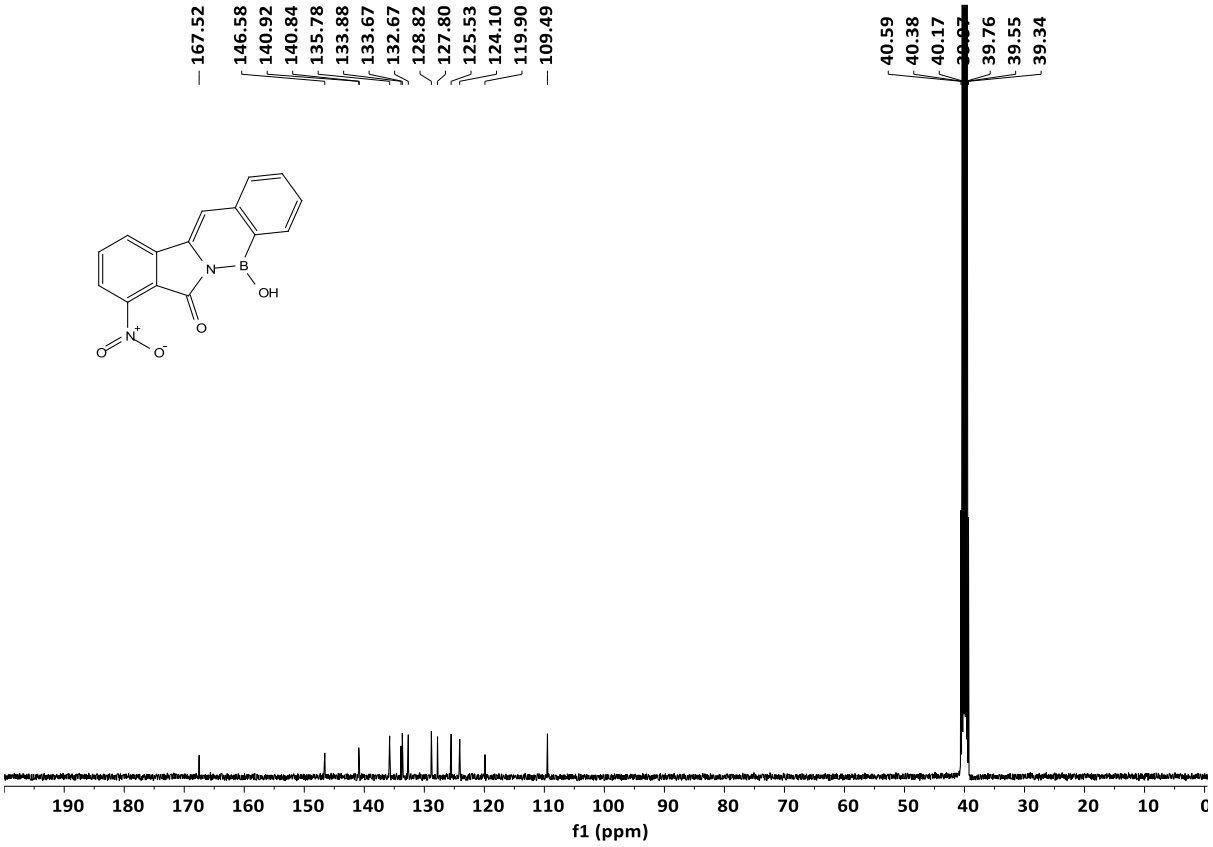

Figure S18. ^{13}C {^{1}H} NMR spectrum (100 MHz) of **NO_2-PBNH 8** in DMSO-d_6 at 25 °C

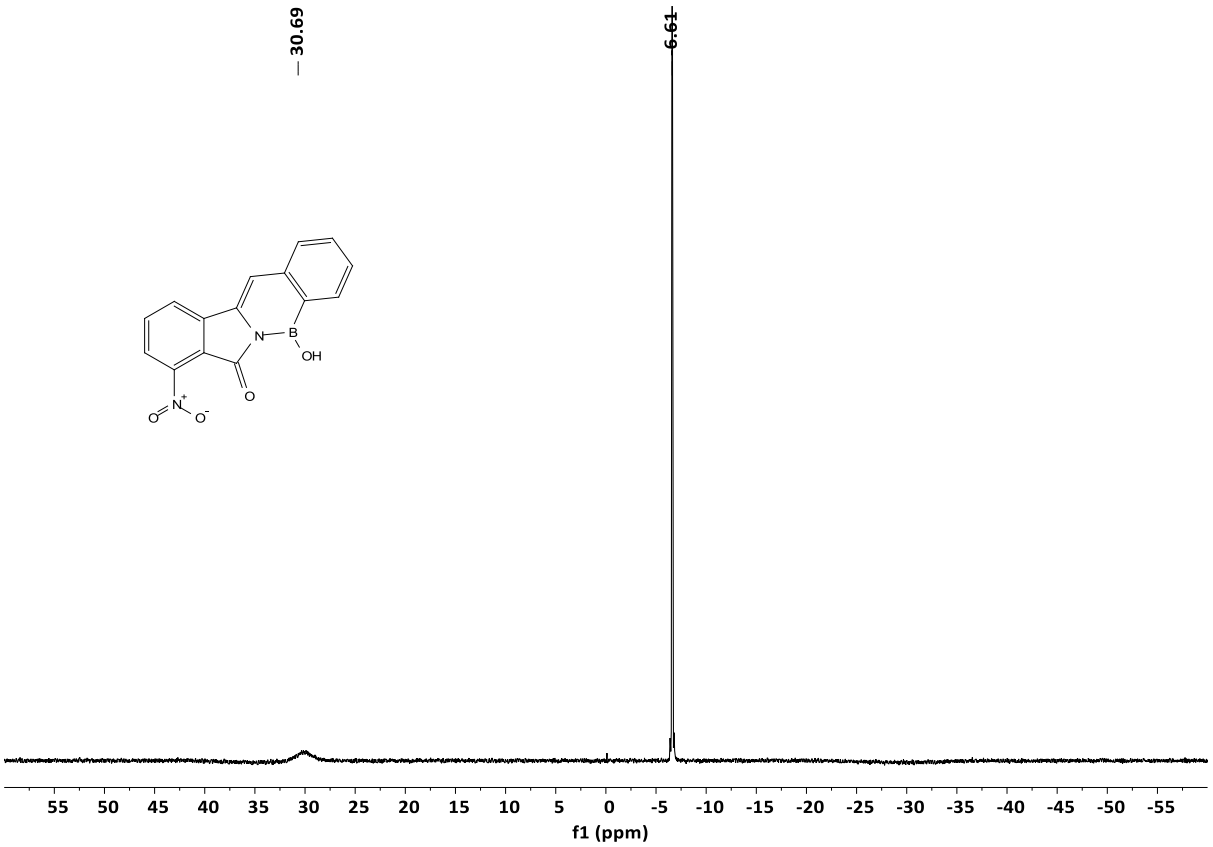

Figure S19. ^{11}B {1H} NMR spectrum (128 MHz) of **NO_2-PBNH 8** in acetone-d_6

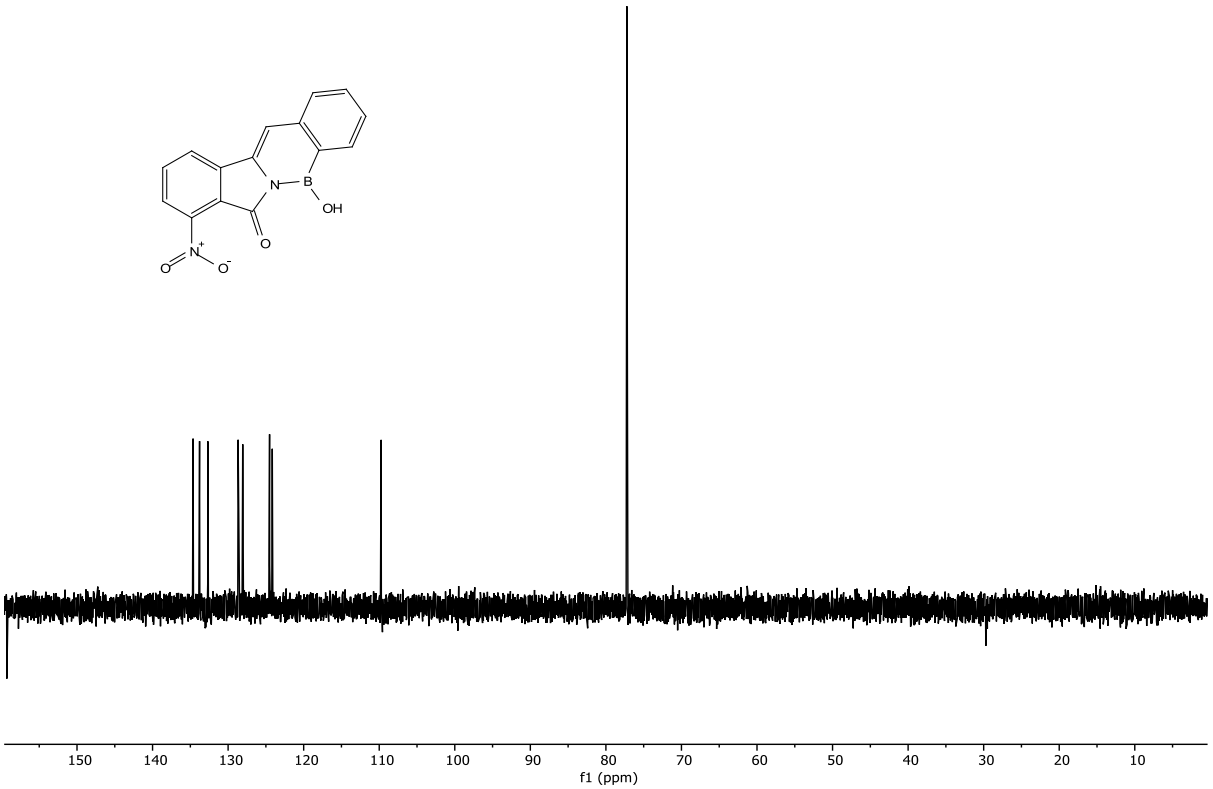

Figure S20. ^{13}C {1H} DEPT 135 NMR (100 MHz) of **NO_2-PBNH 8** in $CDCl_3$ at 25 °C

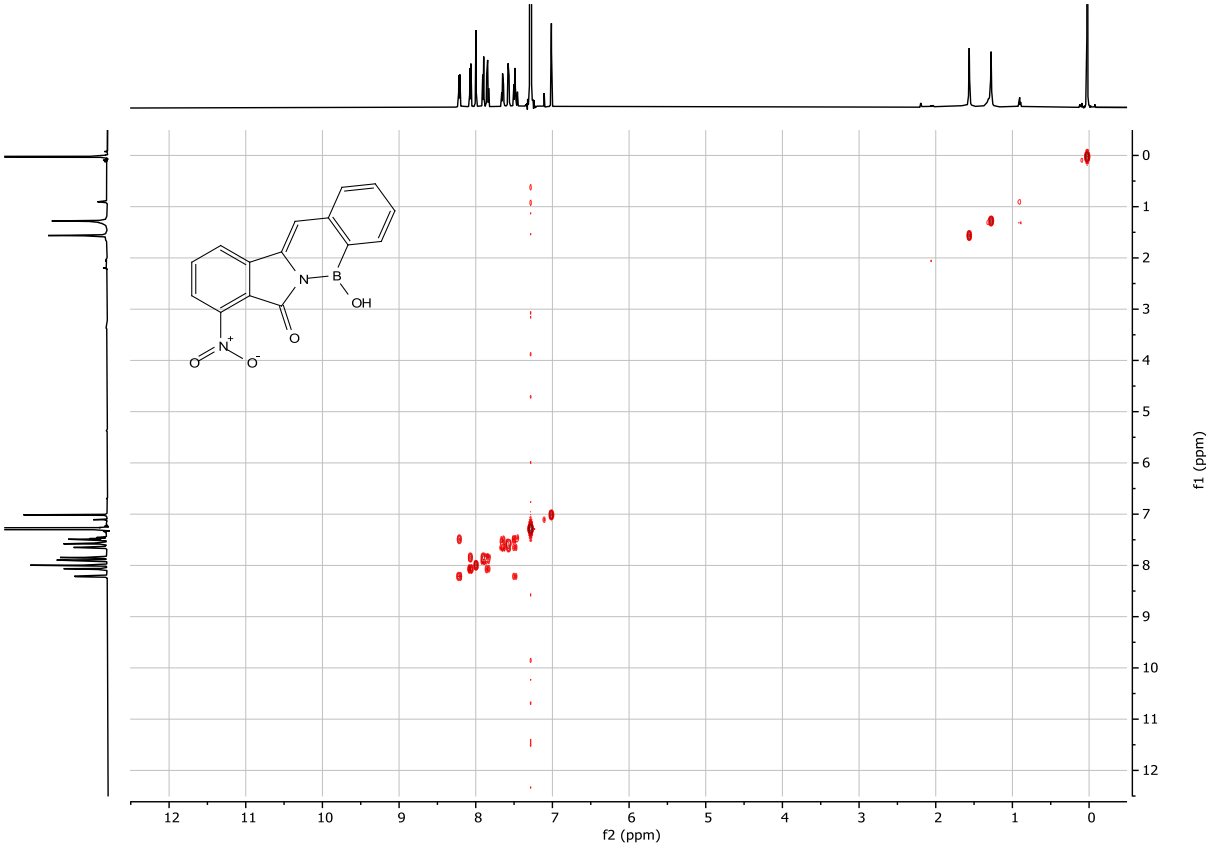

Figure S21. ^{1}H-^{1}H COSY spectra of **NO_2-PBNH 8** in $CDCl_3$ (400 MHz)

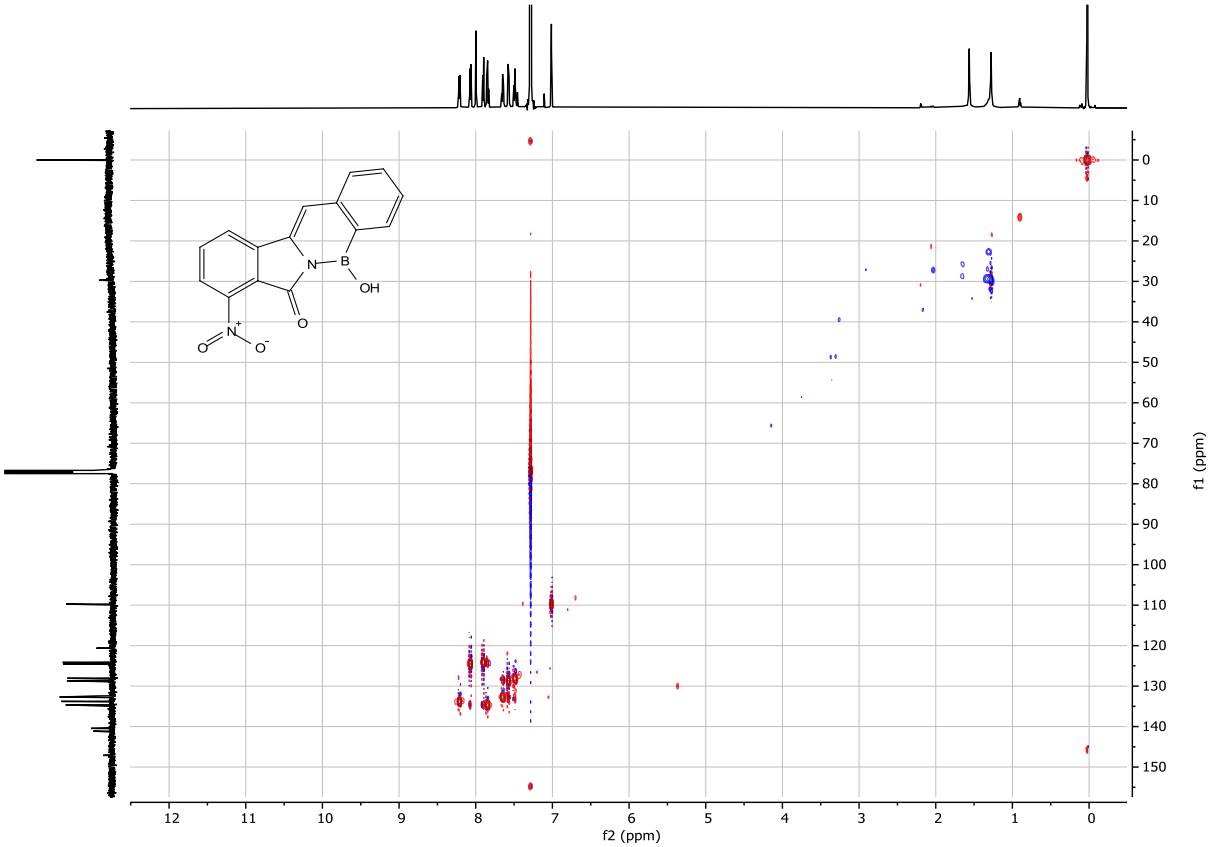

Figure S22. HSQC NMR spectra of **NO_2-PBNH 8** in $CDCl_3$ (400 MHz)

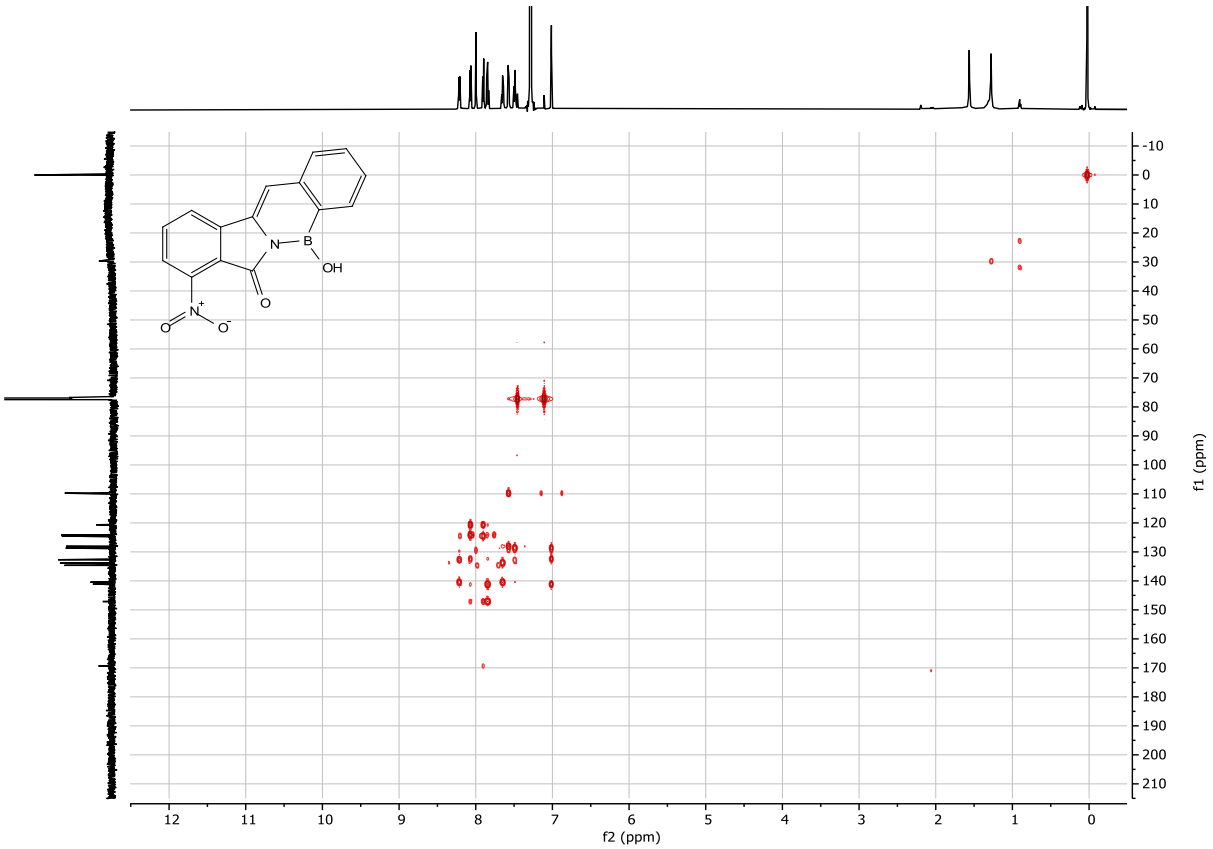

Figure S23. HMBC NMR spectra of **NO_2-PBNH 8** in $CDCl_3$ (400 MHz)

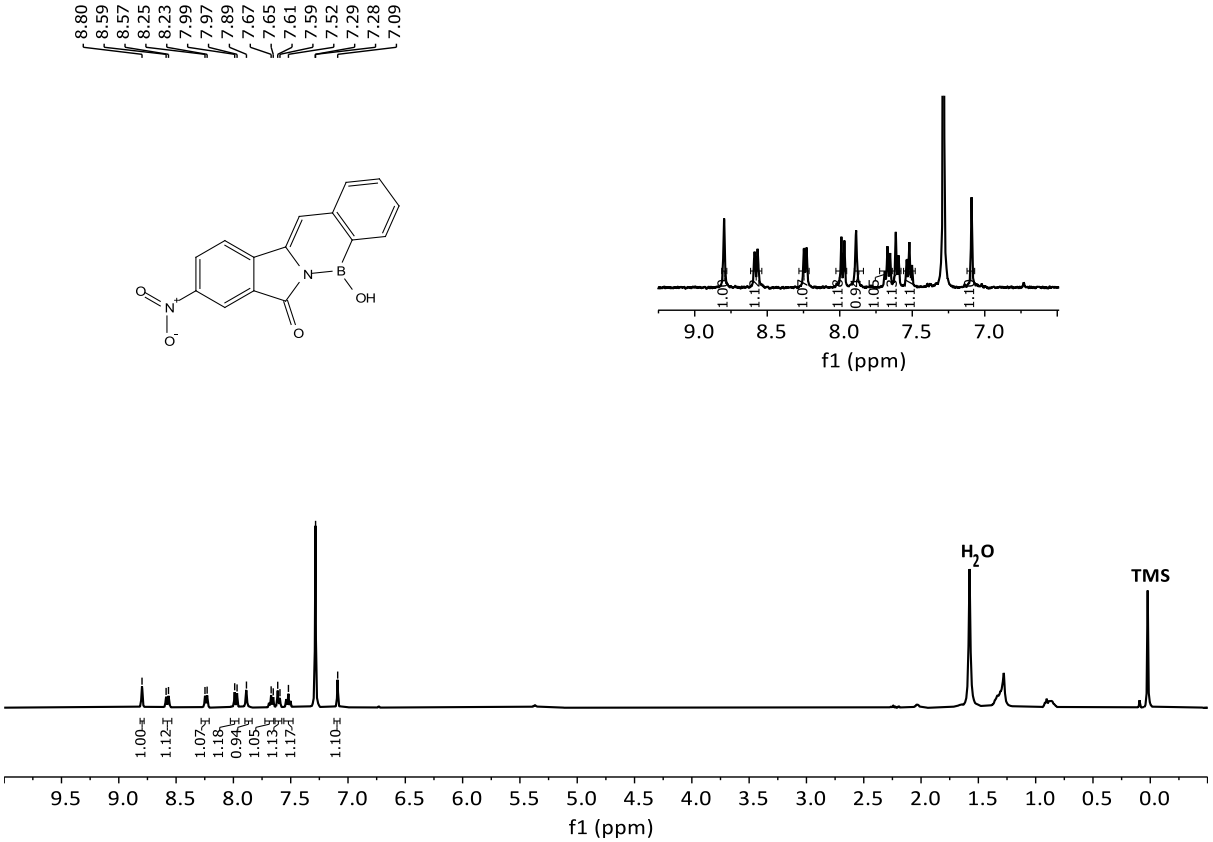

Figure S24.[1]H NMR spectrum (400 MHz) of **NO_2-PBNH 9** in $CDCl_3$ at 25 °C

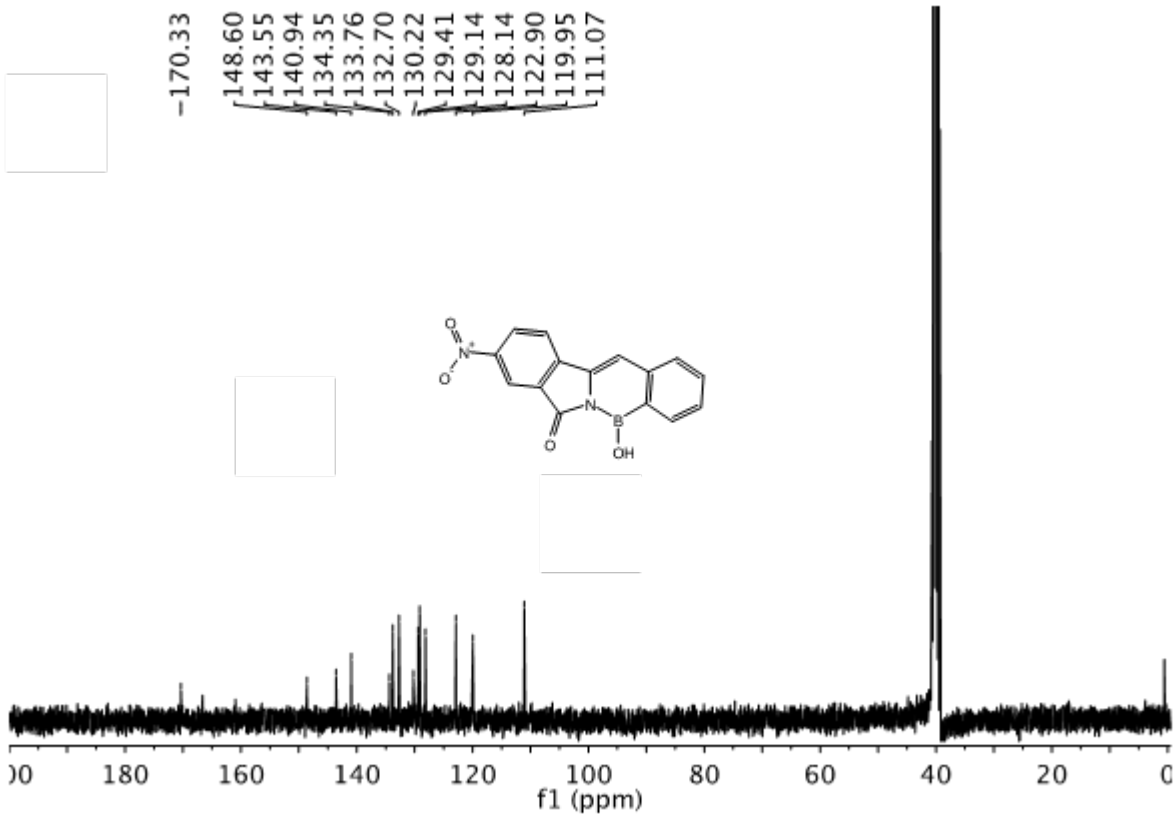

Figure S25. ^{13}C {^{1}H} NMR spectrum (100 MHz) of **NO_2-PBNH 9** in DMSO-d_6 at 25 °C

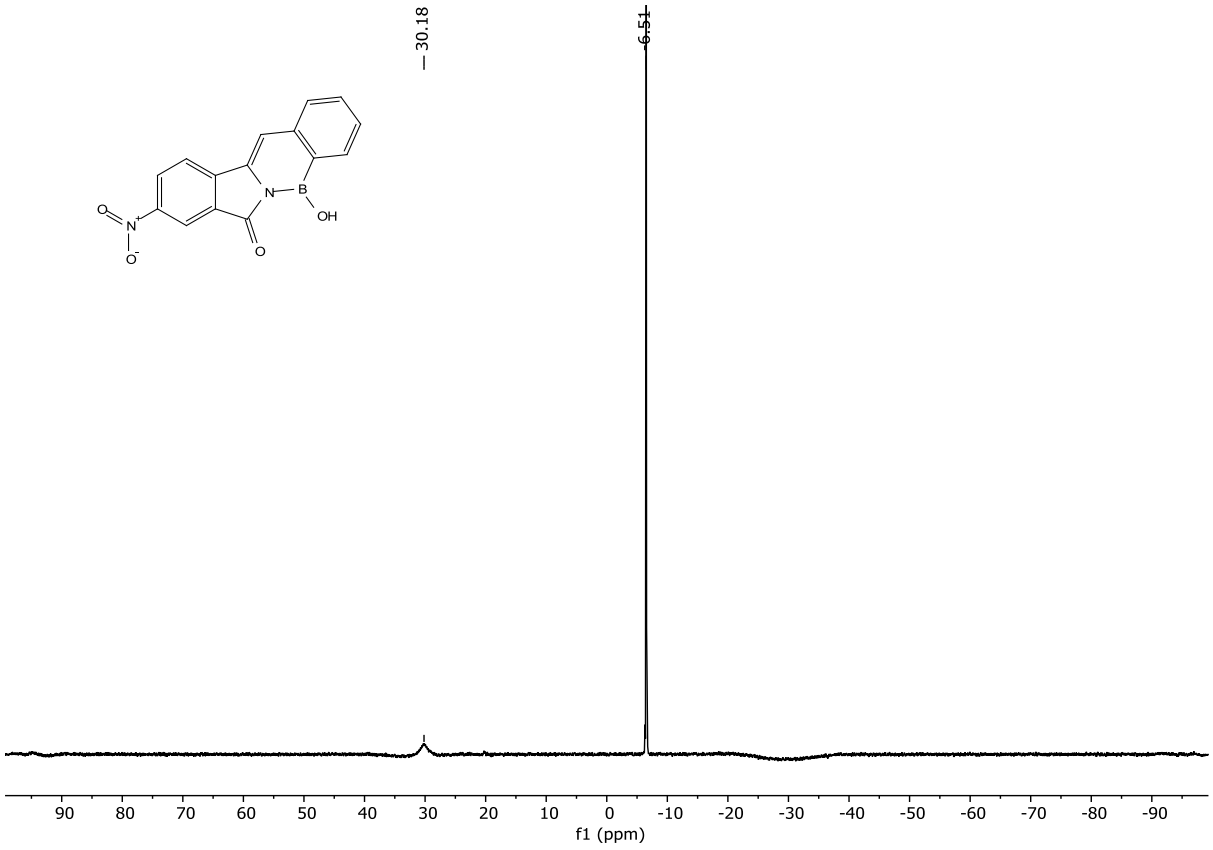

Figure S26. ^{11}B {1H} NMR spectrum (128 MHz) of **NO_2-PBNH 9** in acetone-d_6

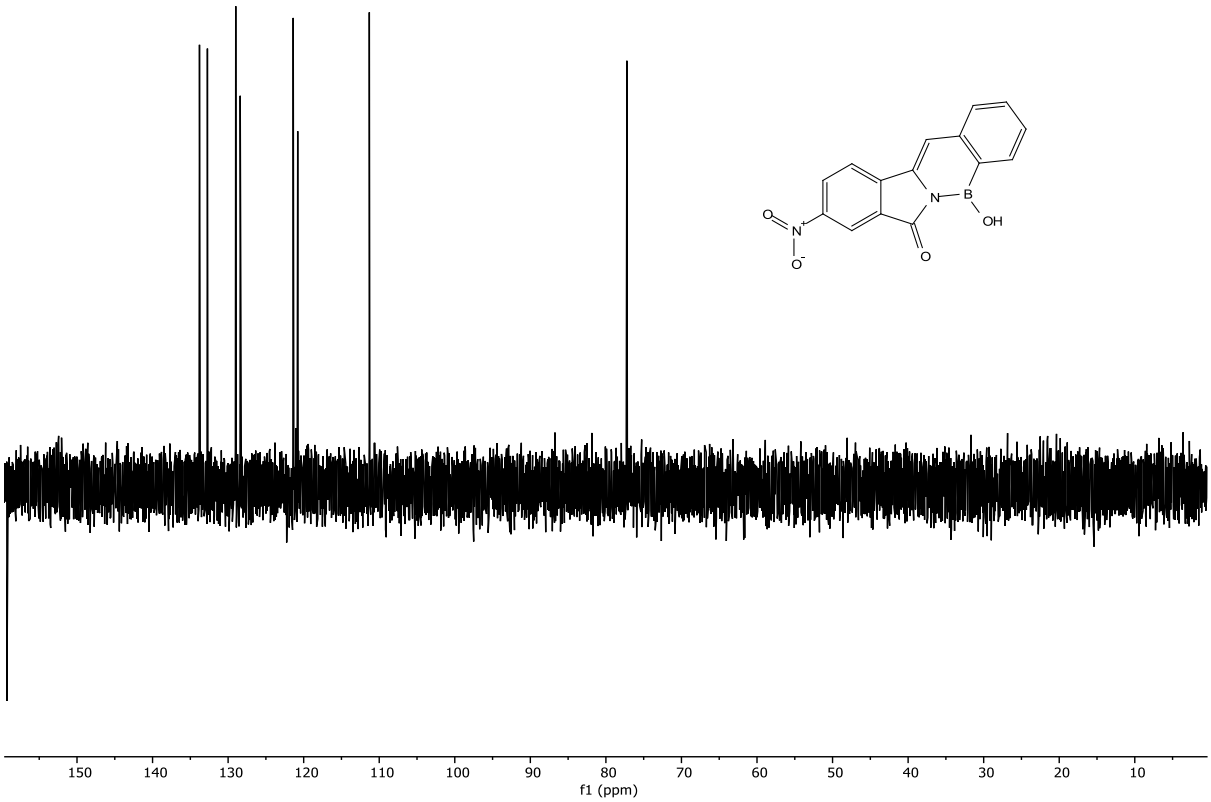

Figure S27. ^{13}C {1H} DEPT 135 NMR (100 MHz) of **NO_2-PBNH 9** in $CDCl_3$ at 25 °C

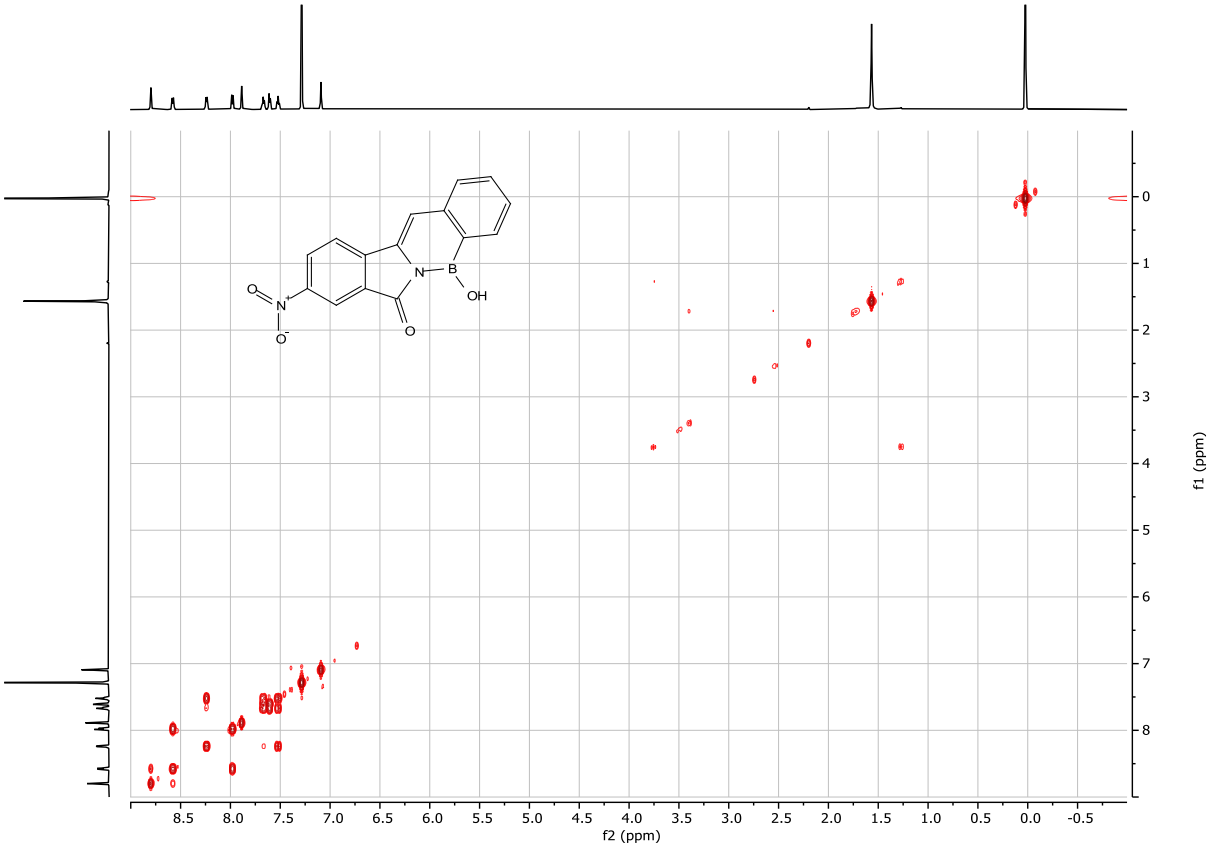

Figure S28. ^{1}H-^{1}H COSY spectra of **NO_2-PBNH 9** in $CDCl_3$ (400 MHz)

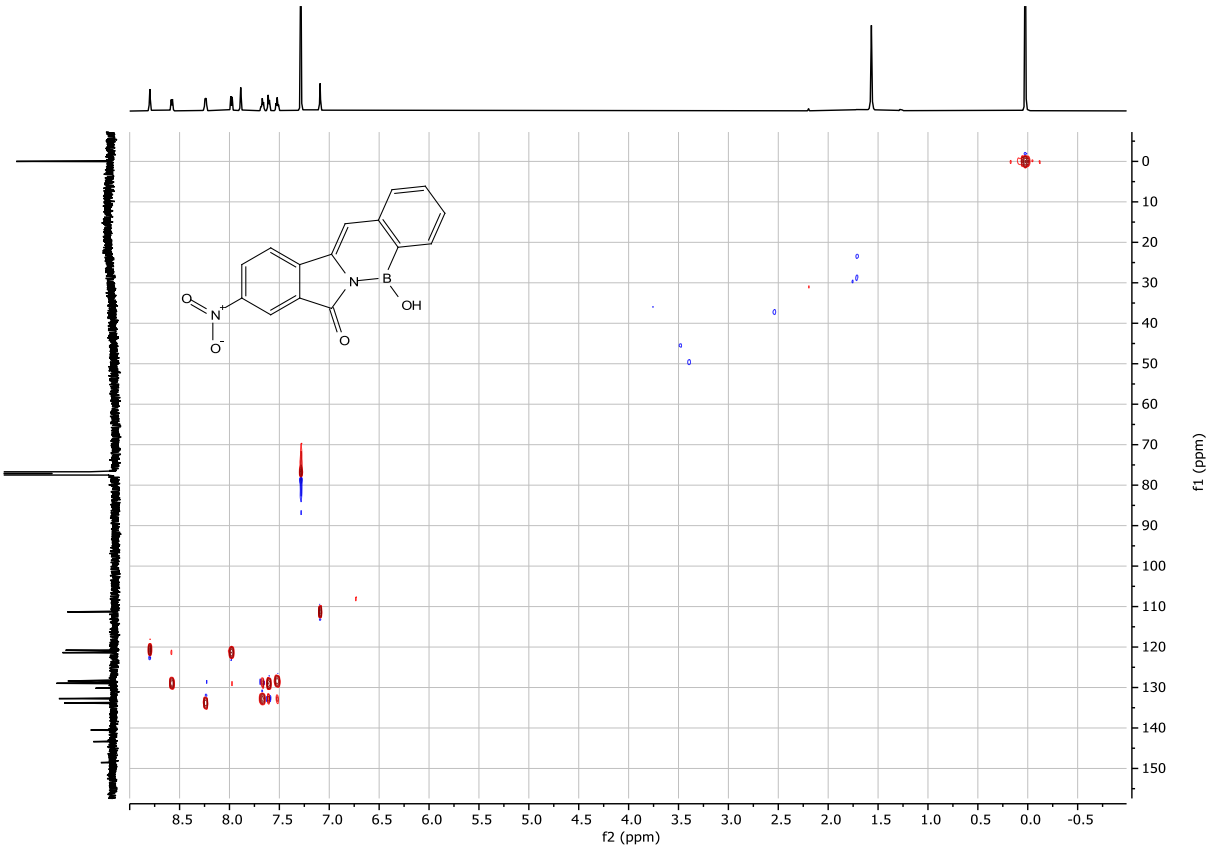

Figure S29. HSQC NMR spectra of **NO_2-PBNH 9** in $CDCl_3$ (400 MHz)

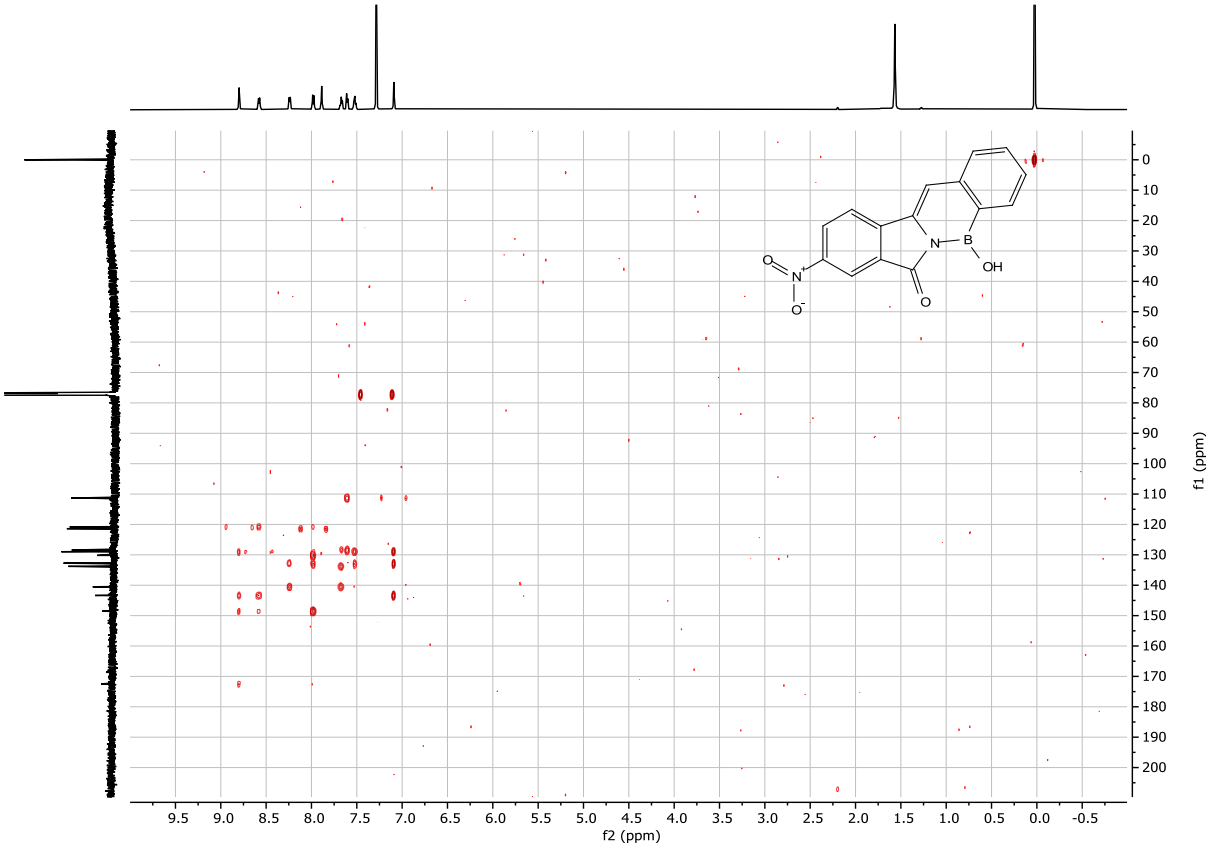

Figure S30. HMBC NMR spectra of **NO_2-PBNH 9** in $CDCl_3$ (400 MHz)

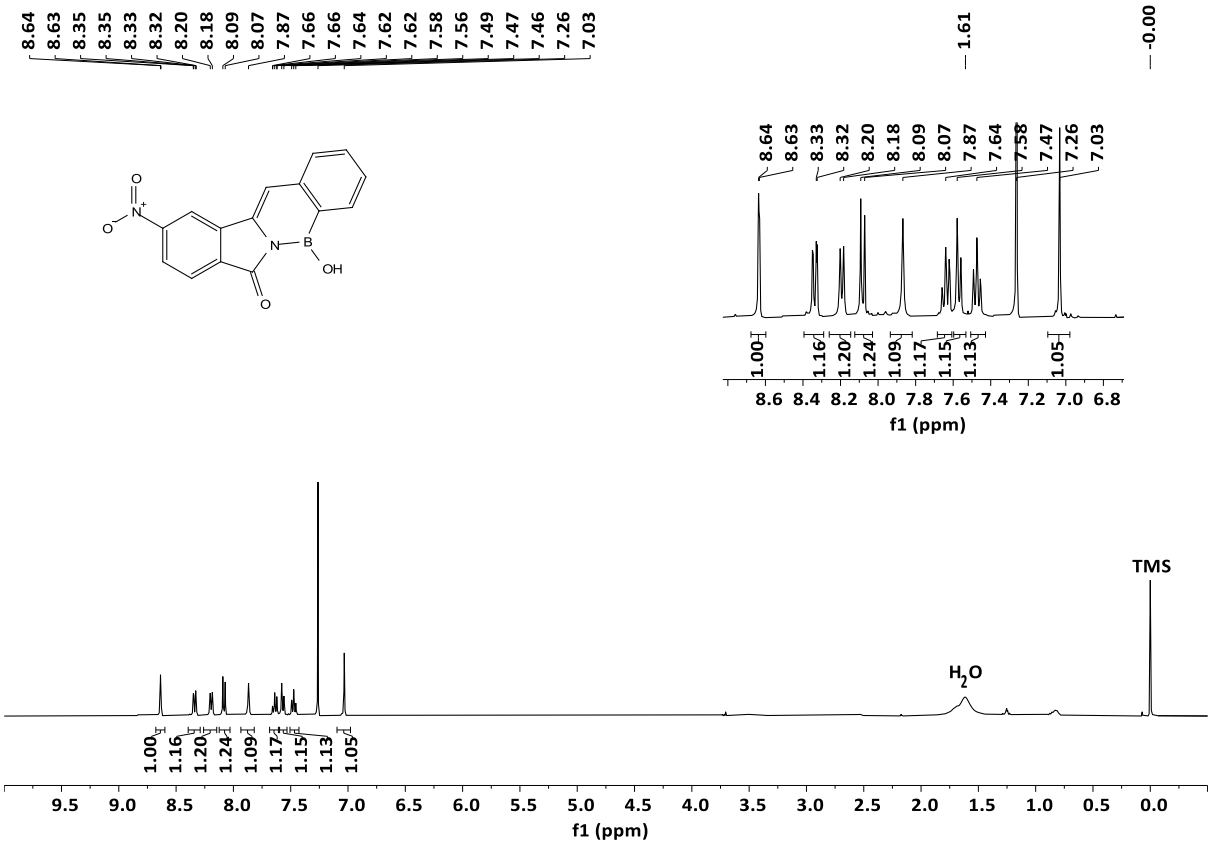

Figure S31. ^{1}H NMR spectrum (400 MHz) of **NO_2-PBNH 10** in $CDCl_3$ at 25 °C

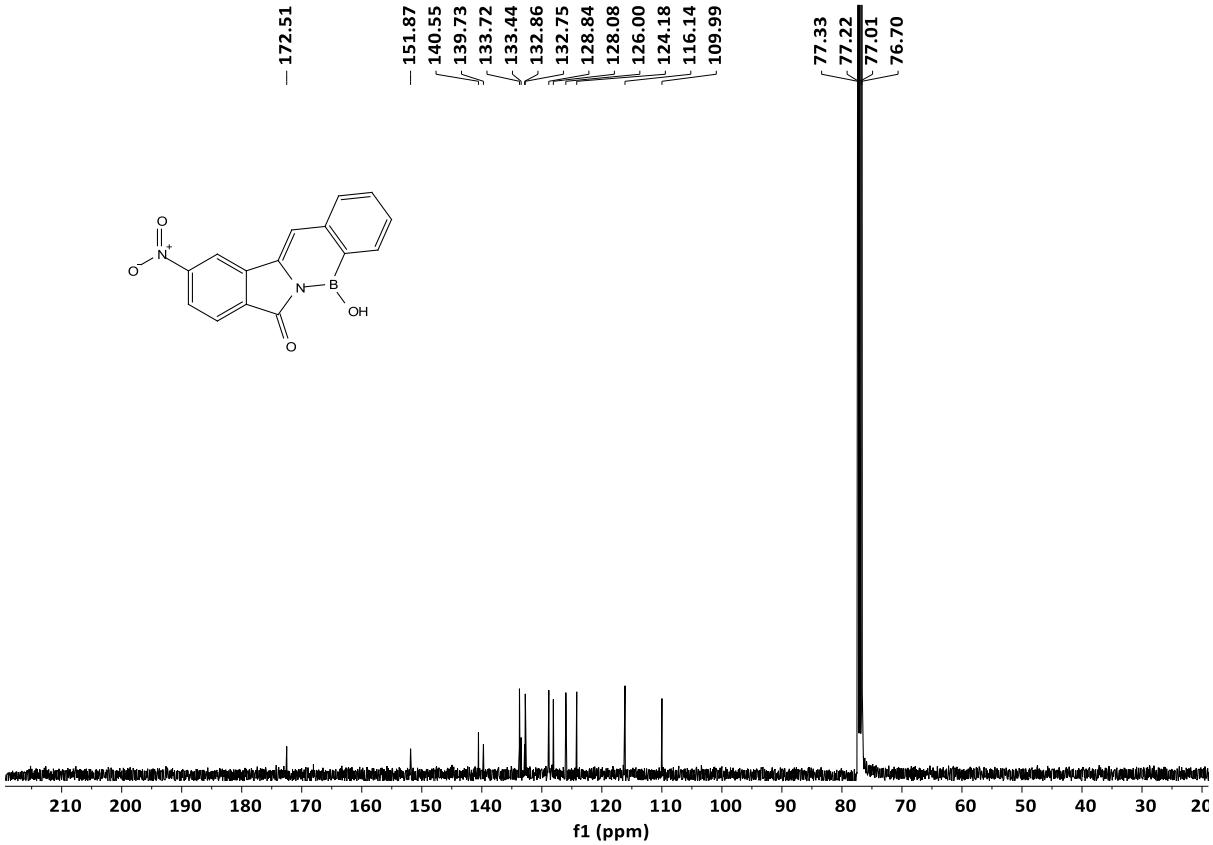

Figure S32. ^{13}C {^{1}H} NMR spectrum (100 MHz) of **NO_2-PBNH 10** in $CDCl_3$ at 25 °C

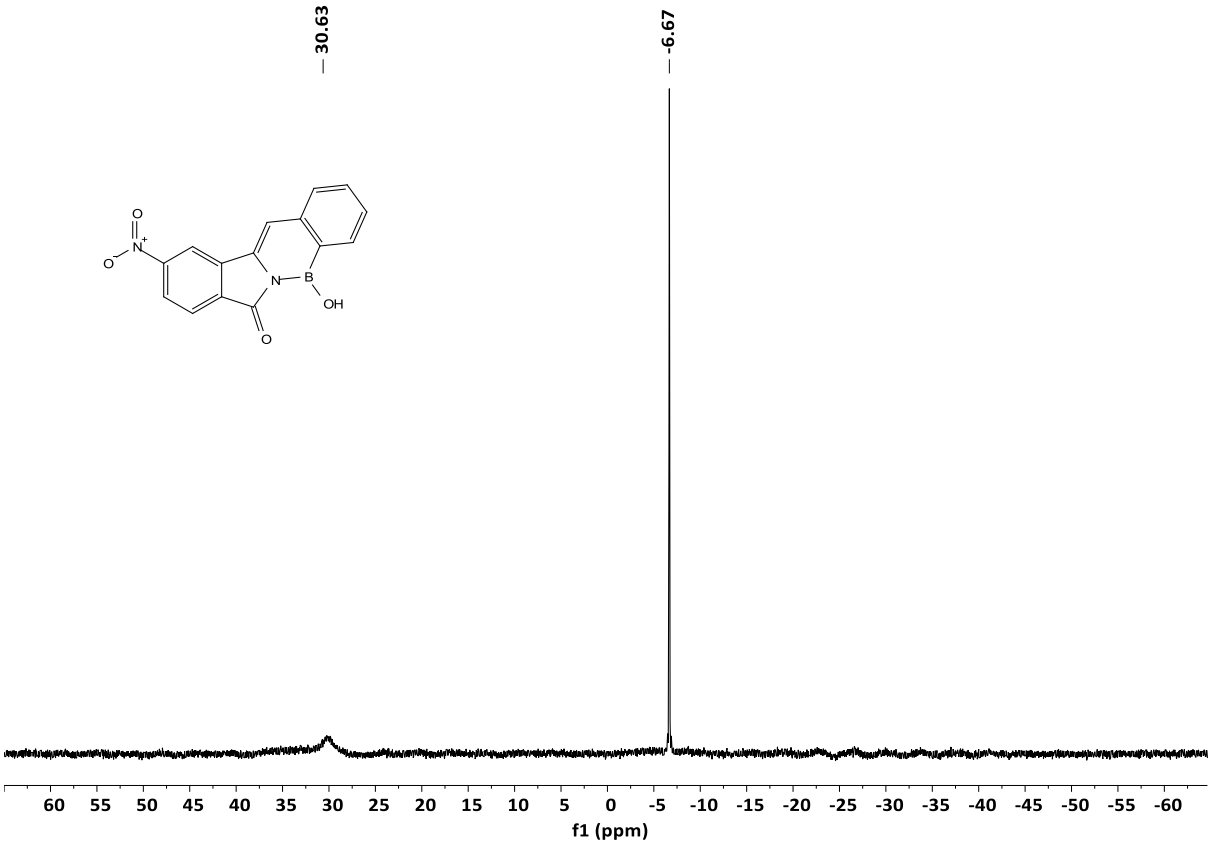

Figure S33. ^{11}B {1H} NMR spectrum (128 MHz) of **NO_2-PBNH 10** in acetone-d_6

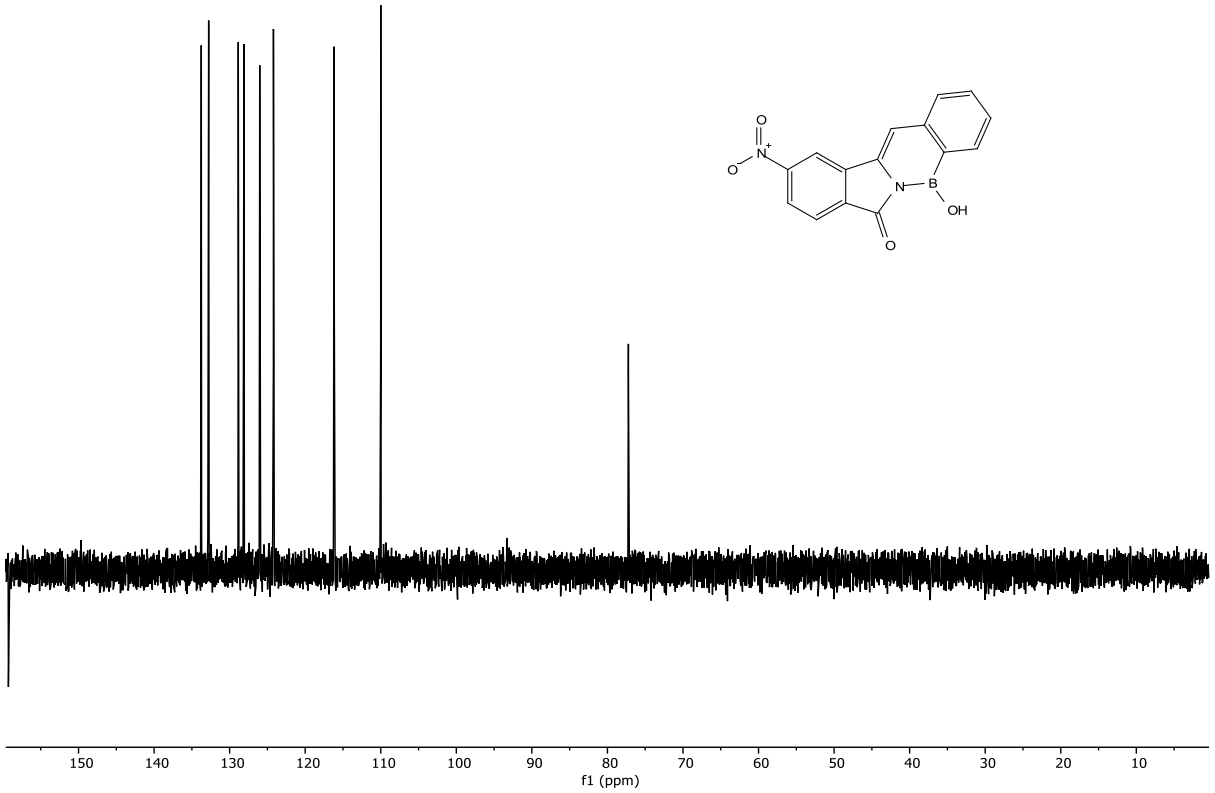

Figure S34. ^{13}C {1H} DEPT 135 NMR (100 MHz) of **NO_2-PBNH 10** in $CDCl_3$ at 25 °C

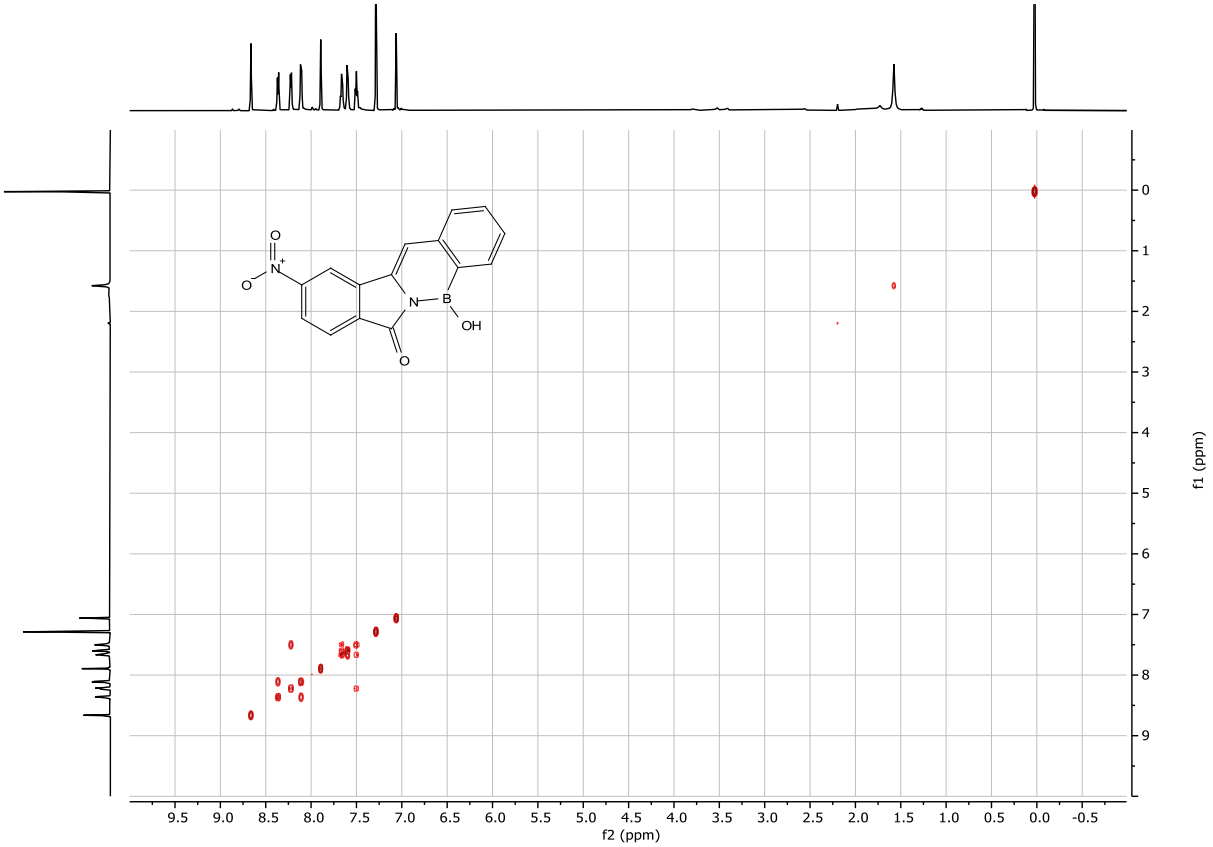

Figure S35. ^{1}H-^{1}H COSY spectra of **NO_2-PBNH 10** in $CDCl_3$ (400 MHz)

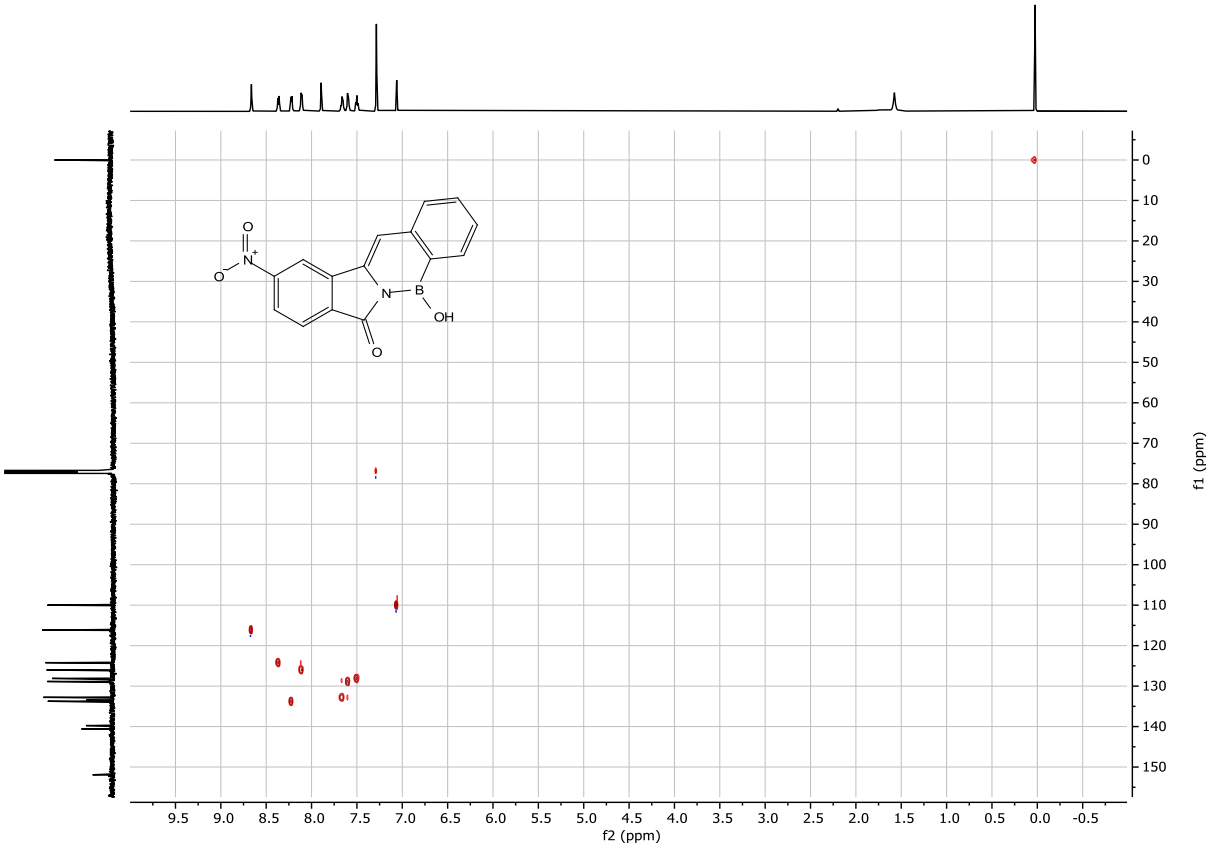

Figure S36. HSQC NMR spectra of **NO_2-PBNH 10** in $CDCl_3$ (400 MHz)

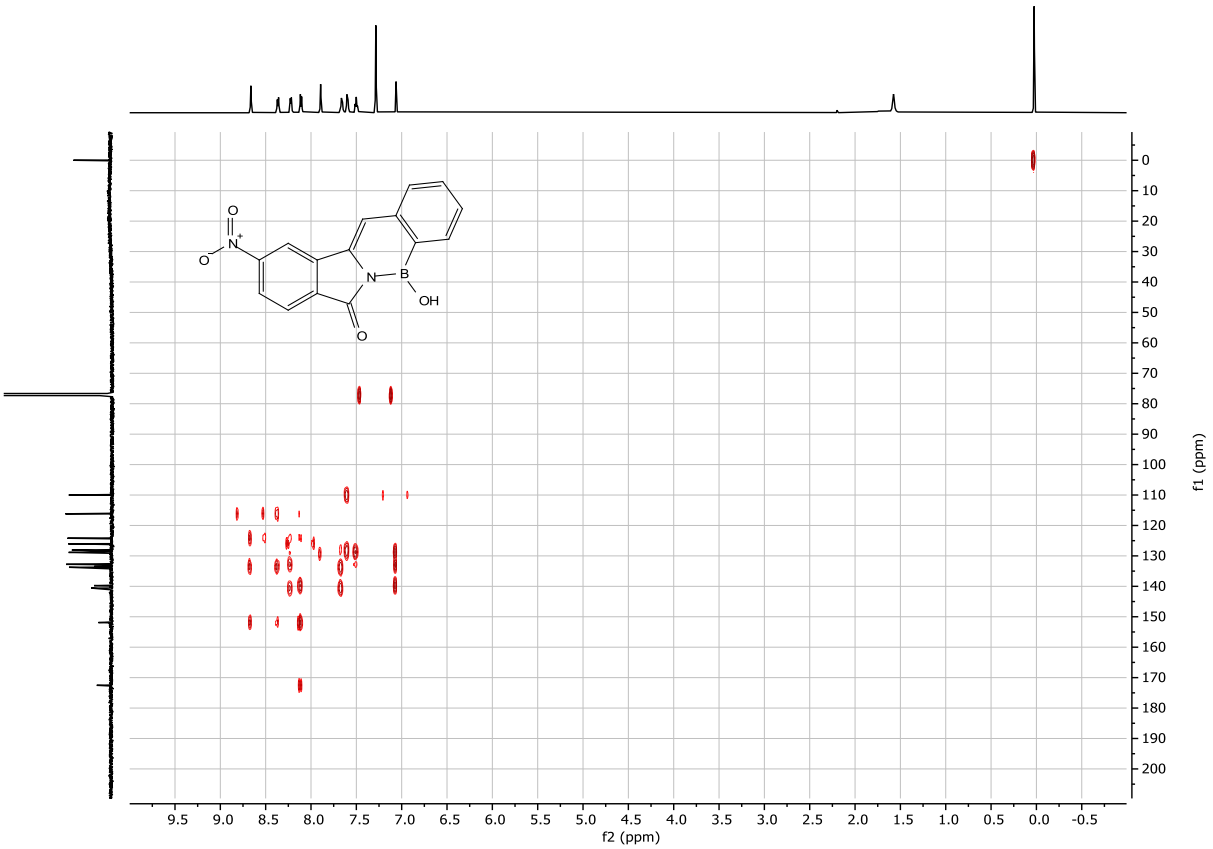

Figure S37. HMBC NMR spectra of **NO_2-PBNH 10** in $CDCl_3$ (400 MHz)

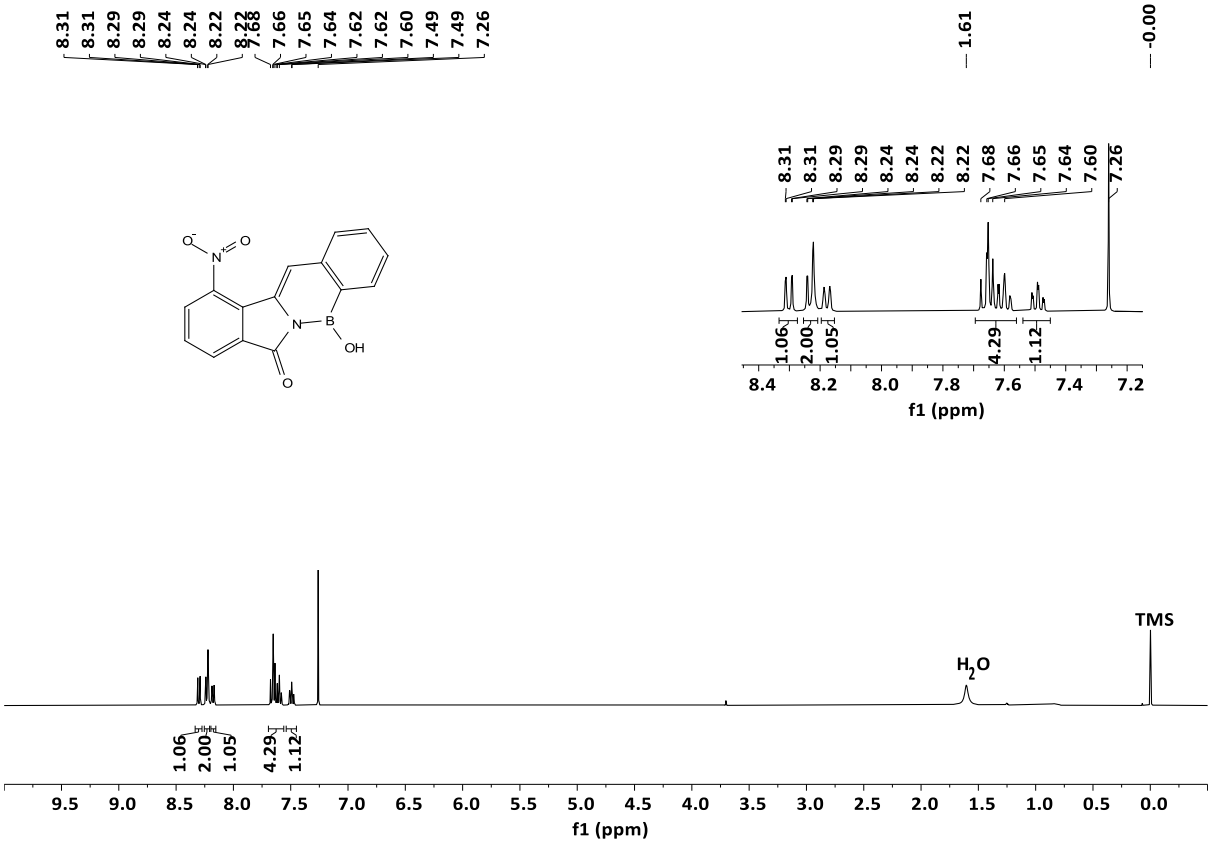

Figure S38.[1]H NMR spectrum (400 MHz) of **NO_2-PBNH 11** in $CDCl_3$ at 25 °C

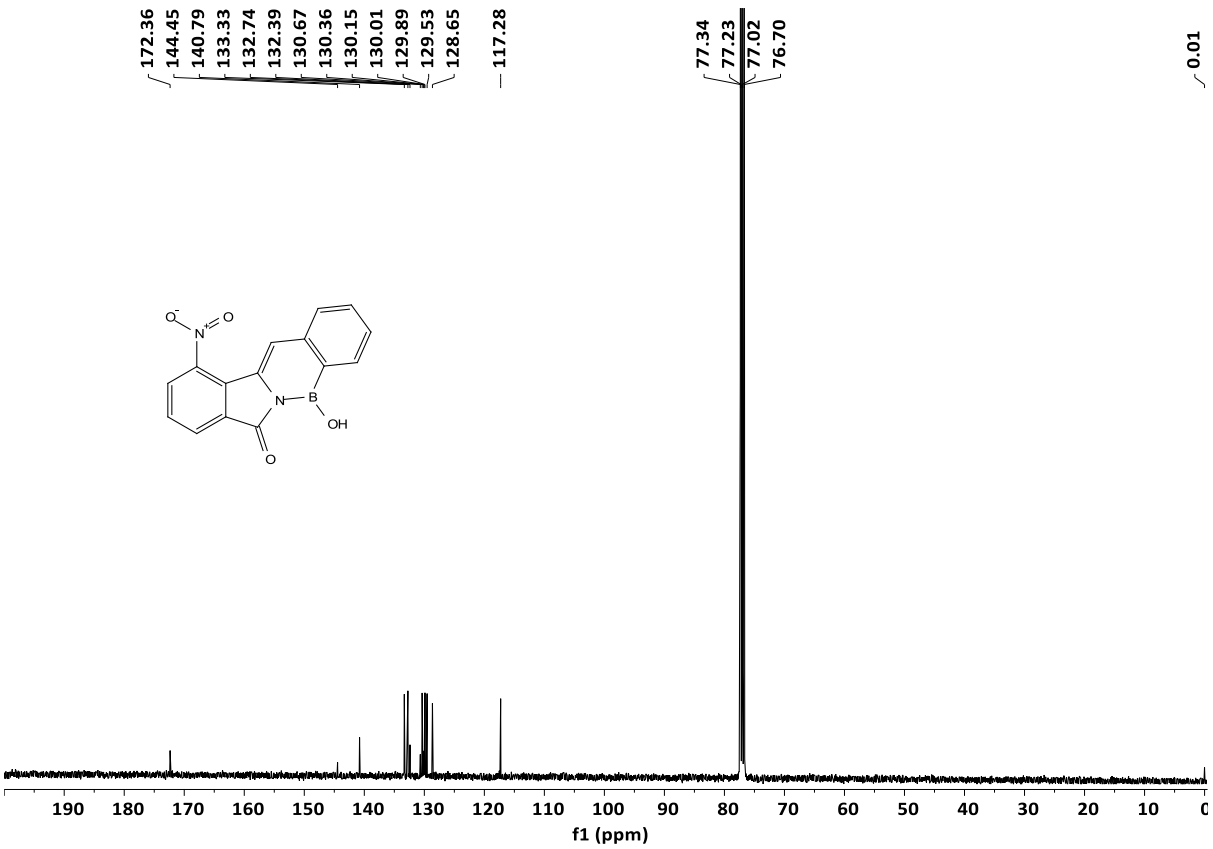

Figure S39. ^{13}C {^{1}H} NMR spectrum (100 MHz) of **NO_2-PBNH 11** in $CDCl_3$ at 25 °C

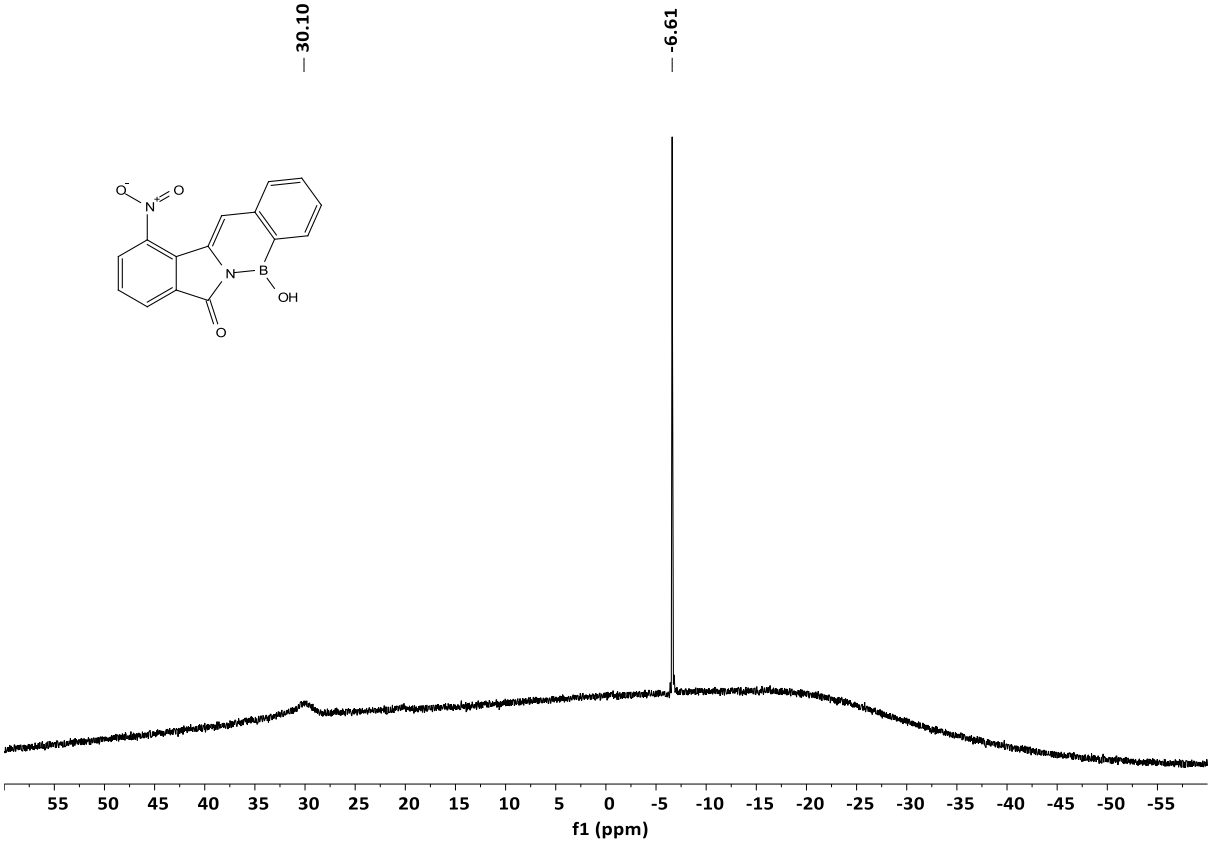

Figure S40. ^{11}B {1H} NMR spectrum (128 MHz) of **NO_2-PBNH 11** in acetone-d_6

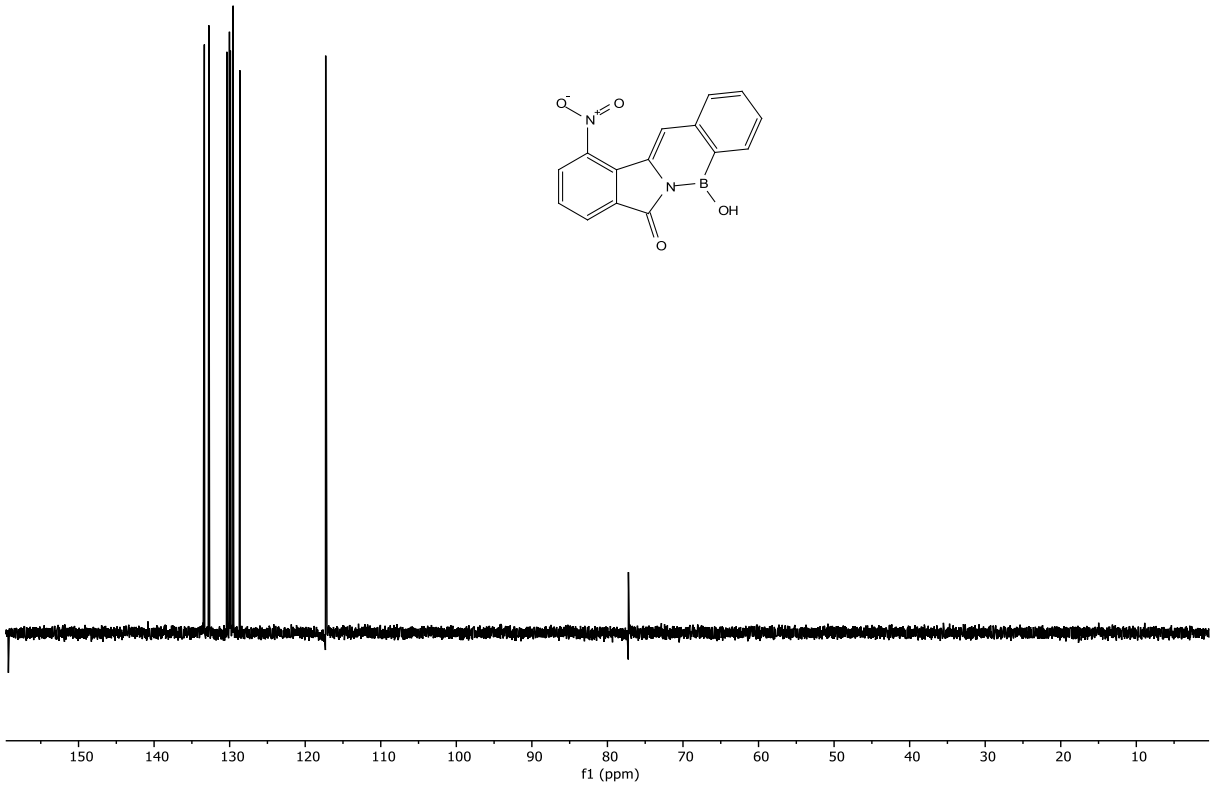

Figure S41. ^{13}C {1H} DEPT 135 NMR (100 MHz) of **NO_2-PBNH 11** in $CDCl_3$ at 25 °C

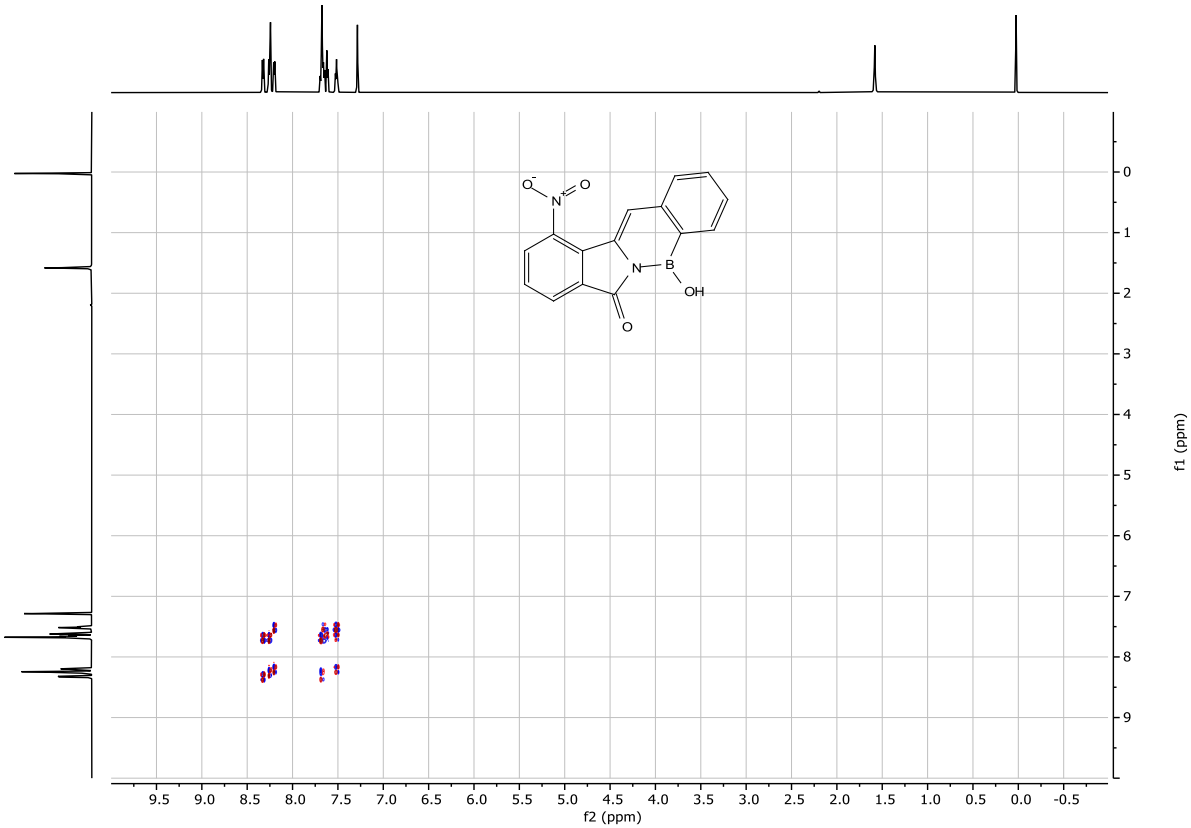

Figure S42. ^{1}H-^{1}H COSY spectra of **NO_2-PBNH 11** in $CDCl_3$ (400 MHz)

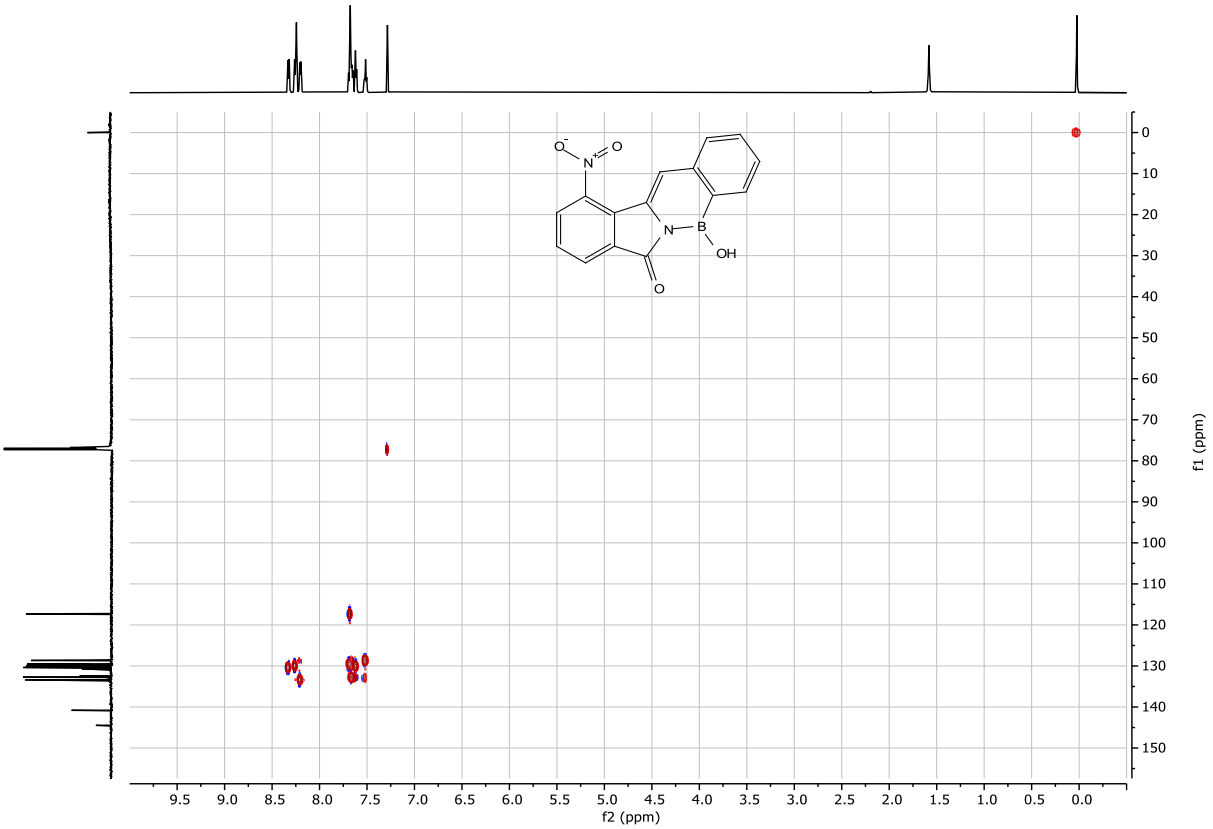

Figure S43. HSQC NMR spectra of **NO_2-PBNH 11** in $CDCl_3$ (400 MHz)

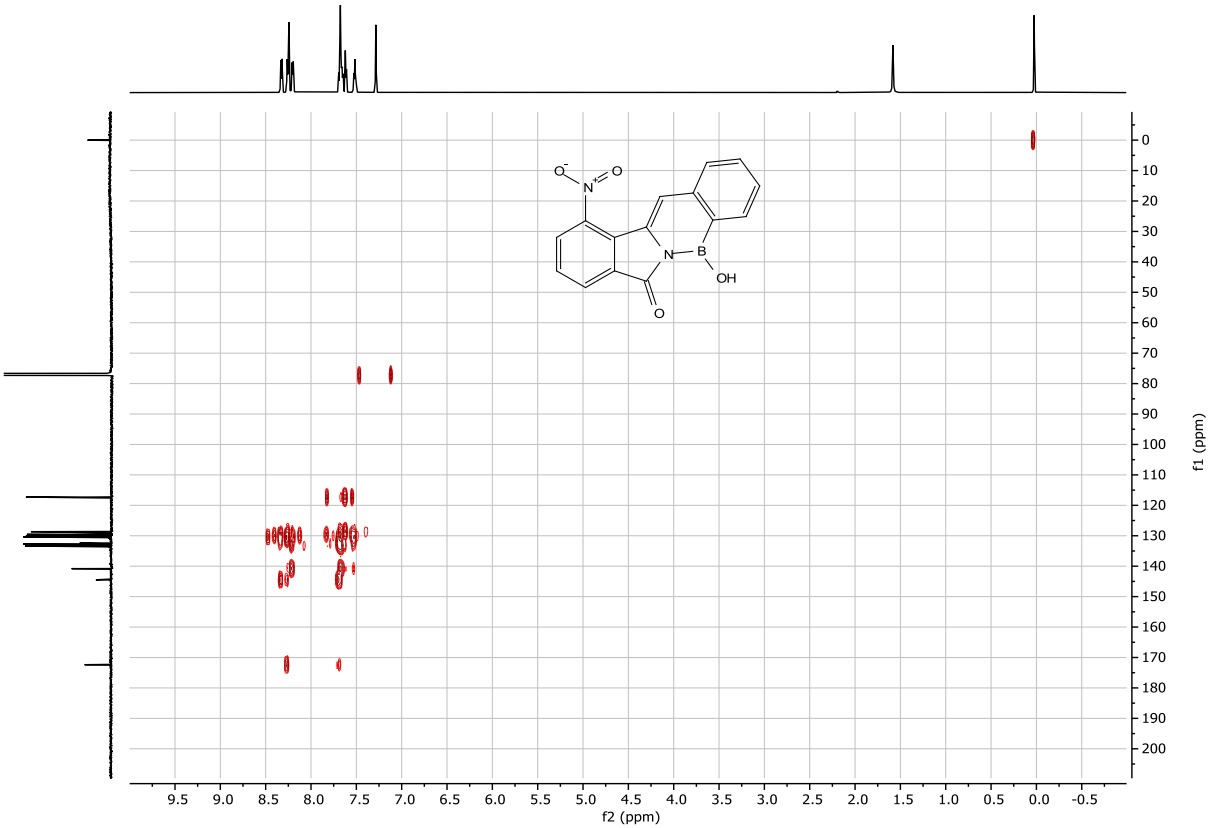

Figure S44. HMBC NMR spectra of **NO_2-PBNH 11** in $CDCl_3$ (400 MHz)

DART-Mass

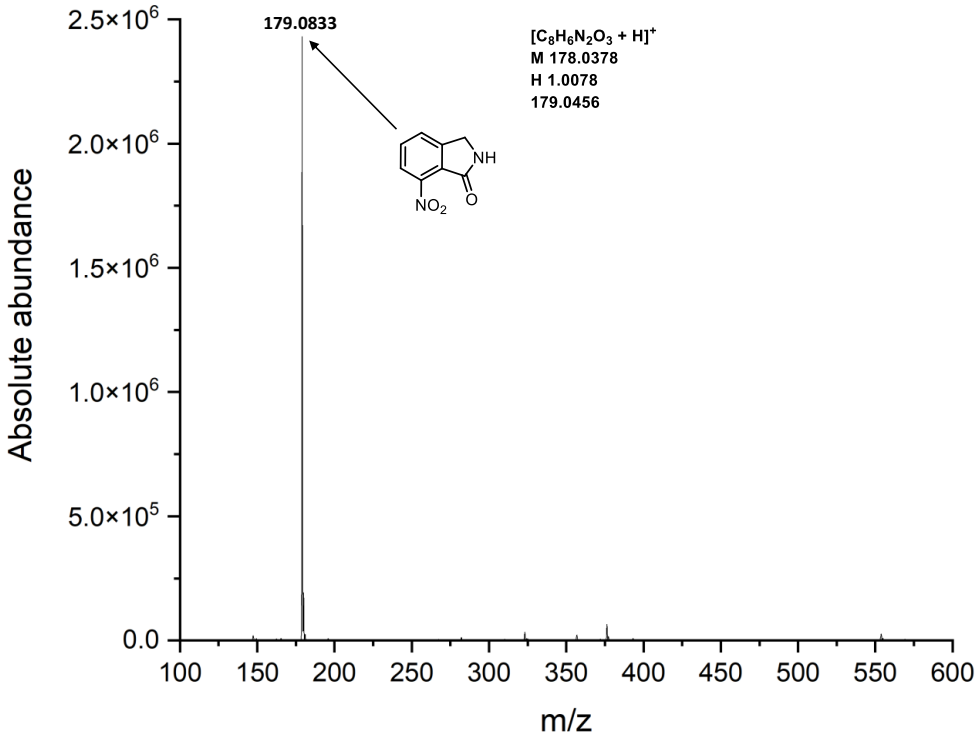

Figure S45. DART Mass spectrum for **2a**

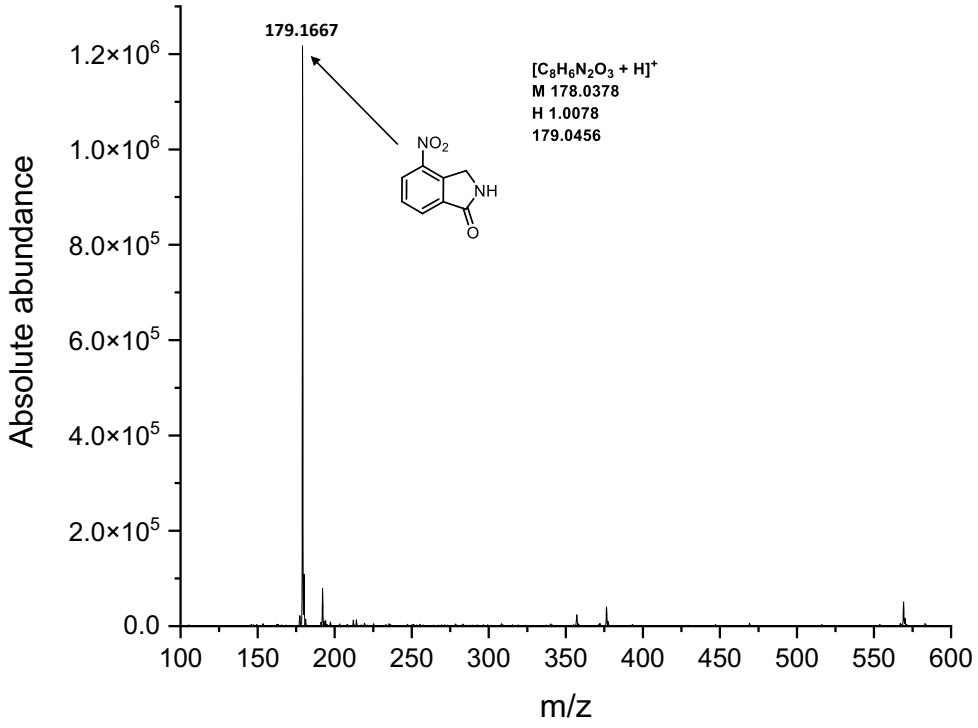

Figure S46. DART Mass spectrum for **2d**

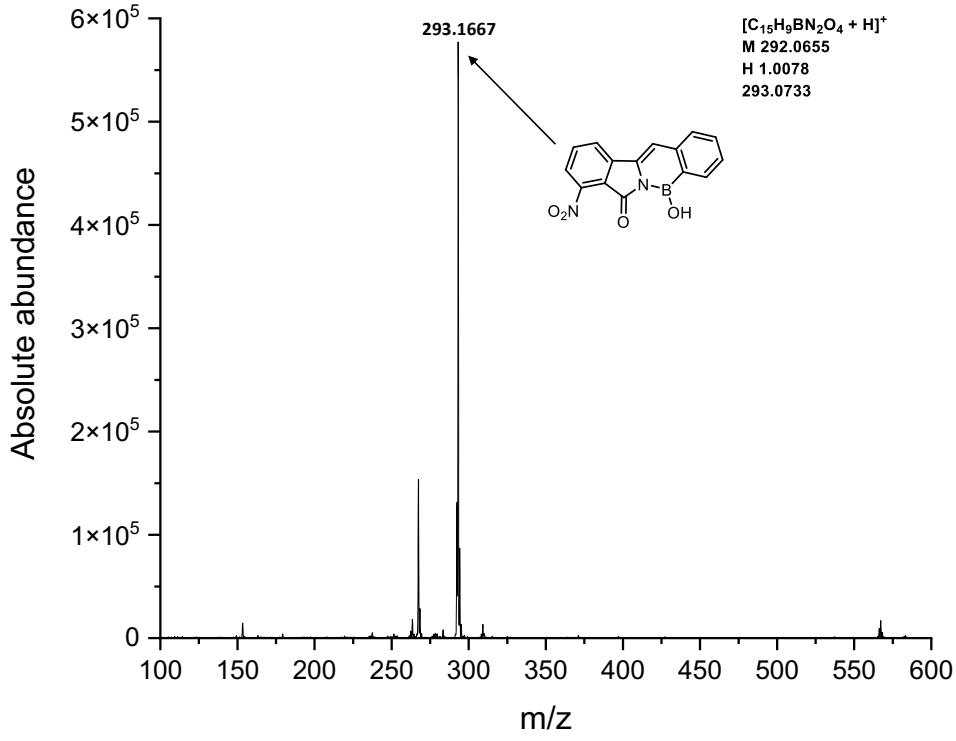

Figure S47. DART Mass spectrum for **NO_2-PBNH 8**

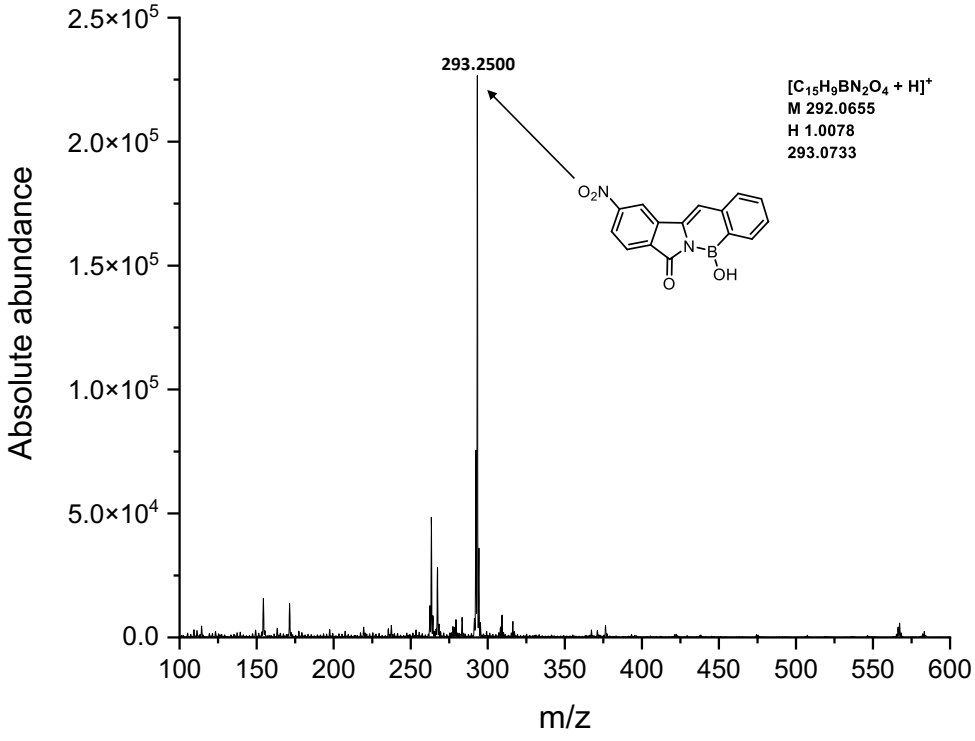

Figure S48. DART Mass spectrum for **NO_2-PBNH 10**

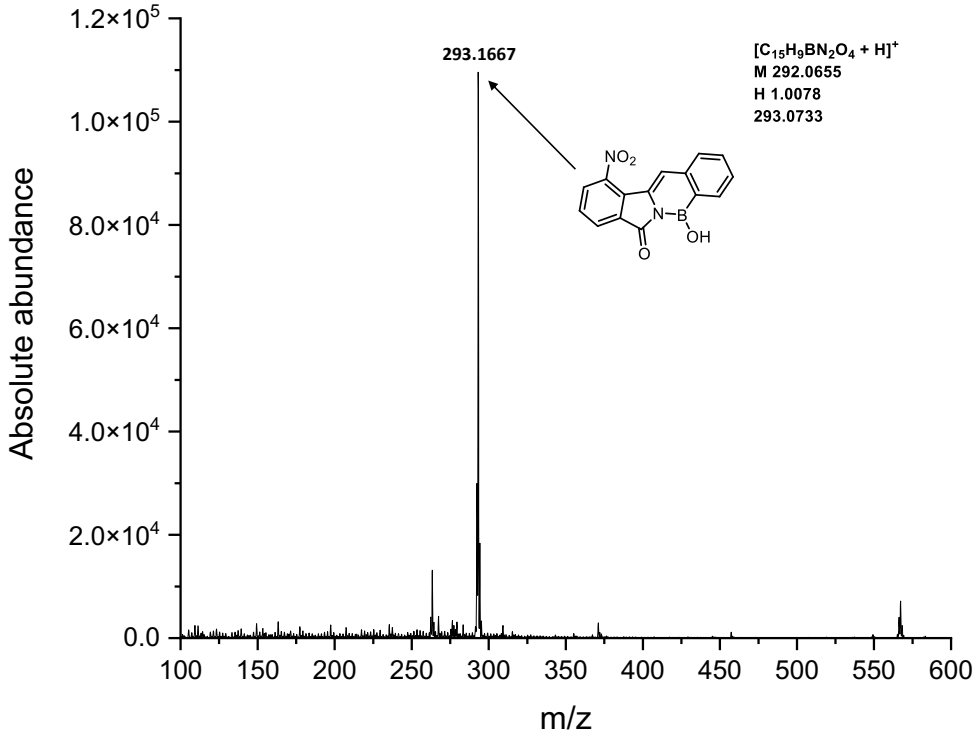

Figure S49. DART Mass spectrum for **NO_2-PBNH 11**

FT-IR

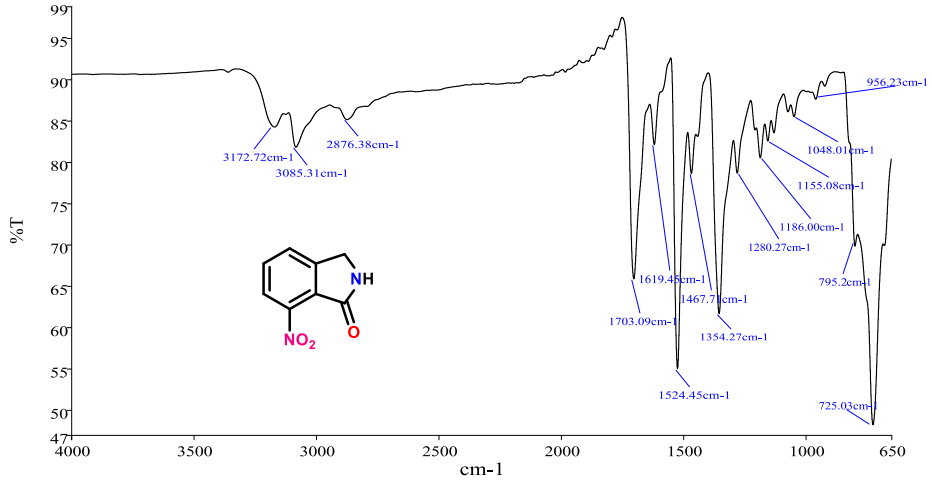

Figure S50. FTIR of compound **2a**

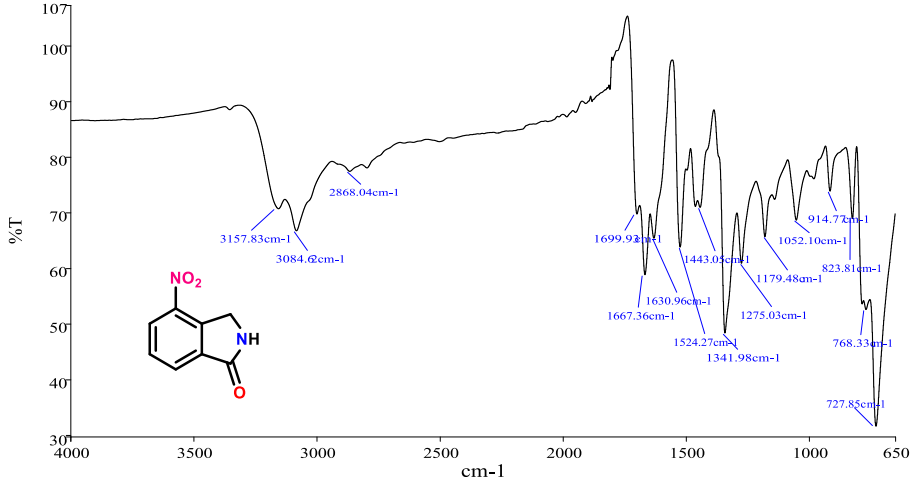

Figure S51. FTIR of compound **2d**

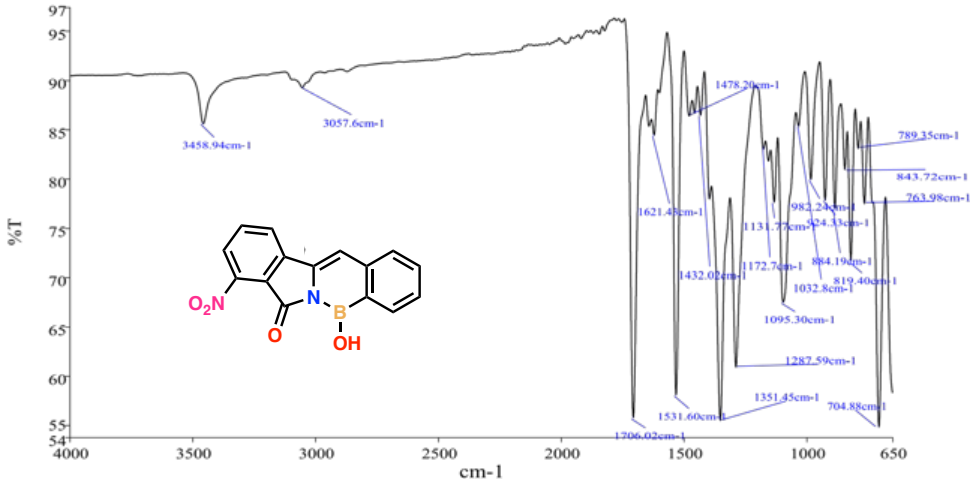

Figure S52. FTIR of **NO_2-PBNH 8**

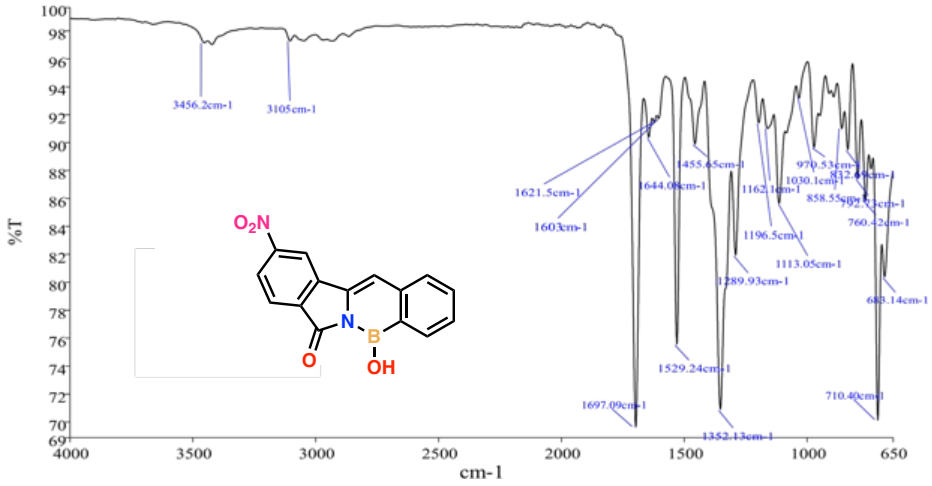

Figure S53. FTIR of **NO_2-PBNH 10**

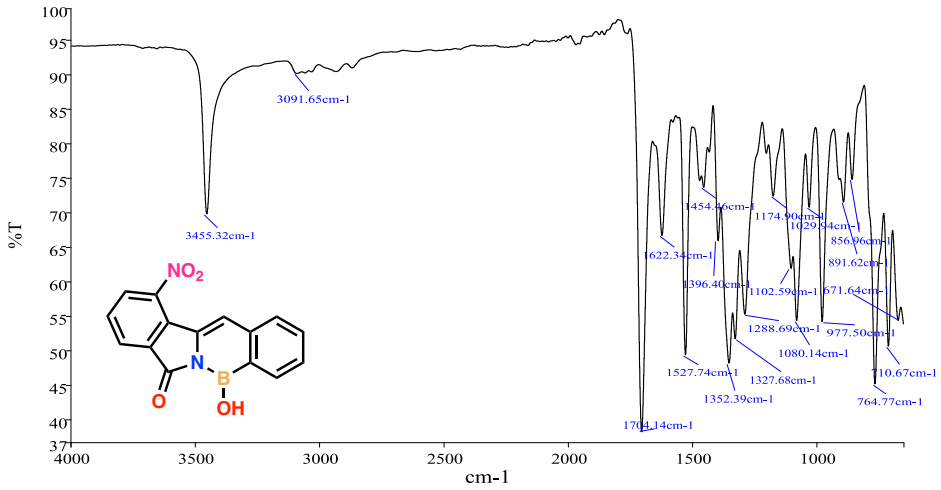

Figure S54. FTIR of **NO_2-PBNH 11**

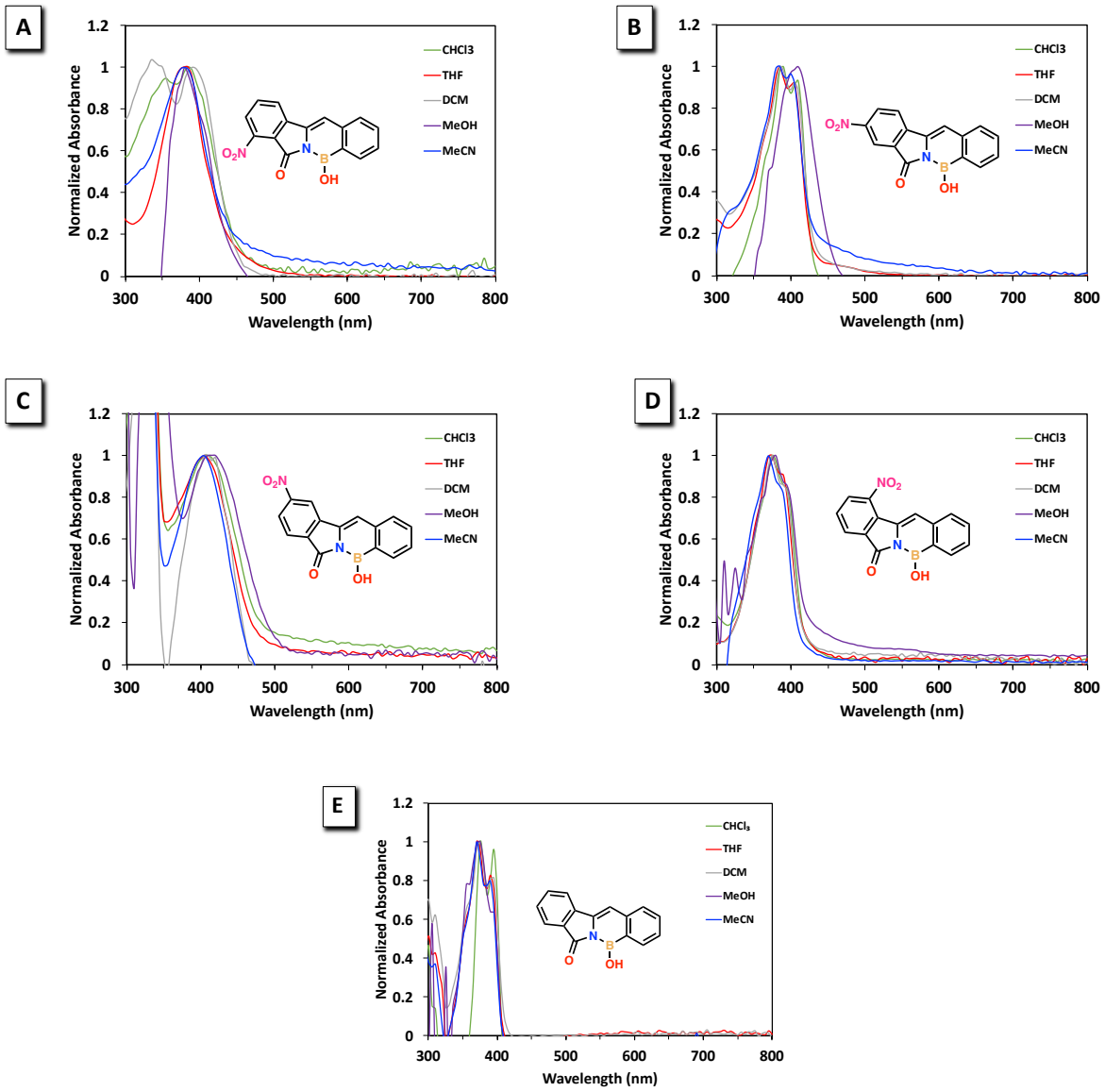

Figure S55. Experimental normalized Uv-vis absorption spectra of (A) **NO_2-PBNH 8**; (B) **NO_2-PBNH 9**; (C) **NO_2-PBNH 10**; (D) **NO_2-PBNH 11**; and (E) unsubstituted **PBNH** in $CHCl_3$, THF, DCM, MeOH and MeCN. (PBNHs concentration = 10^{-6} M in solution)

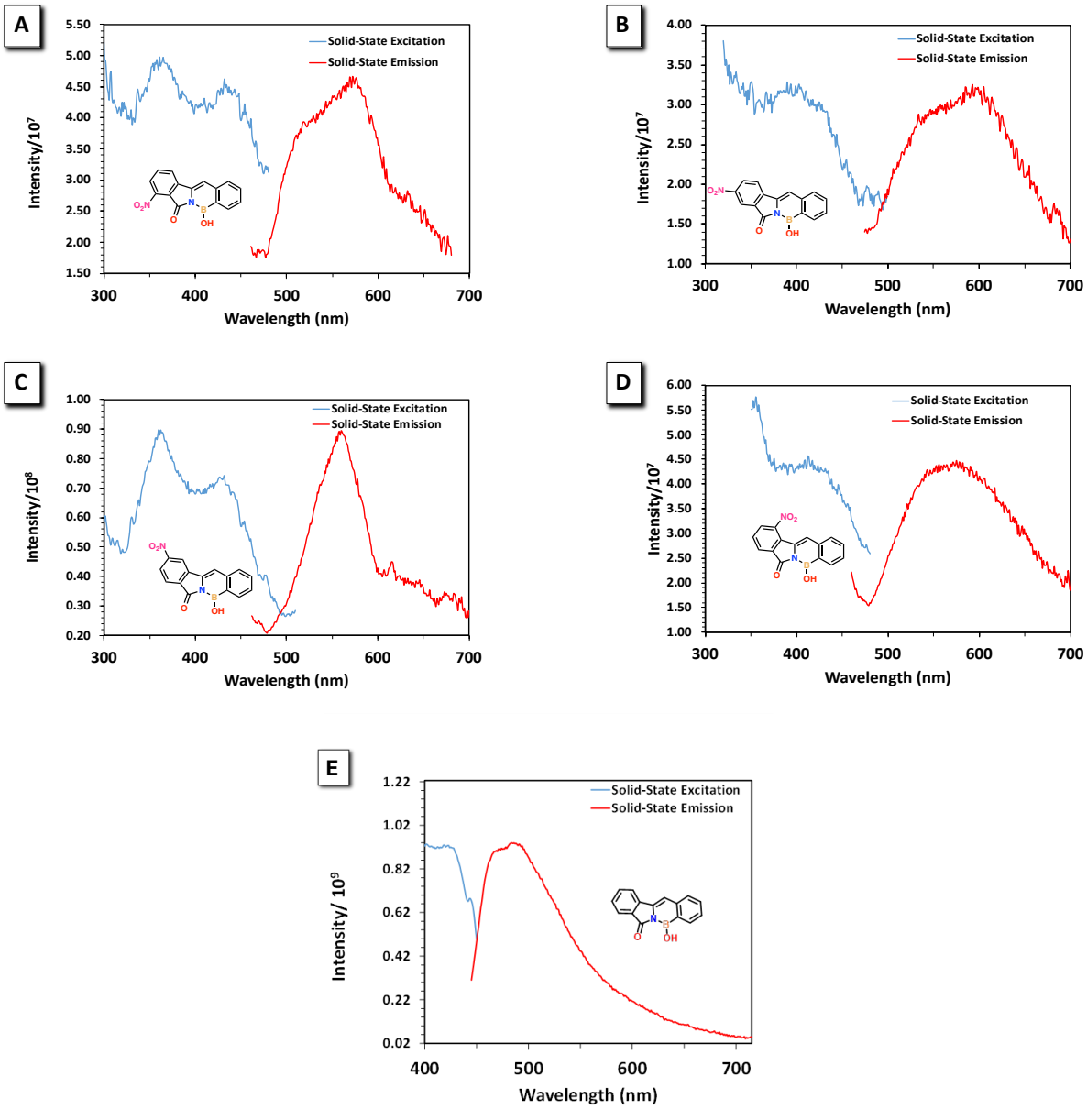

Figure S56. Experimental solid-state excitation and solid-state emission spectra of (A) **NO_2-PBNH 8**; (B) **NO_2-PBNH 9**; (C) **NO_2-PBNH 10**; (D) **NO_2-PBNH 11**; and (E) unsubstituted **PBNH**.

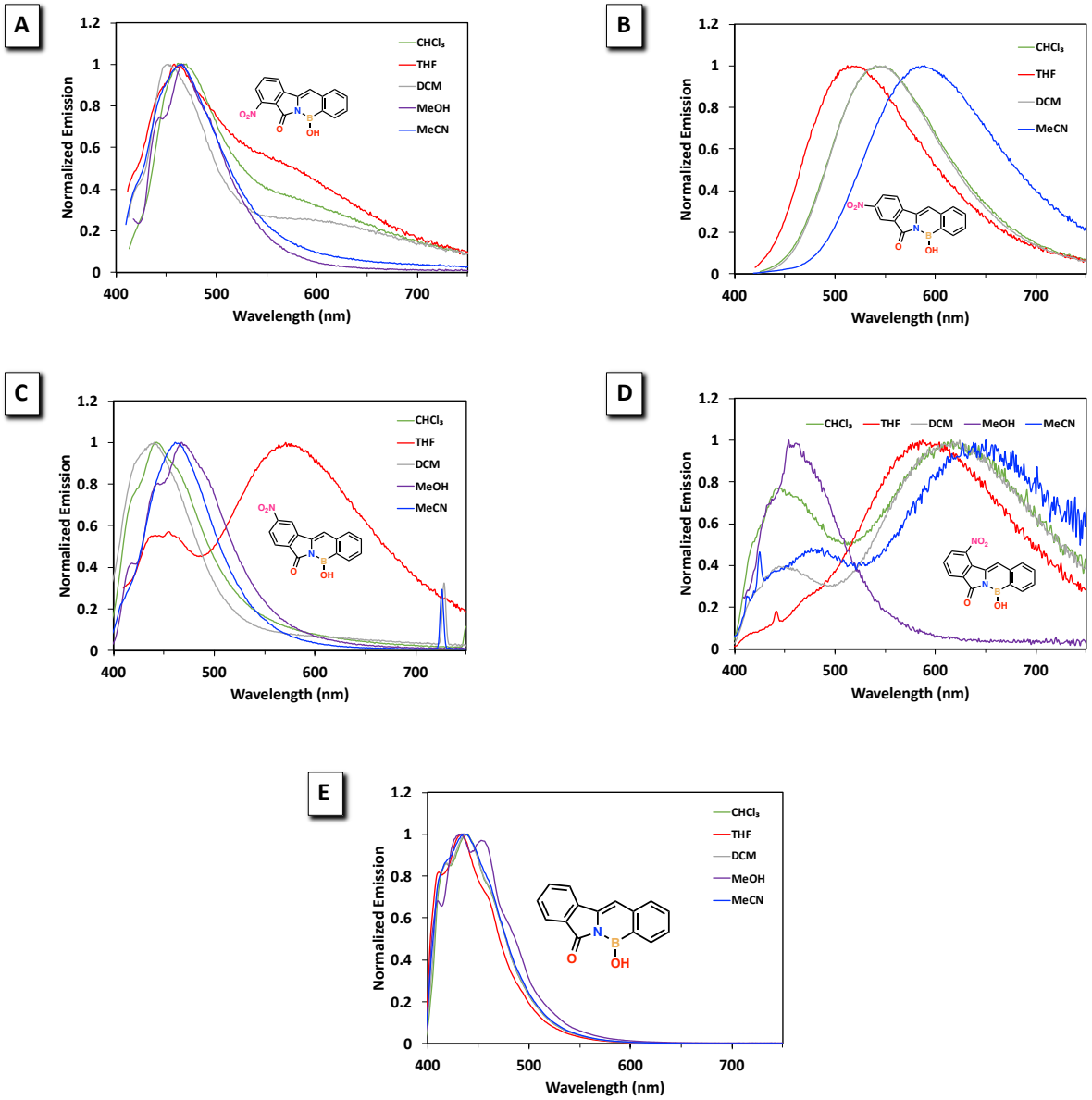

Figure S57. Experimental normalized emission spectra of (A) **NO_2-PBNH 8**, (B) **NO_2-PBNH 9**, (C) **NO_2-PBNH 10**, (D) **NO_2-PBNH 11**, and (E) unsubstituted **PBNH** in $CHCl_3$, THF, DCM, MeOH and MeCN. (NO_2-PBNHs concentration = 10^{-5} M in solution, λ_{exc} are in manuscript Table 2)

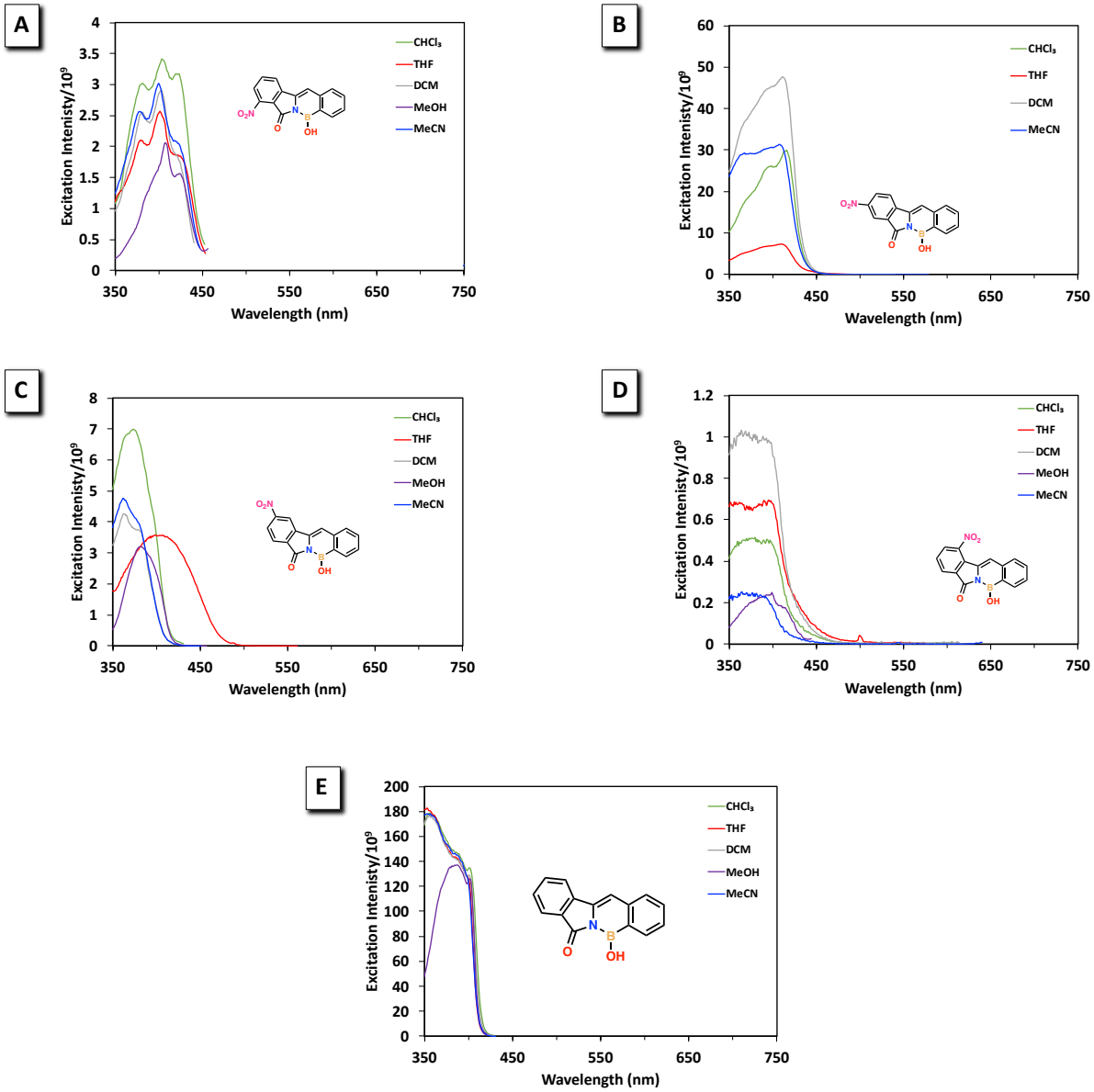

Figure S58. Experimental excitation spectra of (A) **NO_2-PBNH 8**, (B) **NO_2-PBNH 9**, (C) **NO_2-PBNH 10**, (D) **NO_2-PBNH11**, and (E) unsubstituted **PBNH** in $CHCl_3$, THF, DCM, MeOH, and MeCN. (NO_2-PBNHs concentration = 10^{-5} M in solution)

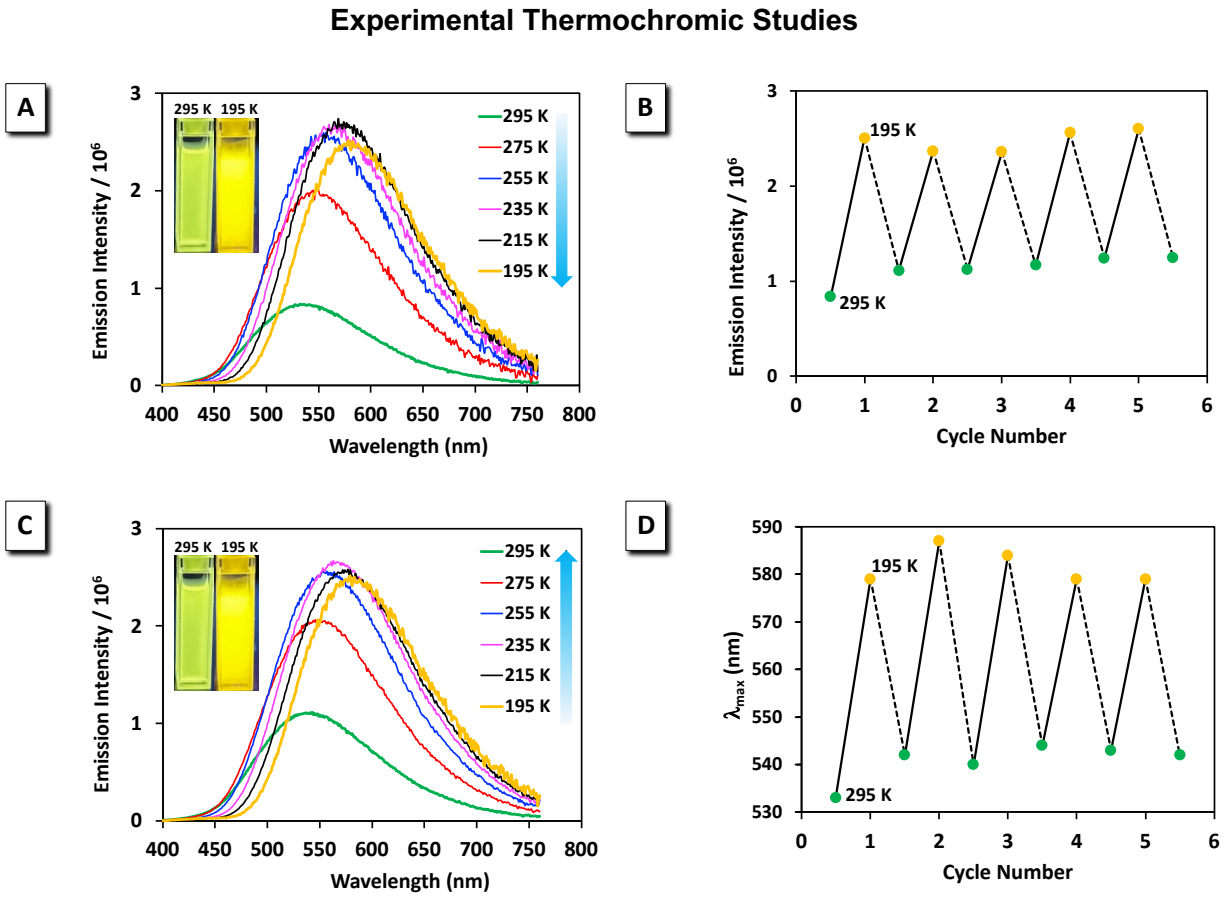

Figure S59. (A) Temperature-dependent emission spectra for **NO_2-PBNH 9** from 295 K to 195 K. (B) Reversible modulation of emission intensity, shown by temperature cycling of **NO_2-PBNH 9**. (C) Temperature-dependent emission spectra for **NO_2-PBNH 9** from 195 K to 295 K. (D) Reversible modulation of emission wavelength, shown by temperature cycling of **NO_2-PBNH 9.** (in distilled DCM, NO_2-PBNH concentration= 10^{-5} M, λ_{ex} = 380 nm)

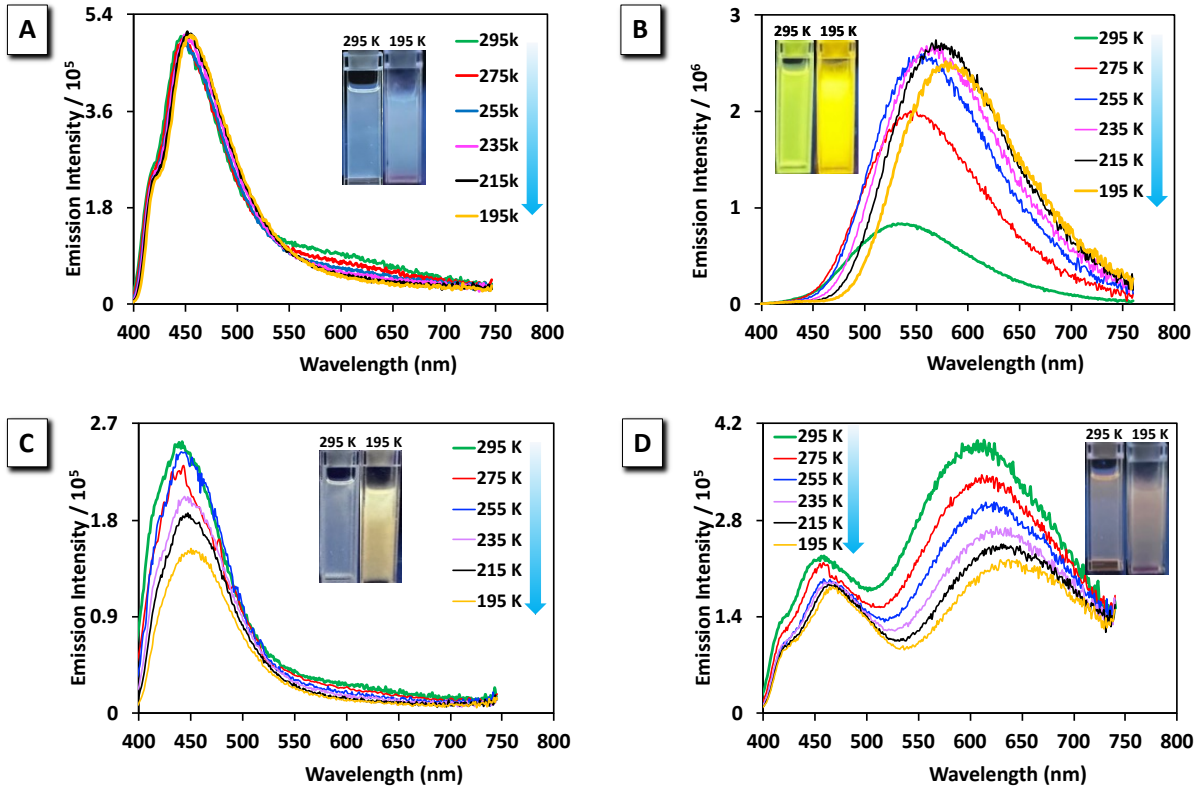

Figure S60. Variable temperature emission spectra (λ_{ex} = 380 nm) in regular DCM for (A) **NO_2-PBNH 8**; (B) **NO_2-PBNH 9**; (C) **NO_2-PBNH 10**; **and** (D) **NO_2-PBNH 11.** (NO_2-PBNH concentration = 10^{-5} M)

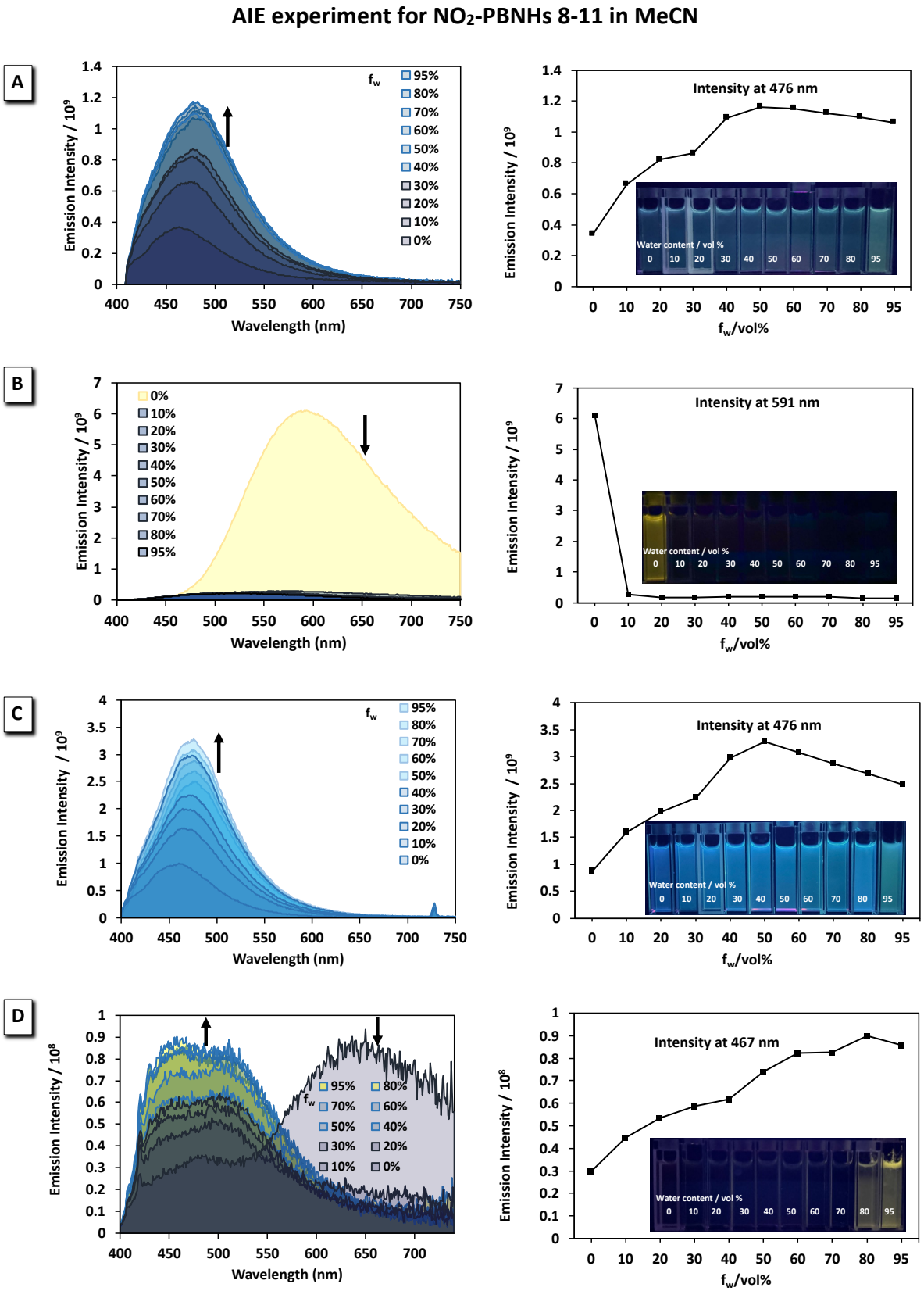

Figure S61. Emission spectra and plots of λ_{em} intensity vs. % water fraction (fw) for **NO_2-PBNHs 8** (A), **9** (B), **10** (C) and **11** (D) in MeCN/water mixtures (0-95% water). Photographs of **NO_2-PBNHs 8** (A), **9** (B), **10** (C) and **11** (D) in MeCN/water mixtures upon increasing the

fraction of water (0% to 95% fw from left to right) under a 365 nm handheld UV-light lamp. (**NO_2-PBNH** concentration= 10^{-5} M).

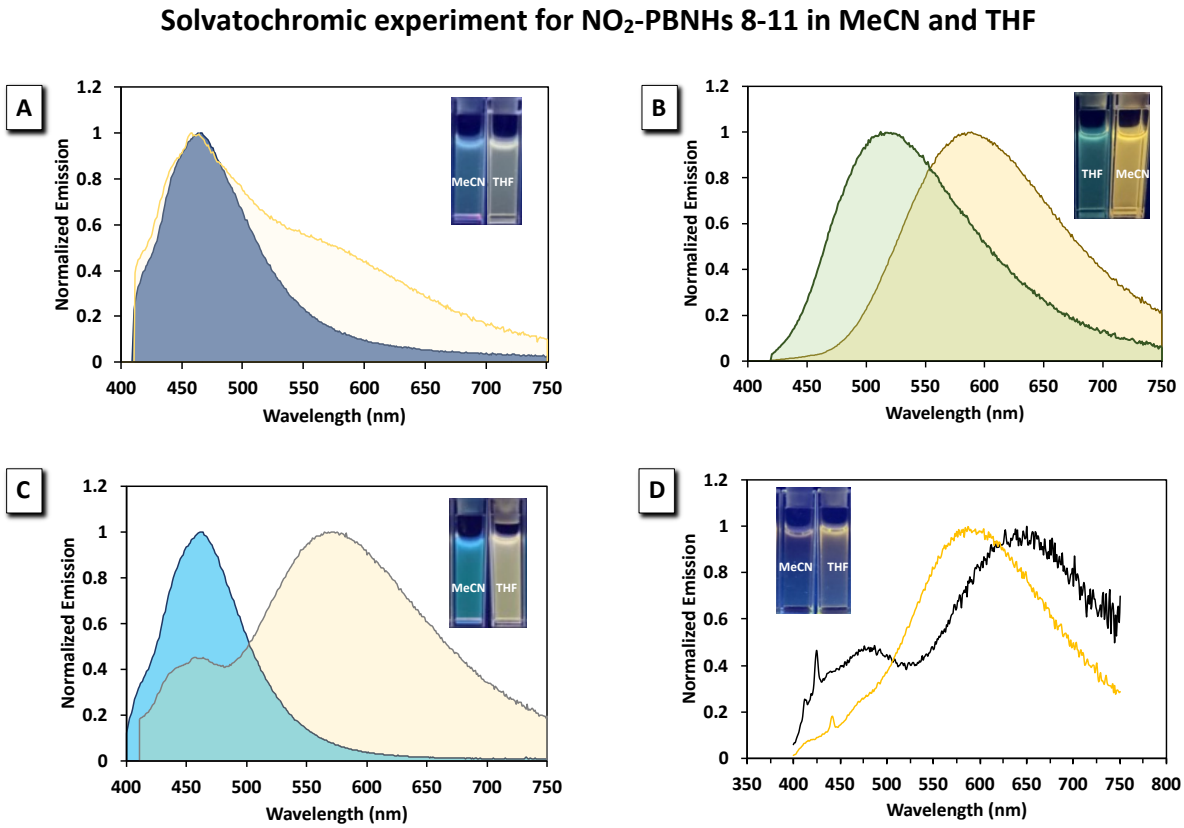

Figure S62. Emission spectra of **NO_2-PBNHs 8** (A), **9** (B), **10** (C), and **11** (D) in MeCN and THF illustrating solvatochromic behaviors. (**NO_2-PBNH** concentration= 10^{-5} M)

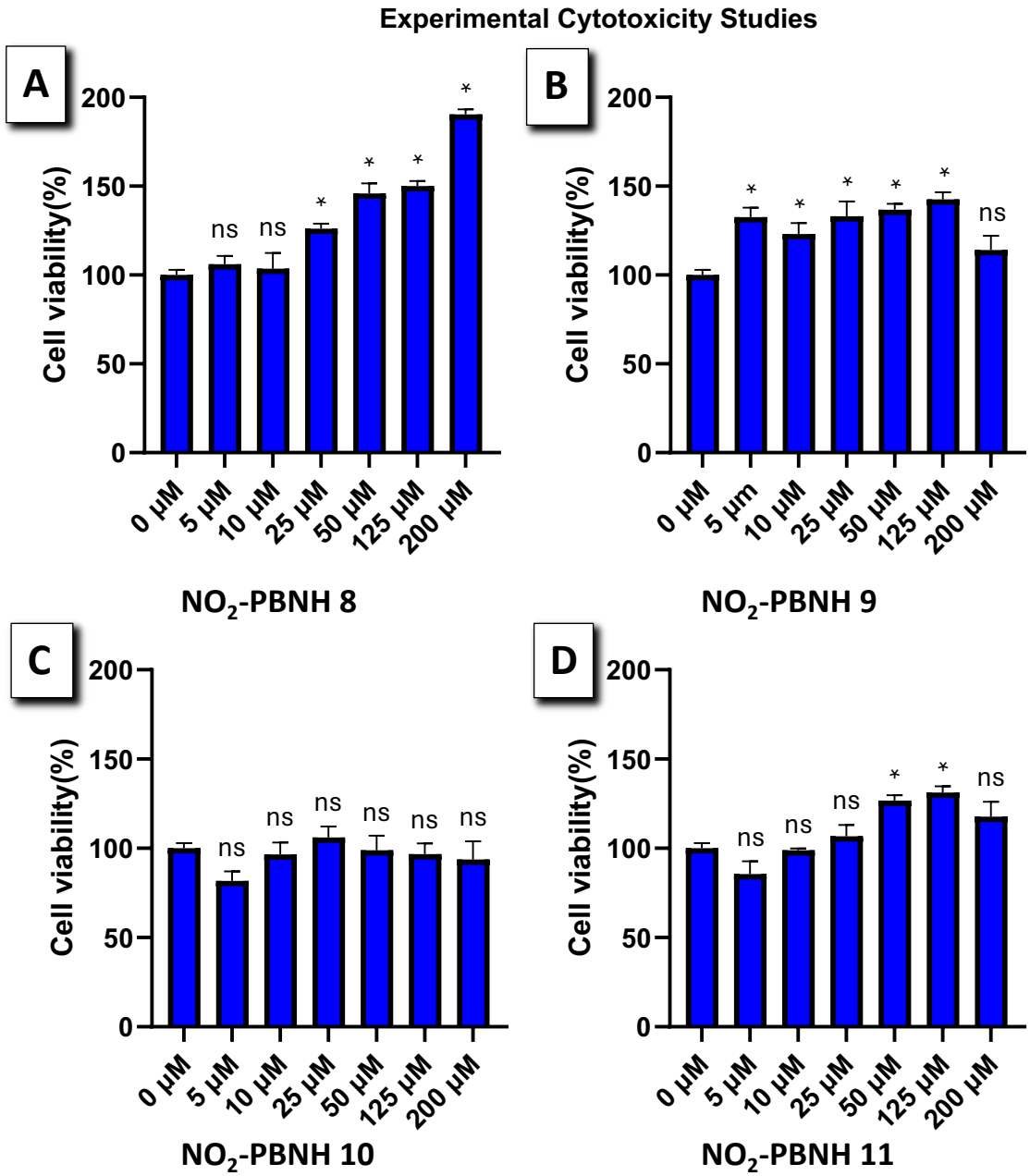

Figure S63. NO_2-PBNHs 8-11 are nontoxic to human HEK293 cells. Cells were incubated in the presence or absence of the indicated concentrations of **NO_2-PBNHs 8** (A), **9** (B), **10** (C), and **11** (D) for 72 h, and viability was determined using MTT assays. Viabilities were normalized to the relative viability of untreated control samples (100%). Data are presented using mean ± standard errors (n = 4). ∗: *p*-value < 0.05, ns: not significant (*p*-value > 0.05)

Table S1. TD-DFT M06-2X/6-311++G(d,p) calculated spectroscopic, electronic, and structural properties of the ground and excited states of the series of **NO_2-PBNHs** studied. All parameters are calculated in acetonitrile. The leading transition is $S_0 \rightarrow S_1$ in all cases with slight contribution from $S_0 \rightarrow S_2$

Compound	λ_{abs} (nm)	Oscillator Strength	HOMO (eV)	LUMO (eV)	LUMO+1 (eV)	E_g (eV)	$E_{LUMO+1} - E_{LUMO}$ (eV)	λ_{em} (nm)	Stokes shift (nm)	Dipole moment (D)	
										S_0	S_1
PBNH	337	0.59	-7.40	-1.71	-0.67	5.68	1.04	439	102	6.02	6.48
NO_2-PBNHA 8	352	0.48	-7.57	-2.14	-1.68	5.43	0.47	465	113	10.48	10.95
NO_2-PBNH 9	356	0.84	-7.61	-2.35	-1.60	5.26	0.75	466	110	8.10	9.02
NO_2-PBNH 10	366	0.38	-7.57	-2.43	-1.45	5.15	0.98	486	120	2.60	2.39
NO_2-PBNH 11	351	0.52	-7.63	-2.14	-1.87	5.50	0.27	520	169	2.54	3.30

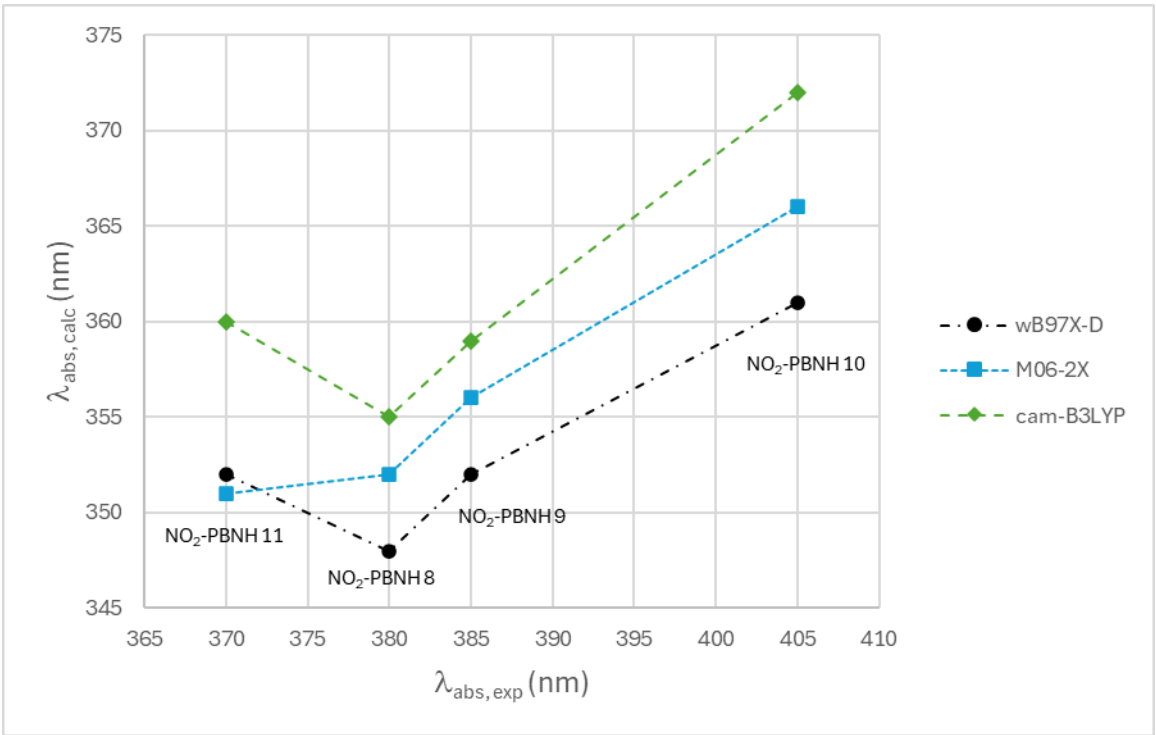

Figure S64. Calculated ($\lambda_{abs,\ calc}$) versus experimental ($\lambda_{abs,\ exp}$) maximum absorption wavelengths for compounds **NO_2-PBNHs 8-11** using different DFT functionals: cam-B3LYP, ωB97X-D, and M06-2X. All calculations were performed using the 6-311++G(d,p) basis set in acetonitrile.

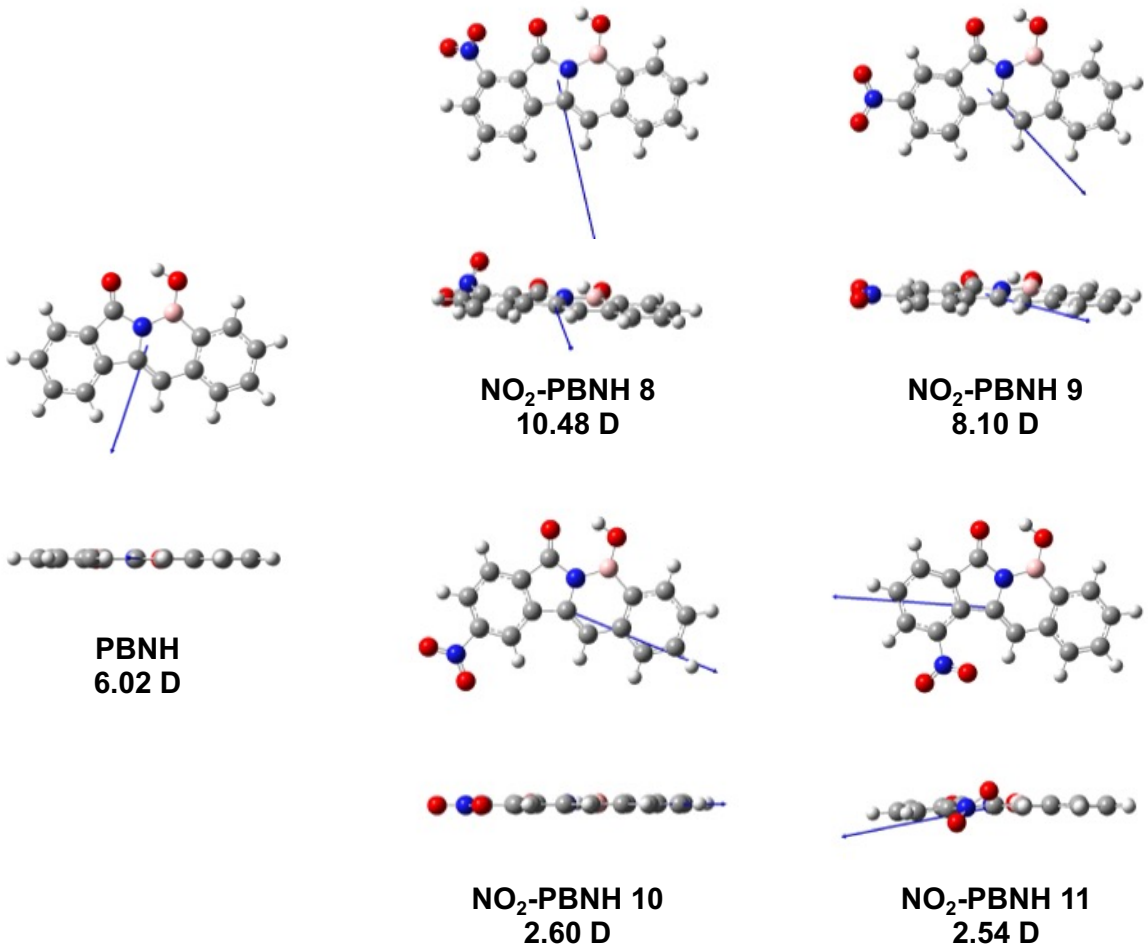

Figure S65. Magnitude (in D) and front (top) and in-plane (bottom) orientations of the ground-state dipole moments for unsubstituted **PBNH** and **NO_2-PBNHs 8–11**. To fit in the same figure, the dipole moment vectors were scaled by 0.8 for unsubstituted **PBNH**, **NO_2-PBNH 8** and **NO_2-PBNH 9** and by 2.8 for **NO_2-PBNH 10 and NO_2-PBNH 11**. Calculated at the M06-2X/6-311++G(d,p) level in acetonitrile.

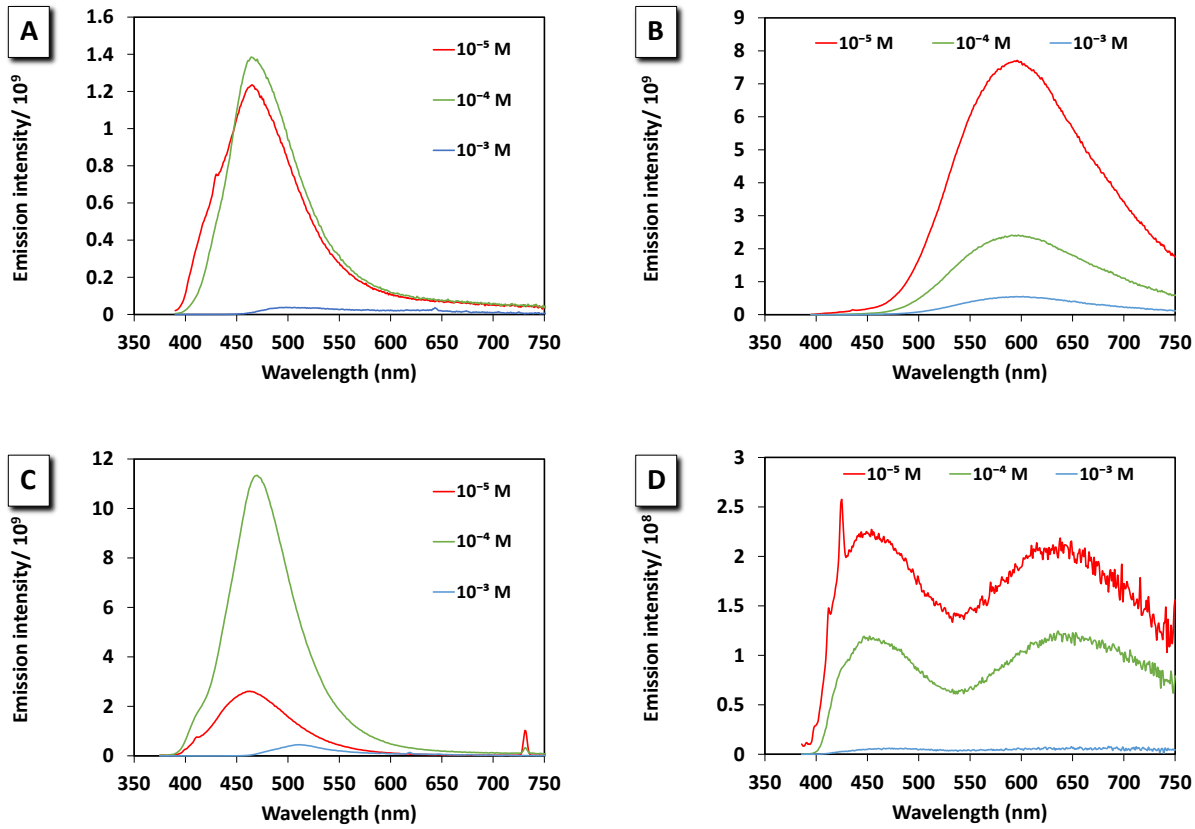

Figure S66. Concentration-dependent fluorescence measurements for **NO_2-PBNHs 8** (A), **9** (B), **10** (C), and **11** (D) at 10^{-5}, 10^{-4}, and 10^{-3} M in pure MeCN to evaluate intermolecular interactions in solution.

X-RAY CRYSTAL DATA

	8	9	11
CCDC Number	**2487849**	**2487850**	**2487851**
Empirical formula	C15H9BN2O4	C15H9BN2O4	C15H9BN2O4
Formula weight	292.05	292.05	292.05
Temperature/K	100.00	100.00	100.00
Crystal system	monoclinic	monoclinic	triclinic
Space group	P21/n	P21/c	P-1
a/Å	7.7216(6)	9.6994(4)	6.9686(4)
b/Å	8.3798(6)	14.1856(5)	8.0866(5)
c/Å	19.2968(14)	9.1953(3)	11.7246(7)
α/°	90	90	79.131(2)
β/°	100.234(3)	101.2730(10)	73.601(2)
γ/°	90	90	81.914(2)
Volume/Å3	1228.74(16)	1240.79(8)	619.77(6)
Z	4	4	2
ρcalcg/cm3	1.579	1.563	1.565
μ/mm-1	0.115	0.114	0.114
F(000)	600.0	600.0	300.0
Crystal size/mm3	0.349 × 0.052 × 0.03	0.127 × 0.097 × 0.027	0.311 × 0.029 × 0.025
Radiation	MoKα (λ = 0.71073)	MoKα (λ = 0.71073)	MoKα (λ = 0.71073)
2Θ range for data collection/°	5.314 to 54.206	4.282 to 54.224	3.666 to 52.708
Index ranges	-9 ≤ h ≤ 9, -10 ≤ k ≤ 10, -24 ≤ l ≤ 24	-12 ≤ h ≤ 11, -18 ≤ k ≤ 18, -11 ≤ l ≤ 11	-8 ≤ h ≤ 8, -10 ≤ k ≤ 10, -14 ≤ l ≤ 14
Reflections collected	27982	23978	28025
Independent reflections	2707 [Rint = 0.0690, Rsigma = 0.0411]	2730 [Rint = 0.0269, Rsigma = 0.0173]	2532 [Rint = 0.0326, Rsigma = 0.0167]
Data/restraints/parameters	2707/0/203	2730/0/203	2532/0/203
Goodness-of-fit on F2	1.046	1.088	1.100
Final R indexes [I>=2σ (I)]	R1 = 0.0450, wR2 = 0.1091	R1 = 0.0489, wR2 = 0.1161	R1 = 0.0391, wR2 = 0.0916
Final R indexes [all data]	R1 = 0.0616, wR2 = 0.1191	R1 = 0.0537, wR2 = 0.1190	R1 = 0.0426, wR2 = 0.0934
Largest diff. peak/hole / e Å-3	0.32/-0.24	0.43/-0.36	0.38/-0.25

References

1 B. Laleu, Y. Akao, A. Ochida, S. Duffy, L. Lucantoni, D. M. Shackleford, G. Chen, K. Katneni, F. C. K. Chiu, K. L. White, X. Chen, A. Sturm, K. J. Dechering, B. Crespo, L. M. Sanz, B. Wang, S. Wittlin, S. A. Charman, V. M. Avery, N. Cho and M. Kamaura, *J Med Chem*, 2021, **64**, 12582–12602.

2 C. J. Saint-Louis, R. N. Shavnore, C. D. C. McClinton, J. A. Wilson, L. L. Magill, B. M. Brown, R. W. Lamb, C. E. Webster, A. K. Schrock and M. T. Huggins, *Org Biomol Chem*, 2017, **15**, 10172–10183.

3 A. Rosowsky, R. A. Forsch, A. Null and R. G. Moran, *J Med Chem*, 1999, **42**, 3510–3519.

4 L. Han, R. Shi, C. Xin, Q. Ci, J. Ge, J. Liu, Q. Wu, C. Zhang, L. Li and W. Huang, *ACS Sens*, 2018, **3**, 1622–1626.

5 Q. Sun, Y. Chu, N. Zhang, R. Chen, L. Wang, J. Wu, Y. Dong, H. Li, L. Wang, L. Tang, C. Zhan and J.-Q. Zhang, *J Med Chem*, 2024, **67**, 7330–7358.

6 B. Peng, A. Thorsell, T. Karlberg, H. Schüler and S. Q. Yao, *Angewandte Chemie International Edition*, 2017, **56**, 248–253.

7 A. D. Campbell, K. Ellis, L. K. Gordon, J. E. Riley, V. Le, K. K. Hollister, S. O. Ajagbe, S. Gozem, R. B. Hughley, A. M. Boswell, O. Adjei-sah, P. D. Baruah, R. Malone, L. M. Whitt, R. J. Gilliard and C. J. Saint-Louis, *J Mater Chem C Mater*, 2023, **11**, 13740–13751.